Redatuming of Sparse 3D Seismic Data

PROEFSCHRIFT

ter verkrijging van de graad van doctor
aan de Technische Universiteit Delft,
op gezag van de Rector Magnificus prof. dr. ir. J.T. Fokkema,
voorzitter van het College voor Promoties,
in het openbaar te verdedigen
op maandag 19 maart 2007 om 10:00 uur

door

Sandra TEGTMEIER

Diplom-Geophysikerin, Ruhr-Universität Bochum
geboren te Hameln, Duitsland

Dit proefschrift is goedgekeurd door de promotor:
Prof. dr. ir. A. Gisolf

Toegevoegd promotor:
Dr. ir. D.J. Verschuur

Samenstelling promotiecommissie:

Rector Magnificus,	voorzitter
Prof. dr. ir. A. Gisolf,	Technische Universiteit Delft, promotor
Dr. ir. D.J. Verschuur,	Technische Universiteit Delft, toegevoegd promotor
Prof. dr. H.P. Urbach,	Technische Universiteit Delft
Prof. dr. M. Tygel,	Universidade Estadual de Campinas, UNICAMP, Brazil
Prof. dr. W.A. Mulder,	Technische Universiteit Delft
Prof. dr. ir. C.P.A. Wapenaar,	Technische Universiteit Delft
Dr. T.A. Alkhalifah,	King Abdulaziz City For Science and Technology, Riyadh, Saudi Arabia

ISBN 978-90-9021678-2

SUPPORT

The research for this thesis was financially supported by the DELPHI research consortium.

Typesetting system: LaTeX.

Printed in The Netherlands by Gildeprint, Enschede.

Anfangs wollt ich fast verzagen
Und ich glaubt, ich trüg es nie;
Und ich hab es doch getragen
Aber frag mich nur nicht wie.

Heinrich Heine (1797 - 1856)

Danke, Thorsten.

Contents

1

Introduction

Anfangen im Kleinen,
Ausharren in Schwierigkeiten,
Streben zum Großen.

Alfred Krupp (1812 - 1887)

Ever since the 1973 oil crisis there has been an ongoing discussion over the world energy demand. With respect to this it has always been of particular interest whether the oil resource base would be sufficient to meet this demand.

The International Energy Outlook published by the Energy Information Administration [2005] projects a growth of the total worldwide energy use from 412 quadrillion Btu[1] in 2002 to 645 quadrillion Btu in 2025. It is, furthermore, expected that fossil fuels such as oil, natural gas and coal will continue to supply most of the energy used with fossil oil being the most important energy source and that there will be sufficient oil to meet the worldwide demand until at least 2025. However, the trend clearly implies that the growing demand for oil cannot be met solely by the remaining reserves but that existing reserves need to be exploited more efficiently and new reserves need to be found.

It is actually this need to discover new reserves and monitor the proven ones that establishes the importance of geophysical exploration techniques and, in particular, the importance of the seismic method. As explained by Telford et al. [1990], the seismic method is especially well suited for the exploration of hydrocarbons. It al-

[1] British Thermal Unit, 1 Btu = 1.05505585262 kJ.

lows a great penetration depth, and the result – an image of the probed subsurface – exhibits high accuracy as well as high resolution.

1.1 The seismic method – seismic data acquisition and data processing

Exploration seismology ('the seismic method') has developed from earthquake seismology. An earthquake usually occurs when a part of the subsurface is fractured. At the fractured surface seismic (elastic) waves are generated. These waves travel outward and can be recorded at the earth's surface. Seismologists then use the recorded data to extract information about the rocks through which the waves traveled.
Exploration seismology basically uses the same type of measurements. Here, artificial sources are used to generate seismic waves. Explosives, vibrator trucks (for land acquisition) and air guns (for marine acquisition) are employed. The reflected waves returning to the earth's surface are recorded with receivers, such as geophones or hydrophones. In Figure 1.1 a typical situation for marine data acquisition is shown. The recorded seismic data of such an experiment consist of a number of so-called traces. Each trace represents the motion of the ground in time, respectively the pressure variations for marine acquisition, which is related to the waves arriving at the receiver.

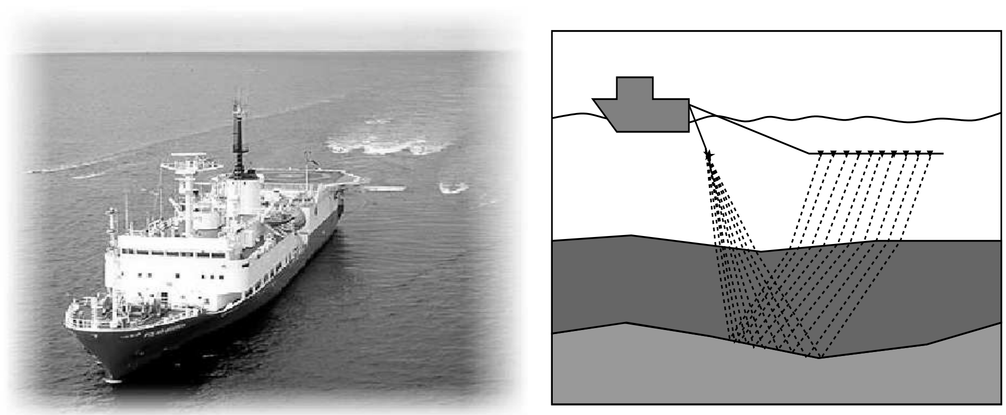

Figure 1.1: *Marine data acquisition. (a) Photograph of a vessel towing the marine acquisition devices (taken from the Veritas website). (b) Sketch of the marine data acquisition. Here, one source and one streamer, which contains the hydrophones, are shown. Furthermore, the raypaths of the reflection from one interface are indicated.*

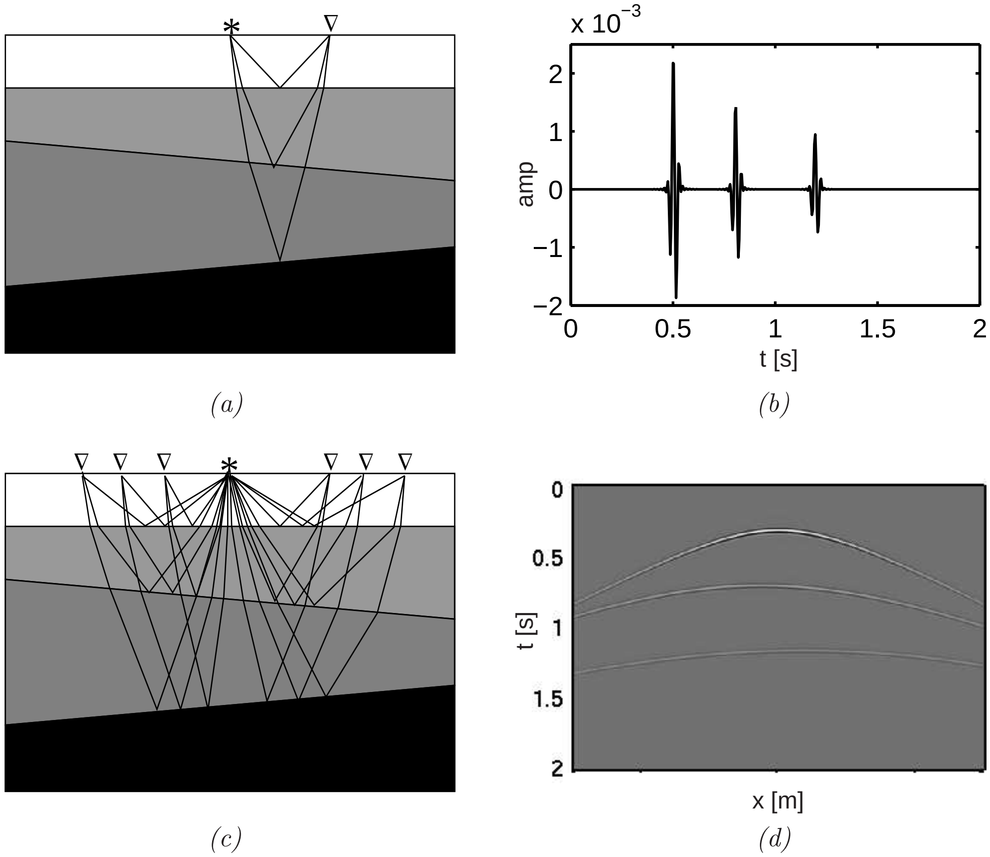

Figure 1.2: *(a) Three reflections occurring on a measurement for one source/receiver pair, (b) the corresponding seismic trace, (c) three reflections occurring on a number of traces of a particular shot gather and (d) the shot gather showing the reflection events.*

The traces contain information about the subsurface, because energy is reflected whenever there is a heterogeneity in the elastic properties of the subsurface, e.g. at the interface between two layers of different types of rock.
In Figure 1.2b a seismic trace is shown containing the reflection events of an experiment for the simple subsurface model presented in Figure 1.2a. However, evaluating only one trace is not enough to build a picture of the subsurface. To cover a large area in the subsurface, a number of geophones is planted along lines (2D seismic) or over a certain area (3D seismic), recording the echoes of a number of shots at different source positions. In Figure 1.2d a so-called shot gather is shown, which contains the reflection events of all traces for the geophones planted along a 2D line for one shot position (see Figure 1.2c). If one takes a look at the shot gather presented, which is representative for the raw data a seismic processor typically gets from a

field crew, it is clear that one still cannot extract any information about the geologic structures of the subsurface. It cannot be done for this simple example, and it is definitely impossible for more complicated data as obtained in the real world. Certain processing steps have to be applied first to get a seismic image of the subsurface. This seismic image, being the end product of the seismic method, is finally handed over to geologists, geophysicists or reservoir engineers who will interpret the result. In Figure 1.3a such a seismic image is presented showing a syncline structure, which can also be found in reality (see Figure 1.3b).

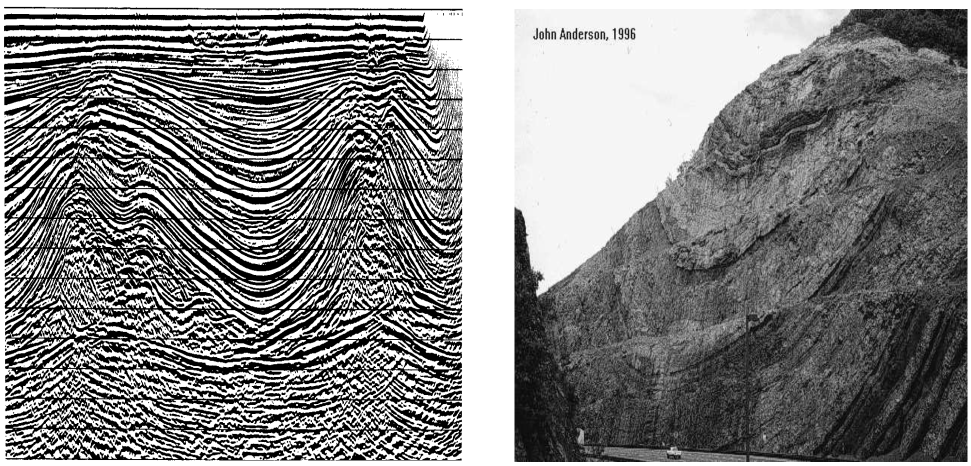

(a) *(b)*

Figure 1.3: *Geological syncline structure (a) in a seismic image, and (b) in reality.*

1.2 Redatuming – a data processing step

Seismic processing has been defined by Sheriff [2002] as: "Changing data, usually to improve the signal-to-noise-ratio to facilitate interpretation." To achieve this, a number of different processing operations are subsequently applied to the input data, such as rearranging the data, filtering, applying different corrections and migration (imaging). Thereby, most of the algorithms applied during seismic processing are optimized for regularly sampled data referenced to a flat surface (datum) and for a simple velocity distribution in the subsurface. Unfortunately in reality, and especially for land acquisition, data are collected on irregularly sampled, rugged surfaces and with complex structures in the subsurface. Typical features of such complexities frequently encountered in the near surface are, for example: varying water table, leached zones, buried river channels, sand dunes and high velocity beds. The variability in velocity and thickness of this near surface layer causes serious distortions of the seismic data acquired at the earth's surface. With the thickness of this near surface layer being usually hundreds of meters, burying sources and receivers for the acquisition at a depth level below the complexities is not a viable option. Therefore, the data will be acquired at the surface, but, prior to further processing, the data can be artificially referenced to a flat surface (new datum) below the distorting complex near surface layer. As a data processing step, signals of virtual sources and receivers at another level than the acquisition surface can be calculated without actually moving them.

1.2.1 Static corrections versus wavefield extrapolation

In data processing the near surface effects are usually accounted for by applying so-called static corrections [see e.g. Marsden, 1993]. Hereby time shifts are calculated independently for every trace, assuming the waves to travel vertically downward from the sources and upward to the receivers through the near surface, low velocity layer, which is assumed to have a relatively smooth velocity distribution. However, in situations of large elevation changes, large distances between surface and new datum level and complex near surface layers with a heterogeneous velocity distribution, the assumption of such vertical raypaths is not realistic (see Figure 1.4). In this case, a processing method taking the true wave propagation in the datum layer into account has to be applied.

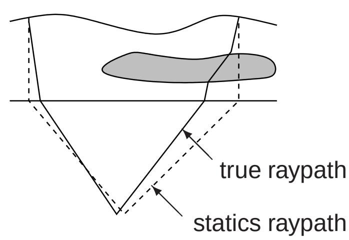

Figure 1.4: *Comparison of the vertical raypath within the near surface layer assumed for static corrections and the true raypath.*

Wavefield extrapolation is such a method. Here, the data recorded at the acquisition surface are transformed into a data set referenced to a new recording surface using the scalar wave equation. That is, in one step the receivers are brought to the new datum; in a second step the sources are moved to the new datum level. This processing step is called *datuming* or *redatuming*, because it references the data to a new datum. Its ability to remove distortions from the input data is illustrated in

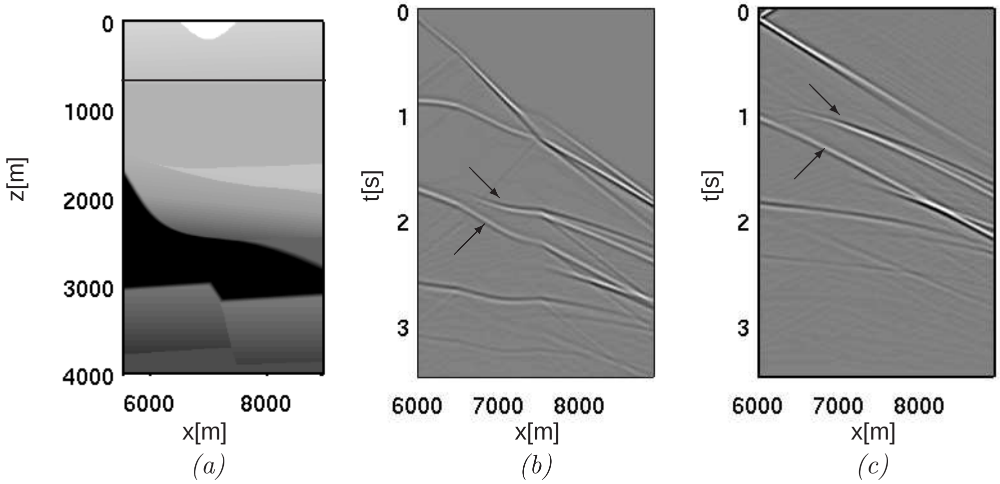

Figure 1.5: *(a) Velocity model with a near surface anomaly. The datum is indicated by the black line. (b) Seismic shot gather distorted by the near surface anomaly. (c) Redatumed seismic shot gather. Note that the distortion has been removed.*

Figure 1.5. Figure 1.5b shows a shot gather, which is clearly distorted by a near surface complexity. For the gather presented in Figure 1.5c redatuming has been performed towards a reference surface below the near surface anomaly. Thereby, the distortions have been removed.

1.2.2 Inventory of existing wavefield extrapolation methods

The wavefield extrapolation techniques can generally be divided into three different categories:

- the Kirchhoff summation methods,
- the phase shift methods,
- the finite difference methods.

All three methods can either be applied to post-stack data, or, by splitting up the extrapolation of the sources and the receivers in two steps, to pre-stack data.

Kirchhoff summation methods

This concept has first been presented by Berryhill [1979] for post-stack data and was later extended to pre-stack data [Berryhill, 1984]. It is based on the Kirchhoff inte-

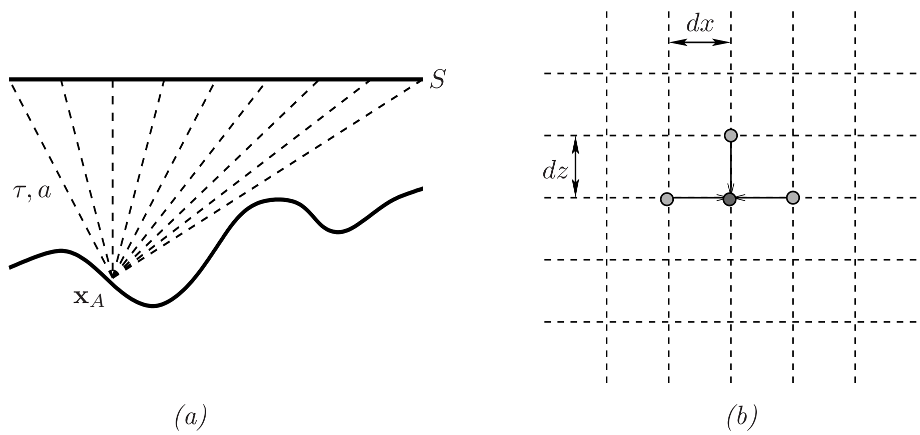

Figure 1.6: *(a) Schematic illustration of the Kirchhoff method. (b) Schematic illustration of the finite difference method.*

gral, which can be derived from the scalar wave equation. By applying this integral to a wavefield, which has been acquired at an arbitrary surface S, the wavefield at any point $\mathbf{x}_A$ lying inside S can be reconstructed. Performing the Kirchhoff integral can be interpreted as calculating a weighted sum of delayed wavefield components of the data acquired at the surface S (see Figure 1.6a). The required amplitude weights a and the time delays τ can be derived from Green's functions describing the wave propagation between the points on S and $\mathbf{x}_A$. These Green's functions are the so-called redatuming operators.
A major advantage of this method is that the wavefield at $\mathbf{x}_A$ can be calculated from measurements along S without the need to construct the wavefield in-between.

■ Phase shift methods

Gazdag [1978] has been the first to introduce the phase shift method. While Kirchhoff summation methods are applied in the space domain, this method is applied in the wavenumber-frequency domain. There, the downward continuation step can be described as a simple multiplication of the wavefield at the acquisition surface with a phase shift factor, the phase shift being defined as the multiplication of the interpolation step Δz in depth direction and the vertical wavenumber k_z. This wavenumber can be derived from the dispersion relation [see for example Claerbout, 1985], and it can be considered constant for small depth intervals where the velocity is constant. An advantage of this method is the ease of implementation and its fast calculation. However, assuming k_z to be constant for the depth interval means that the implementation has to be done in a recursive way in order to handle vertically varying velocities correctly. Furthermore, it is limited to handling small lateral variations of the velocity. To overcome the latter problem, various methods have been developed including the ones of Gazdag and Sguazzero [1984] and Stoffa et al. [1990]. In these so-called split-step methods parts of the computations are performed in the space domain to account for the lateral velocity variations. However, also for these approaches the lateral velocity variations are treated only in an approximate way. A more exact treatment of lateral velocity variations can only be guaranteed if the multiplication of the wavefield in the wavenumber-frequency domain is replaced by a convolution in the space-frequency domain [see for example Holberg, 1988; Blacquiere et al., 1989; Thorbecke and Berkhout, 1994]. In this approach the higher accuracy is paid for by larger computational effort.

■ Finite difference methods

The paper of Claerbout and Doherty [1972] has been the starting point in the development of the theoretically most accurate but computationally most demanding method used for wavefield extrapolation: the finite difference method. For this method, the derivatives of the one-way wave-equation are approximated by finite differences. The finite-difference wave-equation can then be used to expand the input wavefield to any given point in time and space by performing a numerical integration. This is illustrated schematically in Figure 1.6b.

In this method, laterally and vertically varying velocities can be handled. In fact, the complexity of the velocity model that can be treated is only limited by the stepsize between adjacent grid points of the gridded velocity model. If one is willing to invest a lot of computation time and memory, densely sampled grids can be used to describe complex subsurface models with strongly varying velocities and complex boundaries. However, in order to extrapolate a wavefield towards a certain location, all points in-between need to be calculated and stored consecutively. Hence, depending on the chosen grid of the velocity model a vast number of calculations has to be performed per step, and a large number of data has to be stored. The demand in terms of runtime and memory might not pose a serious problem in a 2D situation, but it can certainly restrict the feasibility of this method with respect to the 3D situation.

Another factor limiting the accuracy of the finite difference method is the chosen implementation. For the implementation an expression for the derivative of the wavefield is needed. As shown by Claerbout [1985], this derivative contains the square root of the differential operator ik_z. However, there is no straightforward finite difference representation of this square-root expression. It can only be implemented if the square root is regarded as a truncated series expansion. Thereby, the truncation of the series expansion introduces errors in the implementation. The more terms are neglected the less accurate the result of the wavefield extrapolation will be. For reasons of computational efficiency, often only the low-order terms are used comprising either one, two, three or four terms of the series expansions. These equations are often referred to as the 5°-, 15°-, 45°- and 60°-equation, respectively.

Another, computationally very demanding, technique that also uses a finite difference method is reverse time migration. There, the two-way wave-equation is used, which enables a stable migration even of steep dips [see McMechan, 1982, 1983; Chang and McMechan, 1989, 1990]. Because of the high computation costs, only in the last few years the application of reverse time migration has become feasible for practical applications [see Farmer et al., 2006]. It can handle 90° dips, turning rays, multi-pathing and anisotropy and therefore overcomes the limitations of other migration methods.

Comparison of the different methods

A very detailed comparison of these three methods has been presented by Bevc [1995]. He actually computed an upward and a downward continuation of synthetic 2D pre-stack data. The data set being used has been modeled for a subsurface including a syncline/anticline interface and two point diffractors placed directly above and below that interface; the acquisition surface is a cosine shaped surface. From there, the data are upward continued toward a flat surface just above the highest point of the acquisition surface, the downward continuation is applied to the upward continued data set back to the original acquisition surface. For the implementation of the Kirchhoff method the near-field term was included, and it was applied in one step in the time domain. For the implementation of the phase shift method Gazdag's approach was used, and the finite difference method was implemented utilizing the 45°-equation for the calculation of the wavenumber k_z.
For both, the upward and the downward continuation, the Kirchhoff summation approach produces the best results with the least artifacts while being the most effective method. Besides this, it is shown that the efficiency can be further increased by neglecting the near-field part while the accuracy is not diminished in most situations. Not only the results of the up- and downward continuation have been compared but they also served as input for a migration whose results have been taken into consideration as well.
Bevc [1995] names the need for a regular computational grid as a major disadvantage for both the phase shift and the finite difference method. Furthermore, he stresses that, unlike these methods, the Kirchhoff method can handle irregular acquisition grids as long as no operator or data aliasing occurs [see for example Biondi, 2001], and it handles the acquisition topography accurately and not in an approximated version. Consequently, the Kirchhoff summation approach is considered to be the most appropriate method to perform redatuming.
The Kirchhoff summation method indeed has been widely used for redatuming. It has been applied successfully to correct for an irregular datum [see for example Shtivelman and Canning, 1988; Bevc, 1997] and for complex subsurface structures [Berryhill, 1986; Larkin and Levander, 1996; Hindriks and Verschuur, 2001; Kelamis et al., 2002], and for subbasalt imaging [see Martini and Bean, 2002a,b].

1.3 Shortcomings of the conventional redatuming methods with respect to sparse 3D data

Redatuming employing the Kirchhoff summation method has only been applied to 2D data. The two other methods have, to the best of our knowledge, not been used to perform redatuming, but have been used in 2D migration schemes. However, nowadays there is a growing demand for 3D redatuming over complex overburdens and from irregular acquisition surfaces because the amount of 3D data increases. Consequently, the suitability of the three different methods and their limitations with respect to the task of redatuming of 3D data need to be examined carefully.

1.3.1 Problem I – sparse input data sets

A problem that we face in the 3D situation that has not been an issue for the 2D situation is the need for a sufficiently sampled input data set. In this context, 'sufficiently' can mean different things for the three different methods being considered.

Kirchhoff summation methods

For a successful application of the Kirchhoff summation approach to redatum a 3D pre-stack data set, the amplitude factors and time shifts correcting for the wave propagation in the datum layer need to be known everywhere. Furthermore, a sufficiently dense areal receiver coverage for each source as well as a sufficiently dense areal source coverage for each receiver of the input data set is needed. And while assigning the amplitude factors and time shifts does not pose a problem, the demand for an input data set with a sufficiently dense areal source and receiver coverage at the acquisition surface poses a serious problem.
The amplitude factors and time shifts, constituting the redatuming operators of the Kirchhoff approach, can either be calculated in a model-driven manner from a known velocity model of the datum layer, or they can be estimated from the input data set applying the data-driven Common Focus Point (CFP) technology that has been developed by Berkhout [1997a,b]. In case of a sparsely sampled input data set, this technique needs to be combined with the infill method described by van de Rijzen et al. [2004].
In order to understand the need for a densely sampled input data set, one has to remember that the redatuming process, employing the Kirchhoff summation method, has just been described as performing a weighted sum over all acquired traces to calculate one redatumed trace. As is known from the principles of integration theory, such a summation will only give correct results if the distance between two adjacent points to be summed together is sufficiently small. If the distances between the neighboring points are too large, aliasing artifacts will be produced by the summation, and the achieved result will not resemble the desired result. In the ideal,

densely sampled case, the summation of the corrected traces gives a constructive interference of the contributing traces. The traces which do not contribute interfere destructively, i.e. they cancel each other. However, choosing, or having to deal with a sampling interval that is too large hampers this process. The non-contributing parts will not cancel each other, but they produce artifacts. Furthermore, the amplitudes of the real events will be affected. That means that the output data of a redatuming method utilizing Kirchhoff summation applied to sparse input data will contain artifacts and show incorrect amplitudes. Therefore, the source and receiver coordinates of the acquired traces, which are added together in the redatuming integral, have to have a sufficiently dense sampling. This is generally the case for the densely sampled 2D lines. Unfortunately, conventional 3D acquisition geometries, such as the cross-spread geometry for land acquisition or the marine parallel line geometry, do not provide a dense sampling of all four coordinates describing the source and receiver positions at the surface (see Figure 1.7). Usually, at least one of these coordinates is sparse, meaning that the Kirchhoff summation approach for redatuming cannot be applied to this kind of data unless it is being combined with some sort of data interpolation process.

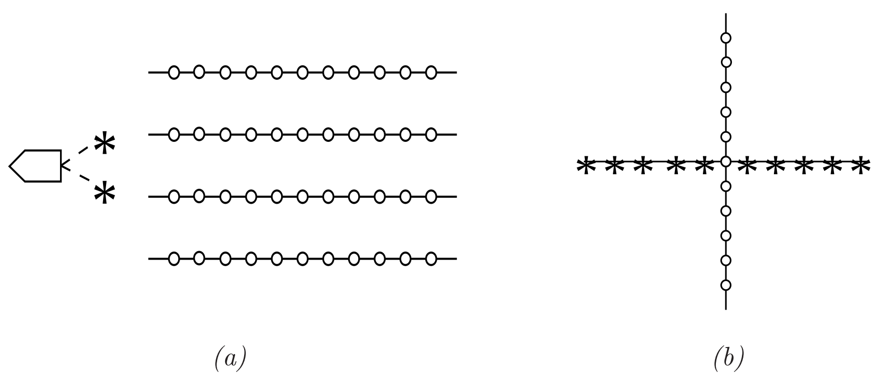

Figure 1.7: *(a) Marine parallel line geometry, and (b) land cross spread geometry.*

Phase shift methods

In order to perform redatuming by applying the phase shift approach to 3D pre-stack data sets, the input data set has to be Fourier-transformed to the wavenumber-frequency domain. Calculating a Fourier transform means, again, the computation of an integral, i.e. the calculation of a weighted sum. Consequently, this method too requires an input data set that has a sufficiently dense areal coverage of the source and the receiver coordinates at the acquisition surface. In addition, the source and receiver coordinates need to be regularly sampled if standard Fourier transforms are

used.
Therefore, the same restrictions apply to this approach as to the Kirchhoff summation approach concerning the density of the data sampling, and, additionally, the requirement of regularly sampled data imposes a further limitation with respect to the applicability to 3D data sets. In reality, a regular sampling of the acquisition surface almost never happens for reasons like streamer feathering for marine data acquisition and obstacles or limited accessibility for land data acquisition. Consequently, the phase shift method for redatuming cannot be applied to 3D pre-stack data as they are acquired in reality unless it is combined with a data interpolation and data regularization step.

Finite difference methods

The equations being used for the finite difference methods expect the data to be acquired on a regular grid. Furthermore, the more complex the subsurface becomes, i.e. the more complex the input data set becomes, the finer the data grid has to be chosen to get correct results. However, this, again, establishes the demand for an input data set which is regularly sampled and exhibits a dense areal coverage of the source and the receiver coordinates. Due to this, the finite difference method for redatuming can also not be applied to 3D pre-stack data as they are acquired in reality unless it is combined with a data interpolation and data regularization step.

1.3.2 Problem II – computational feasibility

It is not only the requirements with respect to the data sampling that restrict the proposed methods in their applicability to realistic 3D situations, but it is also the amount of data which limits the computational feasibility of all three approaches in the 3D situation. First of all, a huge amount of data has to be handled, even if the data set is called sparse with respect to the demands of redatuming. Usually, a data set consists of millions of traces adding up to several terabyte of data. A large number of traces is involved in the calculation of one redatumed trace for all three methods, i.e. data storage and handling are forming a challenge. Secondly, extensive computations have to be performed for all three methods. In order to perform redatuming applying the Kirchhoff summation method, a four-dimensional integral needs to be computed for each frequency component or output time sample. For one redatumed trace using the phase shift method a number of five-dimensional integrals need to be calculated successively. Here, already the calculation of these integral expression is, at the least, computationally demanding and might not even be feasible. In case the finite difference approach is chosen to perform the redatuming, no integral needs to be computed. Instead, the wavefield, which is known on certain grid points, is used to extrapolate the wavefield successively towards other grid points until the new datum is reached. For every calculation step a number of data points is used and needs to be stored. Depending on the grid size considered, a large number of calculation steps needs to be performed and a huge amount of data has to be stored. This can also form a task which is, at least, computationally demanding and might not be feasible.

1.3.3 Conclusions on the conventional redatuming methods

Considering the observations made above concerning the applicability of the existing redatuming methods to a 3D input data set as it is produced from conventionally used acquisition geometries, it can be concluded that none of the methods is particularly suitable for this problem. A successful application of all of these methods requires a sufficiently dense areal source and receiver coverage at the acquisition surface. This generally is not available. In addition, the finite difference and the phase shift approach both require the input data set to be regularly sampled, which is almost impossible to acquire in practice. Therefore, the existing methods cannot be applied to a 3D data set from a conventionally used acquisition geometry without an additional data regularization and data interpolation step. Furthermore, all three methods can be called computationally demanding and might not even be feasible.

1.4 Research objectives

The aim of my research, which will be documented in this thesis, is to develop and to test a new redatuming method, which is applicable to sparse 3D data acquired with conventionally used 3D acquisition geometries. The results of this new method should be comparable to the results the application of the Kirchhoff summation method would have delivered if applied to a densely sampled input data set. The proposed method should be computationally feasible. Therefore, for the new approach it is aimed to reduce the amount of data needed to calculate one output sample.

In this thesis, a new approach to redatuming is presented, that satisfies these requirements. The choice has been made to formulate the redatuming process in terms of a data mapping problem. In order to do this, certain assumptions about the velocity model below the new datum level need to be made, which is different from the conventional methods. However, in this new approach the number of traces involved in the calculation of one output sample is reduced considerably, and the dimensionality of the integral expression describing the process is reduced. Here, only a 2D integral needs to be calculated to compute one output sample as opposed to a 4D integral for the conventional 3D redatuming approach.

The data mapping approach is generally applicable to all sorts of input data sets, but, as already mentioned, the primary interest of this work is to develop an approach applicable to data sets that do not have a dense areal coverage of sources and receivers at the acquisition surface. For the approach too it can still happen that the required traces have not been acquired, even if it uses considerably less traces per output sample. In case this happens, the data mapping approach needs to be combined with some sort of data infill procedure. Fortunately, certain information, which can be obtained from the assumptions of the medium below the new datum level, can be used to apply the infill method developed by van de Rijzen et al. [2004]. Hence, by combining the data mapping approach with the data infill method, the new approach to redatuming becomes applicable to 3D data sets from conventionally used acquisition geometries.

1.5 Outline of the thesis

A schematic outline of the thesis is presented in Figure 1.8. After an introduction to the seismic method in general and redatuming in particular (**Chapter 1**), the methodology of the proposed redatuming approach is described conceptually in **Chapter 2**. **Chapter 3** concentrates on the theoretical derivation and implementation of the data mapping approach to redatuming. In **Chapter 4** this newly developed redatuming approach is evaluated on fully sampled synthetic and real 2D data sets. The series of tests being performed has to ensure that the developed method produces kinematically and dynamically correct results.
Chapter 5 describes the infill step, which will be combined with the new redatuming approach to handle sparsely sampled 3D data sets. This infill step is performed by applying a well-established method, which will be described here. Furthermore, the abilities and limitations are further assessed by means of tests performed for synthetic 3D data sets and on a 3D data set, which has been acquired in a physical modeling facility (see **Chapter 6**). First, I investigate on fully sampled data whether the data mapping approach to redatuming has been extended correctly to the 3D situation. Thereafter, the redatuming of sparsely sampled data by means of the data mapping approach to redatuming combined with the proposed infill is tested.
Chapter 7 presents additional modules of the presented redatuming method. It discusses the implementation of the method for PS-data and, furthermore, presents a modification of the methodology such that it can be used for the prediction of datum layer-related multiples as they appear in the redatumed data. At last, in **Chapter 8**, conclusions will be drawn from the results of the previous chapters and recommendations for future research will be given.
Additionally, certain aspects that have not been addressed explicitly but are important are discussed more thoroughly in the Appendices. **Appendix A, Appendix B** and **Appendix C** are related to the theory and the implementation of the data mapping approach to redatuming. **Appendix A** presents the derivation of the expression for the redatuming of 3D pre-stack data using the Kirchhoff summation method. **Appendix B** is dedicated to the estimation of ray parameters from redatuming operators, and **Appendix C** explains the estimation of the eigenvalues for

the Hessian matrix of the corrected traveltime function. **Appendix D** is related to the implementation of the infill approach the redatuming is combined with for sparsely sampled input data sets.

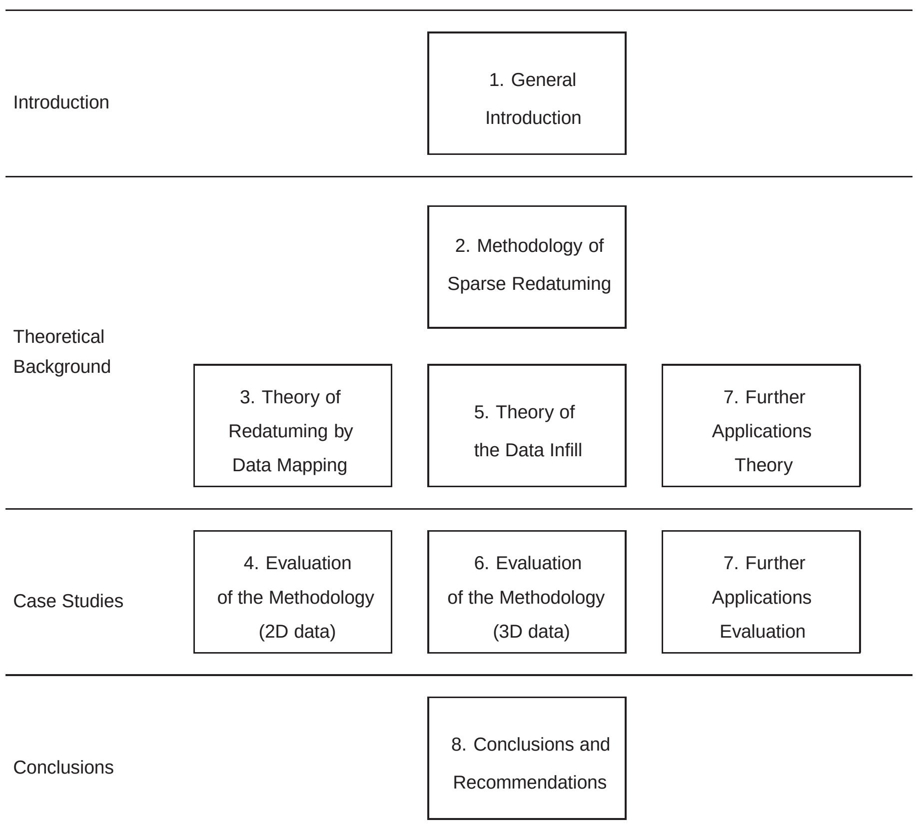

Figure 1.8: *Schematic outline of the thesis.*

2

Methodology of the redatuming of sparse 3D seismic data

Überall geht ein frühes Ahnen
dem späteren Wissen voraus.

Alexander von Humboldt (1769 - 1859)

In this chapter, a new approach to redatuming is presented for which the amount of data needed to calculate one output sample is reduced with respect to the conventionally used methods. We have chosen to formulate the redatuming process in terms of a data mapping problem along the lines of Bleistein and Jaramillo [2000]. They define Kirchhoff data mapping (KDM) as a procedure which transforms data with a certain source/receiver configuration belonging to a certain background model of the earth to another data set with a different source/receiver configuration and background earth model. The normal move-out (NMO) correction, the dip move-out (DMO) correction, the azimuthal move-out (AMO) method and redatuming can be thought of as special cases of this general concept. For the NMO, DMO and AMO correction, the background earth model being used is generally very simple. A homogeneous medium is assumed as background model for every time sample that needs to be calculated with the velocity being the stacking velocity related to the time sample considered. Then, in the NMO correction and DMO correction, all trace offsets are changed to be zero offset. The AMO method can be described as a generalization of these two procedures. Here, besides the offset, also the azimuth of the traces is changed. In comparison to this, the most important aim of redatuming is certainly not to change the offset and the azimuth of a certain input data set, but to produce an output data set which is referenced to a new datum level. However, offset and azimuth changes can be incorporated as well.

Bleistein and Jaramillo [2000] derive a general formula considering a single reflector, multiple and multi-pathing free seismic data set. The formula they derive is a multidimensional integral equation with the integration parameters being the source and receiver coordinates of the input data set and the the so-called earth model parameters, which basically describe the single reflector and which are influenced by the chosen background earth model. This integration over the physical model space needs to be solved analytically in order to derive formulas describing NMO, DMO, AMO and redatuming. In their paper they note that the application of the KDM formalism has already successfully been used to derive the formulation of 2.5D DMO. For redatuming, this has not been accomplished yet.

To develop the new redatuming method, the general thought of KDM is being adopted here, i.e. a simplified background model of the earth is assumed in order to map an input data set referenced to the acquisition surface to an output data set referenced to the new datum level. However, the derivation of the formalism follows a different, slightly simpler line of thought. In the end, the proposed approach meets the requirements. The formalism describing the data mapping approach to redatuming (DMR) can be interpreted as a simplified version of Kirchhoff summation redatuming method (KSR), where one of the 2D integrals over the acquisition coordinates can be solved analytically. Furthermore, fewer traces of the input data set are involved in the calculation of one output sample because the knowledge of the velocity model is utilized to pre-select potentially contributing traces of the input data set.

The assumptions about the background earth model, which are made for this new approach, do not only provide the opportunity to develop a new, efficient approach for redatuming. At the same time, the information of the background model can also be used to combine the redatuming method with a trace infill method such that it becomes applicable to sparse 3D input data sets.

2.1 The background earth model

It has just been discussed that all KDM techniques require a background earth model. With respect to the application of KDM to redatuming, a distinction has to be made between the datum layer and the medium below the datum.

2.1.1 The datum layer

As for the conventional KSR method, redatuming operators will be used to account for the one-way wave-propagation between the sources or the receivers at the acquisition surface and at the new datum level. These redatuming operators represent Green's functions. In general, there are two possible ways to derive the operators: a data-driven or a model-driven way.

In the data-driven way, the operators are extracted from the input data set applying the Common Focus Point (CFP) technology developed by Berkhout [1997a,b]. With this technology the operators can be estimated correctly from the input data set without requiring an accurate velocity model of the datum layer. However, the estimation procedure demands the input data set to be densely sampled as well. Hence, if the redatuming operators are to be extracted from a sparse input data set, this process is also combined with a trace infill method such as the method described by van de Rijzen et al. [2004].

For the model-driven estimation of the redatuming operators, an accurate velocity model of the datum layer is needed [see for example Bevc, 1997]. This model is then used to calculate the operators either by ray tracing or by applying some sort of wavefield modeling method.

In the end, the redatuming operators contain amplitude factors and time shifts, describing the wave propagation in the datum layer, no matter whether they are computed in a data-driven or in a model-driven manner.

2.1.2 The medium below the new datum

For the conventional KSR approach information about the medium below the new datum level is not required. The considered redatumed traces are estimated by the application of two weighted summations (Fresnel stacks) to the input data set, which has been corrected for the wave propagation in the datum layer. One Fresnel stack is applied to estimate the contributing receivers and the second one is applied to identify the contributing sources. However, for the DMR approach, which is described in this chapter, it is aimed at utilizing a background model of the earth below the new datum level to map the input data set referenced to the acquisition surface to the desired output data set referenced to the new datum level. A crucial point, with respect to this, is the definition of the assumed background model.

This model should be as simple as possible. If a very complex model for the medium below the datum level was needed to get correct results, the whole redatuming process would become superfluous. Besides this, the background medium should not include any restrictions of the shape and the position of the potential reflectors. It is intended to construct a surface of all possible reflection points and, thereby, account for all possible dips and azimuths of the subsurface reflectors. In other words, a reasonable estimate of the velocity associated with the given reflection time t_{red} of the considered time sample of the redatumed trace is needed, but no assumptions will be made on the shape of the potential reflector. It is assumed, and will be demonstrated by the results, that a simple dip independent root mean square (RMS) velocity field is accurate enough to serve this purpose. This assumption implies the following:

- a constant velocity describes the medium below the new datum for the calculation of one output sample,
- the velocity being used changes for every output sample,
- the possible reflection points belonging to the considered time sample lie on an ellipsoidal surface, a so-called isochrone[1] [see Staude, 1882].

2.2 The locus

The information gained from the isochrones can be employed to identify time samples in the input data set, which are possibly contributing to the considered time sample of the redatumed trace; that is, a locus[2] of possibly contributing time samples can be created in the input data set. Such a locus will be a 1D line in source and receiver coordinate space for the redatuming of a 2D input data set and a 2D surface for the redatuming of a 3D input data set. It is comparable to the DMO surface [see for example Hale, 1991] and the AMO saddle [see for example Biondi et al., 1998; Biondi, 2006]. The DMO surface can be derived from the DMO ellipse/ellipsoid, the AMO saddled is derived by cascading the formula of DMO and inverse DMO.
The estimation of the locus for the DMR approach is carried out straightforwardly (see Figure 2.1). For every possible reflection point on the considered isochrone ray tracing is performed through the redatumed source and receiver location towards the acquisition surface. Thereby, the part below the new datum level is simple. Straight rays can be employed here since the medium below the new datum level is assumed to be homogeneous. The transition at the boundary of the medium below the datum layer and the medium above the datum layer is conducted by applying Snell's law, i.e. the ray parameter ϱ is kept constant. Finally, the raypaths are continued upwards through the datum layer towards the acquisition surface. This is done by extracting information about the ray parameter from the traveltimes of the redatuming operators. The theoretical description of this concept will be given in Chapter 3. By doing this, the true raypath in the datum layer, which will be bending or crooked depending on the structure of the datum layer, is taken into account.

[1]Isochrone: an imaginary line or a line on a chart connecting points at which an event occurs simultaneously or which represents the same time or time difference [see Merriam Webster].

[2]Locus: The curve or other figure constituted by all the points which satisfy a particular equation of relation between coordinates, or generated by a point, line, or surface moving in accordance with any mathematically defined conditions [see Oxford Dictionary of English].

A similar approach to redatuming has been chosen by Alkhalifah and Bagaini [2004, 2006] using the so-called topographic datuming operator (TDO). For the derivation of this operator a constant velocity is assumed for the medium below the new datum level. However, in contrast to the approach presented here, they decided to simplify the background medium of the datum layer as well. In their approach the datum layer is assumed to be laterally varying with a locally constant velocity belonging to the considered source and receiver position. This velocity is calculated, for example, from refraction statics. As a consequence, the rays in the datum layer, which are used to identify possibly contributing traces from the input data set, become straight rays. Alkhalifah and Bagaini [2004, 2006] also show that, if the velocity below the new datum layer is set to infinity, static corrections can be interpreted as a limit of their approach. In that case, the rays in the datum layer are vertical.

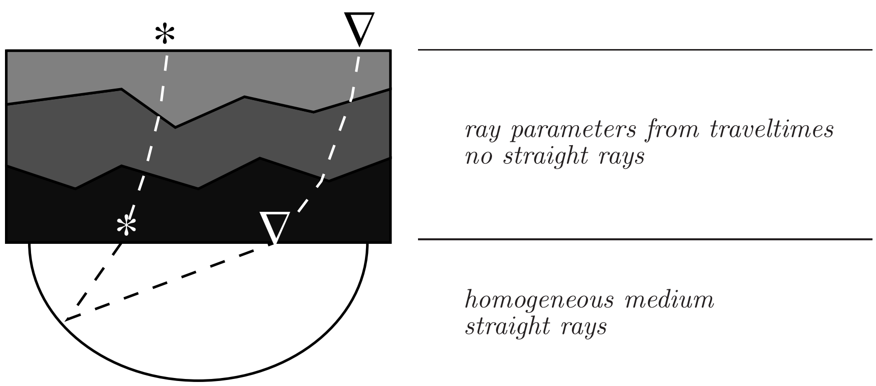

Figure 2.1: *Raypaths for one source/receiver pair at the surface, which is possibly contributing to the considered output sample of the redatumed trace.*

2.3 The weighted stack along the locus

As previously described, for every point on the isochrone one source/receiver pair at the acquisition surface is selected, which belongs to the specular reflection at this point. The two-way traveltime of the sample in this trace, that is needed in the isochrone stack, can be determined. In this way, a locus of possibly contributing time samples in the input data set is determined. Once this locus is known, a weighted stack has to be calculated along it, to compute the time sample considered of the redatumed trace. This step is similar to the stack along the DMO surface or the stack along the AMO saddle applied in the other KDM techniques. It is important to note that the locus is a 2D surface for 3D redatuming and a 1D line for 2D redatuming [see Bagaini and Alkhalifah, 2003]. Hence, for the calculation of

a redatumed time sample by means of the DMR approach only a 2D integral needs to be computed [see Tegtmeier et al., 2004]. This is a considerable reduction of the computational effort compared to the KSR approach, where a 4D integral has to be computed for the redatuming of 3D input data.
The derivation of the correct weights applied in the stack of the DMR approach is a challenge. In order to judge whether the weights have been chosen correctly a desired outcome of the proposed redatuming approach needs to be defined. For this purpose, the result of the conventional Kirchhoff summation method applied to an input data set with a sufficiently dense areal coverage of sources and receivers at the acquisition surface has been selected. The theoretical derivation of the weights and the derivation of the formalism describing this new redatuming approach are being described in Chapter 3.

2.4 The trace infill

The DMR method is generally applicable to any kind of input data sets. However, the focus of this research is the application to input data sets acquired with conventional 3D acquisition geometries. As already mentioned, these data sets are usually sparsely sampled in at least one of the four coordinates describing the source and receiver positions at the acquisition surface. It needs to be examined whether these data sets are to be considered sparse with respect to the requirements of the DMR approach. If these data sets are, indeed, sparse, all problems related to the sparseness need to be identified and possible solutions have to be evaluated.
The requirement of the new approach with respect to the sampling of the input data set is that the locus needs to be sampled sufficiently densely. A problem most likely to occur for sparsely sampled input data is that a trace, which has been pre-selected along the locus, does not exist in the input data set. If, in this case, the weighted stack is applied without taking this into account, the result will be incorrect.
To prevent this from happening, the new redatuming approach is combined with a trace infill step, which will be performed prior to the application of the weighted stack along the locus. As already mentioned in Chapter 1, the trace infill method described by van de Rijzen et al. [2004] has been selected, because this method is particularly well suited for the given situation. However, the discussion of the reasons to prefer this method to other available methods and the description of the methodology and theory behind it are beyond the scope of this chapter. A detailed discussion on this subject is provided in Chapter 5.

2.5 The data mapping approach – step-by-step

To summarize the previous sections a flowchart is presented in Figure 2.2. It illustrates the different steps that have to be performed successively to calculate one output sample of a redatumed trace. As one can see, firstly, the isochrone describing the positions of all possible reflection points in the subsurface below the new datum level needs to be determined. Thereafter, this information is translated into a locus, which indicates all time samples on certain traces referenced to the acquisition surface, which are possibly contributing to the considered output sample. Thirdly, it needs to be checked whether all traces along the locus have been acquired and missing traces need to be filled in. In the end, the weighted stack along the locus is applied. This procedure has to be repeated for every output sample of all desired output source/receiver combinations, because the isochrone of possible reflection points will be different for every output sample.

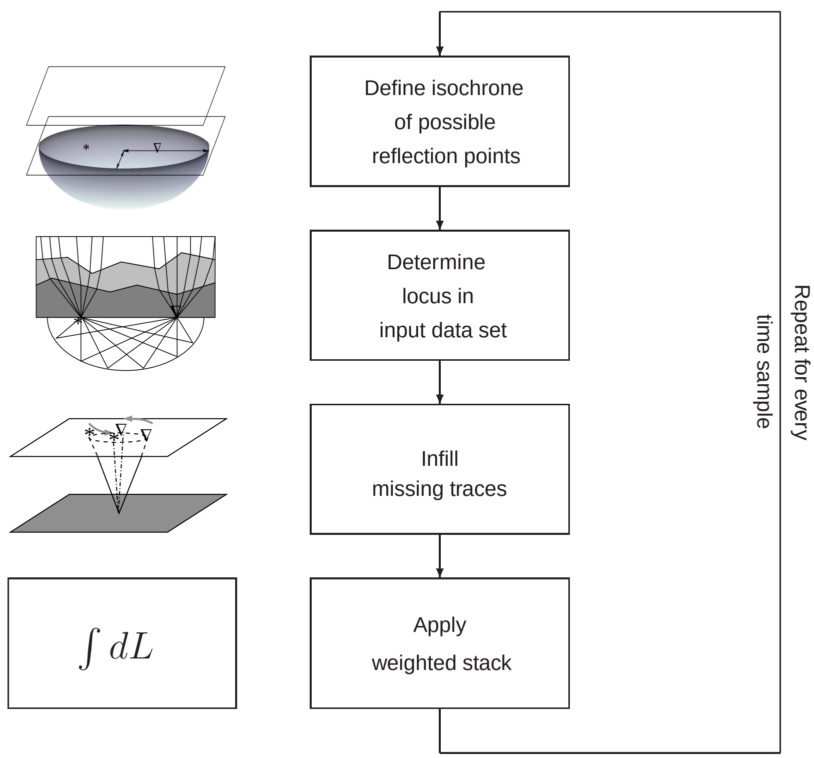

Figure 2.2: *Flowchart of the data mapping approach to redatuming.*

2.6 Influence of the velocity model below the new datum

It certainly needs to be examined how accurately the velocity model below the new datum has to be known to get correct results from the new redatuming approach. A first quick observation is that there is no reflector dip information required in the model, because all possible dips are represented in the ellipsoidal isochrone and all points of the ellipsoid are included in the isochrone stack. Hence, only velocities are needed. The following simple argument tells why using a simple RMS velocity field probably is sufficient.

As illustrated in Figure 2.3, any event arriving at the redatumed receiver can approximately be characterized by three parameters: the arrival time, the emergence angle and the radius of curvature of the wavefront [see Hubral, 1983]. The redatuming procedure outlined above is carried out for every time t_{red} of the redatumed trace; hence, all possible arrival times are covered.

For every arrival time, the ellipsoid assures that all possible emergence angles are covered. So, the only parameter that is still missing is the radius of curvature of the wavefront. This radius is actually directly related to the RMS velocity of the medium for that particular output time.

Conceptually, redatuming is migration to an image point and demigration to the new datum. In this view, the datum layer is traversed only once, whereas the medium below the new datum is traversed twice, in opposite directions. It looks very plausible to assume that inaccuracies in the medium below the new datum cancel out, therefore. The final proof of the concept will be given by applying the new redatuming approach assuming different velocity models for the medium below the new datum. The results, which are presented in Chapter 4, show that the dependency of the redatumed result on the assumed velocity model is, indeed, weak, and that it is sufficient to use simple RMS velocity fields.

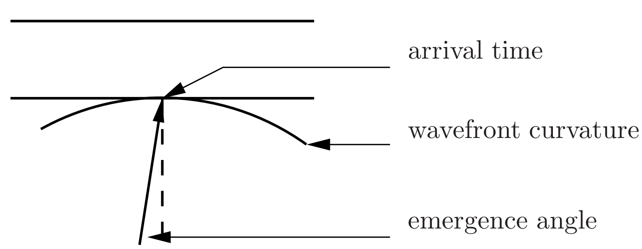

Figure 2.3: *Features of an event occurring at a receiver at the new datum level.*

2.7 Classification of the DMR method

In this chapter the new DMR methodology has been described. This new approach can be classified as a data mapping technique similar to DMO, AMO, TDO and, as the most simplified version of data mapping, statics. In Table 2.1, the most distinct features of these approaches are compared. These features are the geometry and reference surface of the output data set, the characteristics of the datum layer, if applicable, and the characteristics of the medium below the reference surface.
On the one hand, the DMR approach converges to the AMO method if the thickness of the datum layer converges to zero and, furthermore, to the DMO method if, additionally, the azimuths are kept constant. On the other hand, the DMR method converges to the TDO redatuming approach if the velocity of the datum layer is assumed vertically homogeneous, and it even converges to the conventional approach of static corrections if, additionally, the velocity of the medium below the reference surface is assumed to be infinite; i.e. the velocity in the datum layer is much lower than the velocity below the datum.

		DMO	AMO	DMR	TDO	Statics
Survey design (Output)	Acquisition geometry	zero offset	arbitrary	arbitrary	arbitrary	as input
	Reference surface	acquisition surface	acquisition surface	new datum	new datum	new datum
Datum layer	Thickness	0 m	0 m	$>$ 0 m	$>$ 0 m	$>$ 0 m
	Complexity			complex	vertically constant	vertically constant
Medium below reference surface		RMS velocities	RMS velocities	RMS velocities	RMS velocities	$v = \infty$

Table 2.1: *Classification of the DMR method with respect to other well-known methods.*

3

Theory of the data mapping approach to redatuming

Es gibt nichts Praktischeres
als eine gute Theorie.

Immanuel Kant (1724 - 1804)

In this chapter the theory underlying the data mapping approach to redatuming (DMR) is derived, which includes the steps 1, 2 and 4 of the flowchart presented in Figure 2.2. Firstly, it is described how a-priori knowledge of a velocity model of the medium below the datum level is translated into an isochrone that defines all possible reflection points belonging to the output time sample considered (step 1, see Section 3.1). After that, the transformation of this information into the locus of all possibly contributing time samples in the input data set is explained (step 2, see Section 3.2). Thereafter, the integral equation describing the weighted stack along this locus is formulated (step 4, see Section 3.3). With respect to this, the derivation of the correct weighting factors is of particular importance (see Section 3.4).
Furthermore, the assumptions of the DMR approach are listed, and its limitations and opportunities are specified (see Section 3.5). Note, that step 3 of the scheme presented in Figure 2.2, the infill procedure, is described in Chapter 5.

3.1 Definition of the reflection point positions

For the determination of the isochrone of all possible reflection points it is helpful to consider its definition, which is illustrated in Figure 3.1:

$$\{(x_A, y_A, z_A) \,|\, t_{red} = t_r + t_s\} \,. \tag{3.1.1}$$

This isochrone indicates a set of points $\mathbf{x}_A$ in the subsurface where a wave, transmitted by the redatumed source positioned at $\tilde{\mathbf{x}}_s$ at time $t = 0$, and received at the redatumed receiver position $\tilde{\mathbf{x}}_r$ at time $t = t_{red}$, has been reflected. t_s and t_r are the traveltimes from the redatumed source to $\mathbf{x}_A$, and from $\mathbf{x}_A$ to the redatumed receiver, respectively. Every point on this isochrone represents a potential specular reflection point.

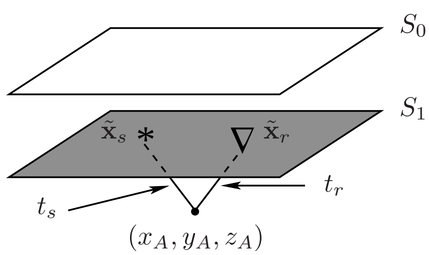

Figure 3.1: *Illustration of the definition of a possible reflection point below the new datum.*

It is impossible to determine the positions of these potential reflection points without any knowledge of the medium below the new datum.
As already mentioned in the previous chapter, it is intended to use a simple dip independent RMS velocity field for this purpose. In practice, the desired RMS velocity field is approximated by redatumed stacking velocities. These redatumed stacking velocities are calculated from conventional stacking velocities, which can be retrieved from the input data set by standard velocity picking. To reference the velocities to the new datum level, they are transformed to interval velocities applying the formula published by Dix [1955]. Thereafter, the layers of the datum layer are removed and, finally, the velocities are inverse transformed to the desired redatumed stacking velocities v_{NMO}.
Once the redatumed stacking velocity $v_2 = v_{NMO}(\tilde{\mathbf{x}}_s, \tilde{\mathbf{x}}_r, t_{red})$, related to the midpoint of $(\tilde{\mathbf{x}}_s, \tilde{\mathbf{x}}_r)$, for the considered time sample is known, the ellipsoidal isochrone can easily be derived. It is defined by its two focal points $\tilde{\mathbf{x}}_s$ and $\tilde{\mathbf{x}}_r$ and by the two parameters a_{ell} and b_{ell} describing the axes of the ellipsoid (see Figure 3.2a). These

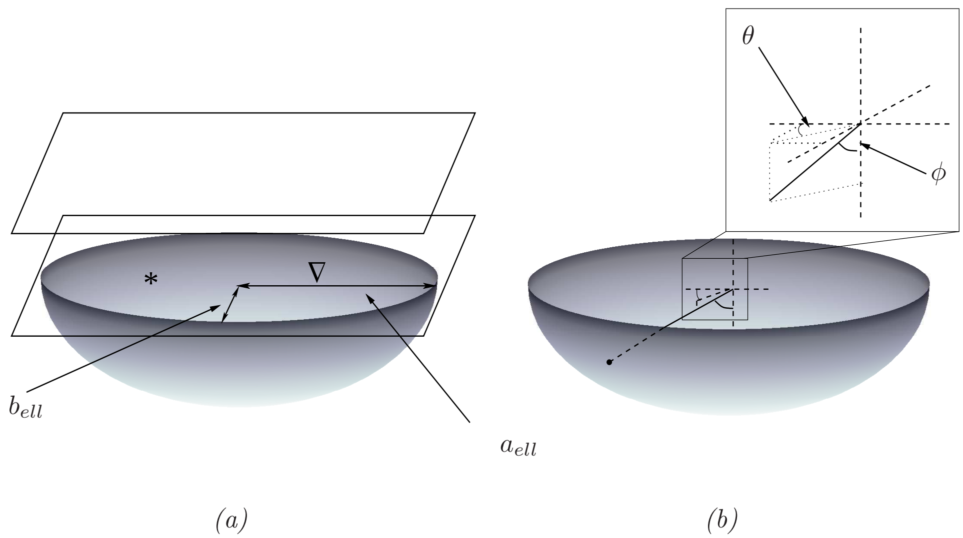

Figure 3.2: *(a) The parameters a_{ell} and b_{ell} describing an ellipsoid. (b) The azimuth θ and polar angle ϕ of a point on the ellipsoid.*

two values can be calculated as follows:

$$a_{ell} = \frac{v_2 t_{red}}{2}, \tag{3.1.2}$$

$$b_{ell} = \sqrt{a_{ell}^2 - \frac{\|(\tilde{\mathbf{x}}_r - \tilde{\mathbf{x}}_s)\|^2}{4}}. \tag{3.1.3}$$

Here, $\|\cdot\|$ indicates the L_2-norm of a vector.
With a_{ell} and b_{ell} being known, the coordinates of the points along the isochrone can be derived. An appropriate sampling of the isochrone surface has to be defined. It has been mentioned earlier that all possible dips of the potential reflector need to be considered; i.e, the sampling of the isochrone should be chosen in such a way that the local dip of selected points on the isochrone in the x-direction δ_x and the local dip δ_y in the y-direction are both equidistantly sampled.
The azimuth θ and polar angle ϕ of the possible reflection point on the ellipsoidal isochrone can be calculated for every (δ_x, δ_y)-pair as:

$$\theta = \arctan\left(\frac{b_{ell}\tan\delta_y}{a_{ell}\tan\delta_x}\right), \tag{3.1.4}$$

$$\phi = \arctan\left(\frac{\sin\theta}{\tan\delta_y}\right), \tag{3.1.5}$$

with $\delta_x \in [-\pi, \pi]$ and $\delta_y \in [-\pi, \pi]$. An illustration of these angles is presented in Figure 3.2b.
Having derived the angles, the coordinates $\mathbf{x}_{iso} = (x_{iso}, y_{iso}, z_{iso})$ of the reflection points along the isochrone a can be determined from the parametric equations of an ellipsoid:

$$x_{iso} = \frac{\tilde{x}_s - \tilde{x}_r}{2} + a_{ell}\cos\theta\cos\phi, \tag{3.1.6}$$

$$y_{iso} = \frac{\tilde{y}_s - \tilde{y}_r}{2} + a_{ell}\sin\theta\cos\phi, \tag{3.1.7}$$

$$z_{iso} = b_{ell}\sin\phi, \tag{3.1.8}$$

with $\tilde{x}_s$ and $\tilde{x}_r$ being the x-coordinates of $\tilde{\mathbf{x}}_s$ and $\tilde{\mathbf{x}}_r$, respectively, and with $\tilde{y}_s$ and $\tilde{y}_r$ being the y-coordinates of $\tilde{\mathbf{x}}_s$ and $\tilde{\mathbf{x}}_r$, respectively.
With respect to Equations 3.1.6 – 3.1.8, two things need to be noted:

[1] The equations are only valid if the redatumed source and the redatumed receiver are positioned at the same depth level, i.e. if $\tilde{z}_s = \tilde{z}_r$. This is approximately true for all examples treated in this thesis. However, if the approach is to be applied in a situation with a none flat datum, with the redatumed sources and receivers at different depth levels, the equations have to be modified accordingly.

[2] The x-axis of the coordinate system being used is oriented in direction of the connecting line between $\tilde{\mathbf{x}}_s$ and $\tilde{\mathbf{x}}_r$.

3.2 Pre-selection of possibly contributing time samples

The information about the isochrone belonging to a certain output time sample is used to determine the locus of corresponding time samples in the input data set in the following way:

[1] The ray parameters $\boldsymbol{\varrho}_s$, consisting of the components $\varrho_{x,s}$ and $\varrho_{y,s}$, belonging to the rays between every possible reflection point and the source position at the new datum are calculated:

$$\varrho_{x,s} = \frac{\sin\left[\arctan\left(\frac{x_{iso}-\tilde{x}_s}{z_{iso}}\right)\right]}{v_2}, \tag{3.2.9}$$

$$\varrho_{y,s} = \frac{\sin\left[\arctan\left(\frac{y_{iso}-\tilde{y}_s}{z_{iso}}\right)\right]}{v_2}. \tag{3.2.10}$$

[2] The source positions $\mathbf{x}_s$ at the surface belonging to a certain reflection point have to be determined utilizing $\varrho_{x,s}$ and $\varrho_{y,s}$. According to Snell's law the ray parameter of a wave traveling through a medium is constant along the raypath. Hence, the required source positions $\mathbf{x}_s$ can be determined by selecting the positions at the acquisition surface, which are connected to the source position at the new datum by rays with the estimated ray parameters $\varrho_{x,s}$ and $\varrho_{y,s}$. Therefor, the ray parameters of the rays inside the datum layer can be extracted from the traveltimes of the redatuming operators, which are assumed to be known (see Appendix B). A selected ray and source position at the surface are presented in Figure 3.3a.

[3] The ray parameters $\boldsymbol{\varrho}_r$, consisting of the components $\varrho_{x,r}$ and $\varrho_{y,r}$, belonging to the rays between the reflection points and the receiver position at the new datum are calculated in a similar way:

$$\varrho_{x,r} = \frac{\sin\left[\arctan\left(\frac{x_{iso}-\tilde{x}_r}{z_{iso}}\right)\right]}{v_2}, \tag{3.2.11}$$

$$\varrho_{y,r} = \frac{\sin\left[\arctan\left(\frac{y_{iso}-\tilde{y}_r}{z_{iso}}\right)\right]}{v_2}. \tag{3.2.12}$$

[4] The receiver positions $\mathbf{x}_r$ at the surface belonging to these parameters and reflection points, respectively, are determined, again, using the redatuming operators above the new datum (see Figure 3.3b).

[5] The traces belonging to the source/receiver pairs $(\mathbf{x}_s(\delta_x,\delta_y), \mathbf{x}_r(\delta_x,\delta_y))$ thus obtained contain time samples which are possibly contributing to the considered output sample. These contributing time samples $t_L(\mathbf{x}_s(\delta_x,\delta_y), \mathbf{x}_r(\delta_x,\delta_y))$ can easily be determined by calculating the traveltime t_{ray} along the rays belonging to the selected source/receiver pairs.

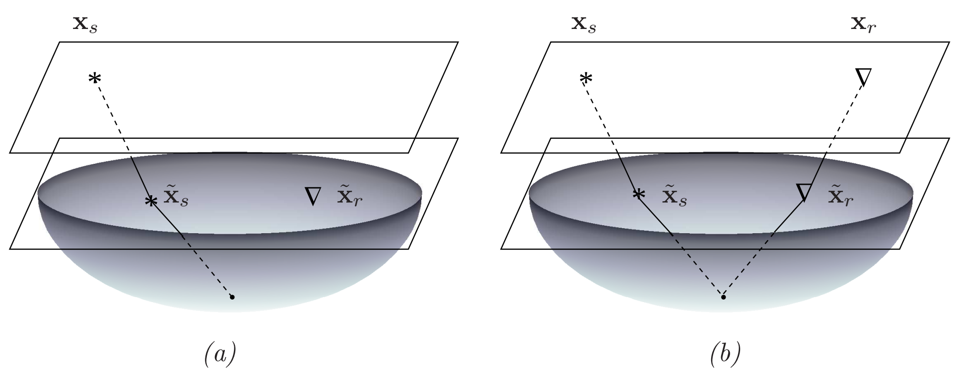

Figure 3.3: *Calculation of one source/receiver pair at the surface describing a trace which is possibly contributing to the time sample t_{red}. (a) The surface position of the source is determined using the information about $\boldsymbol{\varrho}_s$. (b) The surface position of the receiver is determined using the information about $\boldsymbol{\varrho}_r$.*

In the end, all possibly contributing time samples on the pre-selected traces form the locus:

$$\left\{ t_L(\mathbf{x}_s(\delta_x, \delta_y), \mathbf{x}_r(\delta_x, \delta_y)) \;\middle|\; \delta_x, \delta_y \in [-90°, 90°] \right\}. \tag{3.2.13}$$

It is important to note that $\mathbf{x}_s$ and $\mathbf{x}_r$ are dependent on each other. They are connected via a point on the isochrone described by (δ_x, δ_y). Hence, $\mathbf{x}_s$ can be expressed as a function of $\mathbf{x}_r$, and likewise, $\mathbf{x}_r$ can be expressed as a function of $\mathbf{x}_s$. As a consequence, t_L can also be described as a function of $\mathbf{x}_s$:

$$t_L = t_L(\mathbf{x}_s). \tag{3.2.14}$$

Unlike for the DMO and AMO method, it is impossible to find an analytic solution describing the locus as a function of the either (δ_x, δ_y) or as a function of $\mathbf{x}_s$ or $\mathbf{x}_r$. The assumption of non-straight rays inside the datum layer makes this impossible. Note, that no restrictions are imposed regarding the number of true reflectors that can be involved per time sample. The DMR method simply calculates the stationary phase contribution from the selected time samples. If there are more than one true reflectors being tangent to the considered isochrone, as in case of multi-valuedness, they will all produce a stationary phase contribution and will all be handled correctly.

3.3 Derivation of the DMR integral equation

The most straightforward formulation of a weighted stack for the DMR approach is:

$$p(\tilde{\mathbf{x}}_s, \tilde{\mathbf{x}}_r, t_{red}) = \int_{S_0} a_w(\mathbf{x}_s)\, p[\mathbf{x}_s, \mathbf{x}_r(\mathbf{x}_s), t_L(\mathbf{x}_s)] d\mathbf{x}_s, \tag{3.3.15}$$

with p being the wavefield in the time domain and a_w being a weighting factor. This expression clearly shows a weighted summation of time samples of the input data set along the locus L. The key challenge here is the correct derivation of the weights a_w. To accomplish this, the desired result of the weighted stack needs to be formulated first. It has been decided to define the outcome of the conventional KSR method as the desired result, because this method gives the correct result, albeit at great expense, and only for full coverage data. The aim is, of course, that the result of the new redatuming approach is dynamically as well as kinematically identical to the result of exact redatuming.

Starting point for the derivation of the integral expression describing the DMR approach is the integral expression of the conventional KSR approach (see Appendix A for its derivation):

$$P(\tilde{\mathbf{x}}_s, \tilde{\mathbf{x}}_r, \omega) = \int\int \frac{(i\omega)^2}{(2\pi v_1)^2} \frac{\cos\alpha_r \cos\alpha_s}{r_r r_s} P(\mathbf{x}_s, \mathbf{x}_r, \omega) e^{i\omega(\tau_r + \tau_s)} d\mathbf{x}_r d\mathbf{x}_s, \quad (3.3.16)$$

with ω being the angular frequency, P being the wavefield in the space-frequency domain and v_1 being the velocity of the datum layer, which is assumed to be constant for the moment. The meaning of α and r is illustrated in Figure 3.4. As

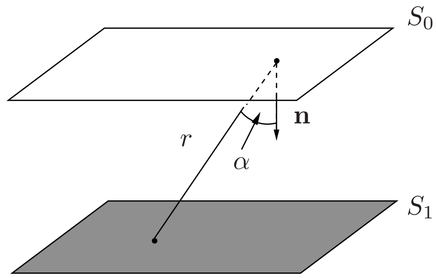

Figure 3.4: *Geometry for downward extrapolation.*

one can see, $r_r = |\tilde{\mathbf{x}}_r - \mathbf{x}_r|$, $r_s = |\tilde{\mathbf{x}}_s - \mathbf{x}_s|$, α_r is the emergence angle between the inward pointing normal vector of S_0 and the local raypath at $\mathbf{x}_r$, and $\tau_r = \frac{r_r}{v_1}$. α_s is the emergence angle between the inward pointing normal vector of S_0 and the local raypath at $\mathbf{x}_s$, and $\tau_s = \frac{r_s}{v_1}$. α_r, r_r and τ_r are functions of $(\mathbf{x}_r, \tilde{\mathbf{x}}_r)$, α_s, r_s and τ_s are functions of $(\mathbf{x}_s, \tilde{\mathbf{x}}_s)$. Only dependencies on relevant parameters will be mentioned in the derivation of the DMR integral.

Equation 3.3.16 is valid for the calculation of all output time samples of the redatumed trace and can, therefore, be formulated in the frequency domain. For the DMR approach the assumed knowledge about the velocity model below the new datum enables one to determine the positions of the possible reflection points belonging to a certain output sample, and it establishes a relationship between sources and receivers at the acquisition surface. However, the isochrone of possible reflection points changes for every output sample. Hence, the DMR approach is dependent on the considered output time, and, consequently, the derivation of the simplified redatuming integral has to be performed in the time domain. The time-domain expression can be obtained by an inverse Fourier transform applied to Equation 3.3.16:

$$p(\tilde{\mathbf{x}}_s, \tilde{\mathbf{x}}_r, t_{red}) = \frac{1}{2\pi}\int d\omega e^{i\omega t_{red}} \iint \frac{(i\omega)^2}{(2\pi v_1)^2} \frac{\cos\alpha_r \cos\alpha_s}{r_r r_s} P(\mathbf{x}_s, \mathbf{x}_r, \omega) e^{i\omega(\tau_r + \tau_s)} d\mathbf{x}_r d\mathbf{x}_s. \tag{3.3.17}$$

Here, the two integrations over the source and the receiver coordinates can be seen as two Fresnel stacks that are performed to determine the contributing traces to the redatumed trace from the input data set. For the DMR method the relationship between sources and receivers at the surface is known. It is established via the considered possible reflection point on the isochrone. As a result of this dependency, the Fresnel stack over the receiver coordinates becomes superfluous, and the integral I_r over the receiver coordinates can be solved analytically. The integral over $\mathbf{x}_r$ in Equation 3.3.17 leads to a $\mathbf{x}_s$-dependent result:

$$I_r(\mathbf{x}_s, \omega) = \int \frac{\cos\alpha_r(\mathbf{x}_r)}{r_r(\mathbf{x}_r)} P(\mathbf{x}_s, \mathbf{x}_r, \omega) e^{i\omega\tau_r(\mathbf{x}_r)} d\mathbf{x}_r. \tag{3.3.18}$$

The application of this integral automatically selects the stationary phase contribution from the input data $P(\mathbf{x}_s, \mathbf{x}_r, \omega)$ for a given surface source location; i.e. it automatically selects the receiver of a possibly contributing trace. However, in the DMR approach it is known how to determine the potential stationary phase point $\hat{\mathbf{x}}_r$ for every source location and output time, via the isochrone. So one can write $P(\mathbf{x}_s, \hat{\mathbf{x}}_r, \omega)$ instead of $P(\mathbf{x}_s, \mathbf{x}_r, \omega)$, where $\hat{\mathbf{x}}_r$ is a function of $(\mathbf{x}_s, t_{red})$.
For every surface source position $\mathbf{x}_s$, it is now assumed that the data $P(\mathbf{x}_s, \mathbf{x}_r, \omega)$ can be described as the reflection at the true reflector tangent to the ellipsoid in the point determined by $\mathbf{x}_s$ and $\tilde{\mathbf{x}}_s$. So, in Equation 3.3.18 $P(\mathbf{x}_s, \mathbf{x}_r, \omega)$ can be replaced by:

$$\Upsilon(\mathbf{x}_s, \mathbf{x}_r, \omega) = a(\mathbf{x}_s, \mathbf{x}_r)\tilde{w}(\omega) e^{-i\omega t_t(\mathbf{x}_s, \mathbf{x}_r)}. \tag{3.3.19}$$

Here, $a(\mathbf{x}_s, \mathbf{x}_r)$ describes the spherical spreading, $\tilde{w}(\omega)$ describes the wavelet and t_t is the two-way traveltime from $\mathbf{x}_s$ to $\mathbf{x}_r$ reflected at the interface tangent to the ellipsoid. In the point $\mathbf{x}_r = \hat{\mathbf{x}}_r(\mathbf{x}_s)$ the analytic extension $\Upsilon(\mathbf{x}_s, \mathbf{x}_r, \omega)$ should coincide with the true wavefield $P(\mathbf{x}_s, \hat{\mathbf{x}}_r, \omega)$:

$$\Upsilon(\mathbf{x}_s, \hat{\mathbf{x}}_r, \omega) \approx P(\mathbf{x}_s, \hat{\mathbf{x}}_r, \omega). \tag{3.3.20}$$

It should be noted here that this assumption is only true for $\hat{\mathbf{x}}_r(\hat{\mathbf{x}}_s)$, with $\hat{\mathbf{x}}_s$ being the surface position belonging to the specular reflection at the true reflector tangent to the ellipsoid belonging to t_{red}. For all other $\hat{\mathbf{x}}_r(\mathbf{x}_s)$ this assumption is not true. This incorrect assumption will, in the end, result in an erroneous curvature of the

corrected event before the Fresnel stack over $\mathbf{x}_s$ is applied. This needs to be corrected for. The derivation of the correction factor accounting for this effect is described in Section 3.4.
It should, furthermore, be noted that the position of $\hat{\mathbf{x}}_s$ is unknown. It is included in the data and implicitly determined by the calculation of the Fresnel stack over $\mathbf{x}_s$.
Substituting Υ, as given by Equation 3.3.19, for P in Equation 3.3.18 yields:

$$I_r(\mathbf{x}_s,\omega) = \int \frac{\cos\alpha_r(\mathbf{x}_r)}{r_r(\mathbf{x}_r)} a(\mathbf{x}_s,\mathbf{x}_r)\tilde{w}(\omega)e^{-i\omega t_t(\mathbf{x}_s,\mathbf{x}_r)}e^{i\omega\tau_r(\mathbf{x}_r)}d\mathbf{x}_r. \tag{3.3.21}$$

The integral I_r can now be calculated by applying the stationary phase method. It has been shown [Bleistein, 1984] that an integral of the form:

$$I(\omega) = \int f(\mathbf{x})e^{i\omega\Gamma(\mathbf{x})}d\mathbf{x} \tag{3.3.22}$$

can be approximated in the high-frequency limit by:

$$I(\omega) \approx \left[\frac{2\pi}{\omega}\right]^{\frac{m}{2}} \frac{1}{\sqrt{\mathcal{A}}} f(\hat{\mathbf{x}})e^{i(\omega\Gamma(\hat{\mathbf{x}})+\mu\frac{\pi}{4})}. \tag{3.3.23}$$

The stationary phase point is defined as $\hat{\mathbf{x}}$ with $|\nabla\Gamma(\hat{\mathbf{x}})| = 0$. Furthermore, $\mathcal{A} = |\det A|$ with $A_{jk} = \left[\frac{\partial^2\Gamma(\hat{\mathbf{x}})}{\partial x_j \partial x_k}\right]$, $j,k = 1,2,\ldots,m$ and m being the dimension of $\mathbf{x}$. $\mu = 2n - m$ with n being the number of positive eigenvalues of A. This is applied to the integral $I_r(\mathbf{x}_s,\omega)$ as follows:

$$\begin{aligned} I_r(\mathbf{x}_s,\omega) &= \tilde{w}(\omega)\int \underbrace{\frac{\cos\alpha_r(\mathbf{x}_r)}{r_r(\mathbf{x}_r)}a(\mathbf{x}_r)}_{f(\mathbf{x}_r)} e^{i\omega\overbrace{[-t_t(\mathbf{x}_s,\mathbf{x}_r)+\tau_r(\mathbf{x}_r)]}^{\Gamma(\mathbf{x}_r)}}d\mathbf{x}_r \\ &\approx \tilde{w}(\omega)\frac{2\pi}{\omega}\frac{1}{\sqrt{\mathcal{A}}}a(\hat{\mathbf{x}}_r)\frac{\cos\alpha_r(\hat{\mathbf{x}}_r)}{r_r(\hat{\mathbf{x}}_r)}e^{i\omega[-t_L(\mathbf{x}_s,\hat{\mathbf{x}}_r)+\tau_r(\hat{\mathbf{x}}_r)]}e^{i\mu\frac{\pi}{4}}, \end{aligned} \tag{3.3.24}$$

with $m = 2$ and $n = 2$ (see Appendix C). As $\mu = 2$, the extra phase factor becomes $e^{i\mu\frac{\pi}{4}} = e^{\frac{\pi}{2}} = \frac{1}{-i}$. This gives:

$$I_r(\mathbf{x}_s,\omega) = \tilde{w}(\omega)\frac{2\pi}{(-i\omega)}\frac{1}{\sqrt{\mathcal{A}}}a(\hat{\mathbf{x}}_r)\frac{\cos\alpha_r(\hat{\mathbf{x}}_r)}{r_r(\hat{\mathbf{x}}_r)}e^{i\omega[-t_L(\mathbf{x}_s,\hat{\mathbf{x}}_r)+\tau_r(\hat{\mathbf{x}}_r)]}. \tag{3.3.25}$$

Substituting this result in Equation 3.3.17 and using Equation 3.3.20 has as result the integral of the DMR approach:

$$p(\tilde{\mathbf{x}}_s, \tilde{\mathbf{x}}_r, t_{red}) = \frac{1}{2\pi} \int d\omega e^{i\omega t_{red}} \int \frac{1}{2\pi v_1^2} \frac{\cos\alpha_r \cos\alpha_s}{r_r r_s} \frac{(-i\omega)}{\sqrt{\mathcal{A}}} \underbrace{a\tilde{w}e^{-i\omega t_L}}_{\approx P(\mathbf{x}_s, \hat{\mathbf{x}}_r, \omega)} e^{i\omega(\tau_r+\tau_s)} d\mathbf{x}_s, \tag{3.3.26}$$

or:

$$p(\tilde{\mathbf{x}}_s, \tilde{\mathbf{x}}_r, t_{red}) = -\frac{1}{2\pi v_1^2} \left[\int \frac{\cos\alpha_r \cos\alpha_s}{r_r r_s} \frac{1}{\sqrt{\mathcal{A}}} \frac{\partial}{\partial t} p(\mathbf{x}_s, \hat{\mathbf{x}}_r, t+\tau_r+\tau_s) d\mathbf{x}_s \right]_{t=t_{red}}. \tag{3.3.27}$$

Here, α_r, r_r, τ_r and $\mathcal{A}$ are functions of $\hat{\mathbf{x}}_r$ and $\tilde{\mathbf{x}}_r$, and of $\mathbf{x}_s$ and t_{red} through the relationship $\hat{\mathbf{x}}_r = \hat{\mathbf{x}}_r(\mathbf{x}_s, t_{red})$. α_s, r_s and τ_s are functions of $\mathbf{x}_s$ and $\tilde{\mathbf{x}}_s$ directly.
It should be noted that the calculation of the amplitude correction factor $\frac{1}{\sqrt{\mathcal{A}}}$ requires the knowledge of the second derivative of the two-way traveltime $t_t(\mathbf{x}_s, \hat{\mathbf{x}}_r)$ of the reflection at the true reflector, which is tangent to the considered ellipsoid. However, the position and shape of the true reflector below the datum is not known and t_t cannot be described analytically. For the implementation of the DMR method it is, therefore, assumed that the second derivative of t_t is small compared to the second derivative of τ_r and can be omitted in the calculation of $\mathcal{A}$. This assumption is true if the true reflector does not have a strong curvature and the distance between the true reflector and the datum is large compared to the thickness of the datum layer. However, if the considered event stems from a shallow reflector or a strongly curved reflector the assumption is no longer valid. In these cases, small errors in the redatumed amplitudes are to be expected.
The derivation for 2D data can be carried out in an analogous manner. Starting point is the integral expression describing the conventional redatuming method in the time domain:

$$p(\tilde{x}_s, \tilde{x}_r, t_{red}) = \frac{1}{2\pi} \int d\omega e^{i\omega t_{red}} \iint \frac{(-i\omega)}{(2\pi v_1)} \frac{\cos\alpha_r \cos\alpha_s}{\sqrt{r_r r_s}} P(x_s, x_r, \omega) e^{i\omega(\tau_r+\tau_s)} dx_r dx_s. \tag{3.3.28}$$

For this situation the one-dimensional stationary phase approximation needs to be applied in order to solve the integral over x_r analytically:

$$\begin{aligned} I(\omega) &= \int f(x) e^{i\omega\Gamma(x)} dx \\ &\approx \sqrt{\frac{2\pi}{\omega}} \frac{1}{\sqrt{|\Gamma''|}} f(\hat{x}) e^{i(\omega\Gamma(\hat{x})+\mu\frac{\pi}{4})}, \end{aligned} \tag{3.3.29}$$

with $\frac{\partial\Gamma(\hat{x})}{\partial x} = 0$, $\hat{x}$ being the stationary phase point and $\mu = sign(\Gamma''(\hat{x}))$.

Finally, the simplified integral of the new redatuming approach for 2D data is:

$$p(\tilde{x}_s, \tilde{x}_r, t_{red}) = \frac{1}{2\pi}\int d\omega e^{i\omega t_{red}} \int \frac{1}{\sqrt{2\pi} v_1} \frac{\cos\alpha_r \cos\alpha_s}{\sqrt{r_r r_s}} \frac{\sqrt{-i\omega}}{\sqrt{|\Gamma''|}} P(x_s, \hat{x}_r, \omega) e^{i\omega(\tau_r+\tau_s)} dx_s, \tag{3.3.30}$$

or

$$p(\tilde{x}_s, \tilde{x}_r, t_{red}) = \frac{1}{\sqrt{2\pi} v_1}\left[\int \frac{\cos\alpha_r \cos\alpha_s}{\sqrt{r_r r_s}} \frac{1}{\sqrt{|\Gamma''|}} D_{\frac{1}{2}} * p(x_s, \hat{x}_r, t + \tau_r + \tau_s) dx_s\right]_{t=t_{red}}. \tag{3.3.31}$$

The term $D_{\frac{1}{2}}$ is a convolution operator corresponding to the frequency domain multiplication by $\sqrt{-i\omega}$.

3.4 Amplitude correction in the DMR method

A crucial part of the DMR approach is the pre-selection of traces possibly contributing to the considered time sample, which is different from the conventional KSR method. The two techniques are illustrated in Figure 3.5 and in Figure 3.6 with as result both showing the true raypaths belonging to the pre-selected source/receiver pairs before the final Fresnel stack is applied. Note here, that for the KSR method the final stack is the second Fresnel stack applied to a half-redatumed data set while for the DMR method only one Fresnel stack is applied to the pre-selected traces applying the source- and the receiver-correction at the same time.
As can be seen in Figure 3.5, for the KSR method the contributing receiver of a certain shot gather is determined by means of the first Fresnel stack, which is applied to redatum the receivers. This process automatically identifies the stationary phase ray; i.e. the contributing trace of the considered shot gather, and needs to be repeated for all shot gathers of the input data set. The result is, as already mentioned, a half-redatumed data set containing a number of possibly contributing traces. In the end, a second Fresnel stack will be applied to this data set to redatum the sources, which automatically determines the stationary phase ray belonging to the redatumed trace from the set of half-redatumed, possibly contributing traces. It is important to note that all possibly contributing traces have been determined correctly by the first Fresnel stack if the applied redatuming operators are correct.
For the DMR approach, presented in Figure 3.6, possible reflection points are assumed to be positioned on an ellipsoidal isochrone below the datum. This information is utilized to identify the potential stationary phase rays and the source and receiver positions of the possibly contributing traces belonging to these rays. However, the true reflector causing the event registered at the considered time t_{red} is most likely not of ellipsoidal shape but will in most cases be a dipping plane tangent to the assumed isochrone in one point. Hence, only one of the assumed reflection

points is positioned correctly, and only one pair of possibly contributing sources and receivers is determined correctly. All other reflection points and pre-selected source/receiver pairs are mispositioned. For the example in Figure 3.5 and Figure 3.6 a plane surface with zero dip has been chosen as true reflector and the true raypaths belonging to the pre-selected source/receiver pairs are indicated for this situation (see Figure 3.6b). Only the source/receiver pair and true raypath belonging to the stationary phase ray are identical for the DMR and the KSR approach. As a consequence of this, the time-corrected reflection event on the selected traces before the final stack is performed has the same apex position for both methods, but its curvature is different. This is displayed in Figure 3.7. Here, experiments on synthetic data with a single dipping layer below the datum have been run for various dips. The results, indeed, show that the apex of the curves indicating the times of the corrected events is always positioned at the correct position in time and space while the corrected events itself have a different curvature. This difference in curvature of the events to be stacked in the two methods gives rise to an amplitude error in the DMR method that needs to be corrected for.
The traveltimes of the corrected event before the final stack is applied for the two methods can be described as follows:

$$\Gamma_{DMR}(\hat{\mathbf{x}}_s, \mathbf{x}_s) = -t_t[\hat{\mathbf{x}}_s, \mathbf{x}_s, \hat{\mathbf{x}}_r(\mathbf{x}_s)] + \tau_r[\hat{\mathbf{x}}_r(\mathbf{x}_s)] + \tau_s(\mathbf{x}_s), \tag{3.4.32}$$

$$\Gamma_{KSR}(\hat{\mathbf{x}}_s, \mathbf{x}_s) = -t_{t,KSR}(\hat{\mathbf{x}}_s, \mathbf{x}_s) + \tau_s(\mathbf{x}_s). \tag{3.4.33}$$

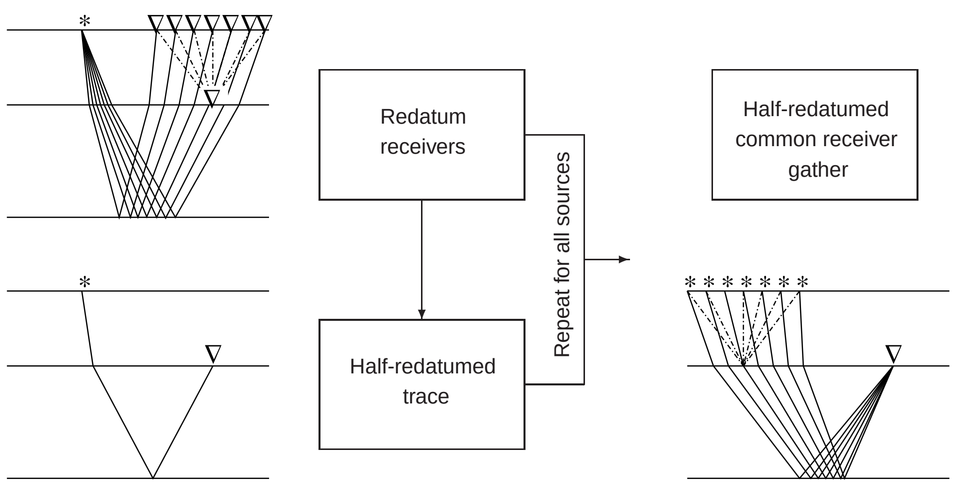

Figure 3.5: *Estimation of the true raypaths of the possibly contributing traces for the conventional redatuming method before the last stack is applied. Note, that the reflector below the new datum is assumed to be flat with zero dip.*

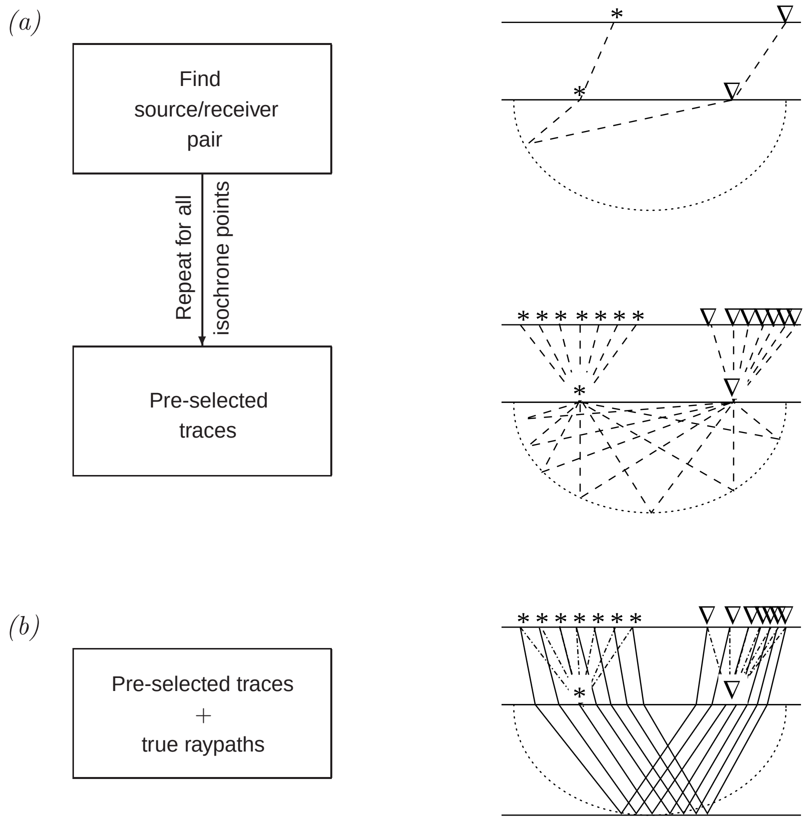

Figure 3.6: *(a) Determination of the raypaths of the possibly contributing traces for the DMR method before the stack is applied. (b) True raypaths, belonging to the selected source/receiver pairs for a reflector below the new datum with zero dip.*

They are both dependent on the surface coordinate $\mathbf{x}_s$ and on the position and shape of the true reflector. The true reflector is tangent to the ellipsoid in a point given by $\hat{\mathbf{x}}_s$ and $\tilde{\mathbf{x}}_s$. It has to be noted here, that this point $\hat{\mathbf{x}}_s$ is not known, but it will be determined implicitly by performing the second redatuming step by means of the KSR method or by calculating Equation 3.4.40, since the information about the true reflector is implicitly included in the seismic data. $t_{t,KSR}$ is the traveltime of a reflection event in a half-redatumed data set after the receivers have been brought to the new datum by means of the conventional KSR approach.
The integral equation describing the DMR method already includes an amplitude correction factor a_Γ employing the curvature of the half-corrected traveltimes as

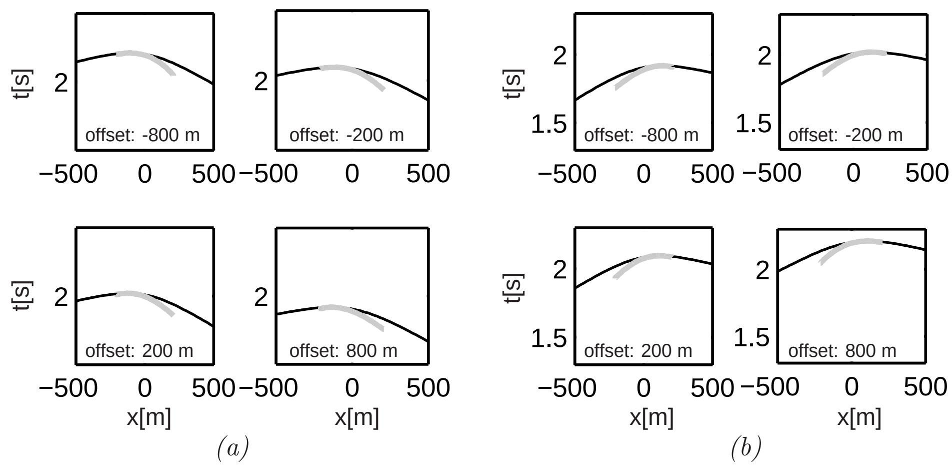

Figure 3.7: *Comparison of the traveltimes of the corrected traces before the last Fresnel stack for the conventional redatuming method (solid line) and for the DMR approach (thick dotted line). (a) shows the situation for a data set for a reflector with a dip of $-40°$, and (b) for a dip of $40°$. The tests have been performed for redatumed traces with an offset of -800 m, -200 m, 200 m, and 800 m.*

follows:

$$a_\Gamma = \frac{1}{\sqrt{\mathcal{A}}}. \tag{3.4.34}$$

It is, therefore, a natural choice to design the amplitude correction for the difference in curvature of Γ_{DMR} and Γ_{KSR} in a similar way:

$$a_c(\hat{\mathbf{x}}_s, \mathbf{x}_s) = \sqrt{\frac{\mathcal{A}_{DMR}(\hat{\mathbf{x}}_s, \mathbf{x}_s)}{\mathcal{A}_{KSR}(\hat{\mathbf{x}}_s, \mathbf{x}_s)}}. \tag{3.4.35}$$

$\mathcal{A}_{DMR}$ and $\mathcal{A}_{KSR}$ are defined as follows:

$$\mathcal{A}_{DMR}(\hat{\mathbf{x}}_s, \mathbf{x}_s) = |\det A_{DMR}(\hat{\mathbf{x}}_s, \mathbf{x}_s)|, \tag{3.4.36}$$

$$\mathcal{A}_{KSR}(\hat{\mathbf{x}}_s, \mathbf{x}_s) = |\det A_{KSR}(\hat{\mathbf{x}}_s, \mathbf{x}_s)|, \tag{3.4.37}$$

with

$$A_{DMR,jk}(\hat{\mathbf{x}}_s, \mathbf{x}_s) = \left[\frac{\partial^2 \Gamma_{DMR}(\hat{\mathbf{x}}_s, \mathbf{x}_s)}{\partial x_{s,j} \partial x_{s,k}}\right], \tag{3.4.38}$$

$$A_{KSR,jk}(\hat{\mathbf{x}}_s, \mathbf{x}_s) = \left[\frac{\partial^2 \Gamma_{KSR}(\hat{\mathbf{x}}_s, \mathbf{x}_s)}{\partial x_{s,j} \partial x_{s,k}}\right]. \tag{3.4.39}$$

Including this amplitude correction in Equation 3.3.27 finally yields the integral expression describing the DMR approach:

$$p(\tilde{\mathbf{x}}_s, \tilde{\mathbf{x}}_r, t_{red}) = -\frac{1}{2\pi v_1^2}\left[\int \sqrt{\frac{\mathcal{A}_{DMR}}{\mathcal{A}_{KSR}}} \frac{\cos\alpha_r \cos\alpha_s}{r_r r_s} \frac{1}{\sqrt{\mathcal{A}}} \frac{\partial}{\partial t} p(\mathbf{x}_s, \hat{\mathbf{x}}_r, t + \tau_r + \tau_s) d\mathbf{x}_s\right]_{t=t_{red}}. \quad (3.4.40)$$

The results of this approach are dynamically and kinematically identical to the results of the conventional KSR approach if the medium below the new datum level is homogeneous. However, as previously discussed, the shape and position of the true reflectors is unknown. Hence, no analytic expression can be found for t_t and $t_{t,KSR}$. As for the calculation of $\mathcal{A}$ it is, therefore, assumed that the second derivatives of t_t and $t_{t,KSR}$ are small and can be omitted in the calculation of $\mathcal{A}_{DMR}$ and $\mathcal{A}_{KSR}$. This assumption is true if the true reflector does not have a strong curvature and the distance between the true reflector and the datum is large compared to the thickness of the datum layer. If the considered event stems from a shallow reflector or a strongly curved reflector the assumption is no longer valid. In these cases, small errors in the redatumed amplitudes are to be expected.
It should be noted, however, that even in case of strong curvature the amplitude errors are small. This is also shown by the results presented in Chapter 4. In such cases one should keep in mind that quantitative analysis of the reflectivities of such amplitudes is impossible, not because of amplitude errors, but because there exists no analytical relationship between media properties and the reflection amplitude of strongly curved events.

3.5 Assumptions, limitations and opportunities

For the derivation of Equation 3.4.40 several assumptions have been made, which can limit the application of the DMR approach. In the following, these assumptions are listed and their consequences are discussed.

3.5.1 Homogeneous datum layer and flat acquisition surface

For the derivation of Equation 3.4.40 the integral expression given in Equation 3.3.16 has been chosen as a starting point. Strictly speaking, this expression is only valid for a homogeneous datum layer with a flat acquisition surface, and only in this case it will give correct results. The redatumed results will be kinematically and dynamically identical to a wavefield which has been acquired at the new datum layer. Only in this situation the redatuming process can be considered as true amplitude redatuming.
In reality, the datum layer will most likely not satisfy these assumptions. Consequently, errors will be introduced in the results of Equations 3.3.16 and 3.4.40. This also happens for most commonly used migration approaches. If the datum layer is

a inhomogeneous, low contrast medium, the amplitude corrections and traveltime shifts of the redatuming operators – the Green's functions – can no longer be calculated analytically. They need to be determined by applying other methods such as ray tracing. For a strongly inhomogeneous datum layer where two-way wave-propagation should be taken into account, redatuming can only be carried out with exact Green's functions, which generally cannot be described by single time shift and amplitude factors. This thesis is limited to datum layers where one-way traveltime operators (Green's functions) with spherical spreading amplitude factors are adequate.
The second assumption underlying the conventional KSR approach and the DMR approach is the assumption of a flat acquisition surface. This stems from the fact that the Rayleigh II integral has been used to derive Equation 3.3.16. This integral is actually a special case of the so-called full Kirchhoff-Helmholtz integral describing wavefield extrapolation for data acquired at arbitrarily shaped surfaces [see for example Wapenaar, 1993]. The Rayleigh II integral will produce correct results if the acquisition surface is flat and if one-way wave-propagation is guaranteed. Applying Equations 3.3.16 and 3.4.40 to data from curved acquisition surfaces will produce redatumed data sets, which are kinematically correct but dynamically incorrect. If it is intended to perform redatuming in this situation, the full Kirchhoff-Helmholtz integral expression should be chosen to describe the conventional KSR method and this expression should be utilized as starting point to derive the data mapping expression.

3.5.2 Multi-valuedness inside the datum

The problem of multi-valuedness arising inside the datum layer equally affects the KSR approach and the DMR approach. For these redatuming methods the estimation of the Green's functions, i.e. the redatuming operators, is crucial for the handling of the multi-valuedness. As already mentioned, the operators are determined in a model-driven way using either ray tracing algorithms or finite difference algorithms [see for example Vidale, 1990; Cerveny, 2001], or they are estimated in a data-driven way employing the CFP-technology. However, these approaches usually consider only first or most-energetic arrivals. They neglect multi-valuedness. They do not consider more than one arrival from the same reflector. For the example presented in Figure 3.8, the operator would contain only one of the two events reaching the same receiver position at the surface from the same focus position at the datum, but it would not contain both events.
It can thus be concluded that neither the KSR approach nor the DMR approach, as they have been derived here, are able to handle multi-valued data sets correctly, if the multi-valuedness arises inside the datum layer. In order to address this problem, it should be examined whether it is possible to combine the presented redatuming methods with the Gaussian beam approach as it has been done by Hill [1990, 2001] for Kirchhoff migration. Hill [1990, 2001] expresses the Green's functions as

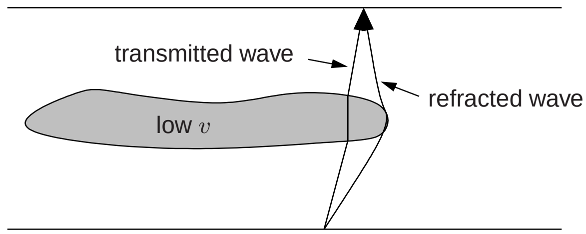

Figure 3.8: *Multi-valuedness inside the datum layer. The transmitted event and the refracted event emitted at the same focus point reach the same receiver.*

Gaussian-beam summations and, in doing so, retains most arrivals. A second option to solve this problem is to calculate the redatuming operators by means of the $x-\omega$ extrapolation [see for example Thorbecke and Berkhout, 1994] or the finite difference approach [see for example Claerbout, 1985], which can both include the multi-valuedness correctly. However, for the application of these approaches an exact velocity model of the datum layer is necessary.
Another way to circumvent the problem of multi-valuedness inside the datum layer is to perform redatuming in a recursive way, i.e. the datum layer is subdivided into a number layers of smaller thickness such that multi-valuedness does not occur inside these thinner layers.
Note that multi-valuedness below the datum does not pose a problem. It will be accounted for automatically by the DMR approach (see Section 3.2).

3.5.3 Flat datum

For the estimation of the isochrone, which is being used in the DMR approach to determine the positions of possible reflection points belonging to the considered output sample, the new datum is assumed to be flat, i.e the redatumed source and the redatumed receiver are expected to be positioned at the same depth level. However, if it is intended to apply the DMR method to a situation with a non-flat datum, that is with large differences in the z-positions of the redatumed source and the redatumed receiver, it is strongly recommended to modify the proposed approach to get kinematically and dynamically correct results.
This modification can easily be accomplished. One just has to orient the axes of the coordinate system used to determine the positions of the possible reflection points accordingly (see Section 3.1). Thereafter, all other steps can be performed as they have been described in this chapter.

3.5.4 Shape of reflectors below the datum

In the derivation of the amplitude weights, which are utilized in the weighted stack of the DMR approach, the potential reflectors below the new datum layer are assumed not to be strongly curved. For most reflectors this will be true. However, it can happen, that strongly curved reflectors have to be treated, or diffraction events, which can be interpreted as reflections from a reflector with infinite curvature. In these cases, the contributions of t_t and $t_{t,KSR}$ cannot be neglected in the correction term derived in Equation 3.4.35. As a result, the event on the redatumed trace can exhibit errors in the amplitude compared to the result of conventional redatuming. The timing of the event will not be affected. However, note the remarks made about the image amplitude of strongly curved events made in Section 3.4.

3.5.5 One-way wavefields

As pointed out in the derivation of the KSR approach, which is the basis for the development of the DMR method, the situation of inverse extrapolation of one-way wavefields is considered. This means that the input data set is assumed to contain primaries only; surface-related multiples should have been removed by prior data processing and internal multiples are assumed to be negligible. Internal multiples that have not been removed will be treated as primaries reflected at mirrored reflectors (see Figure 3.9). As long as the multiple event did not travel inside the datum layer the redatumed result of the KSR approach will be kinematically and dynamically correct, because the assumption that, inside the datum layer, a one-way wavefield is treated is still valid.
For the calculation of the redatumed result by means of the DMR approach also the assumptions being made about the medium below the datum layer are important. In particular, the correctness of the positioning of the possible reflection points and of the velocity used to describe the medium below the datum layer is crucial. As one can see in Figure 3.9, the reflection point belonging to the internal multiple is assumed to be at the mirrored reflector. That is, the velocity belonging to this point

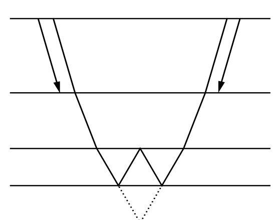

Figure 3.9: *Raypath of an internal multiple. The dashed line indicates the mirrored reflector, the dotted line indicates the raypath of the primary event belonging to the mirrored reflector.*

will be used for the DMR approach instead of the correct velocity belonging to the true reflector. However, in most cases the difference between these two velocities will be negligible, and, therefore, the redatumed result of the DMR approach will be kinematically and dynamically correct as well.
The considerations made above are not true for datum layer-related multiples, which are events that have a downward reflection inside the datum layer or at the surface. In this situation, the assumption of an either up-going or down-going one-way wavefield inside the datum layer is violated. However, the DMR approach can be extended such that it can be used to predict and remove datum layer-related multiples. This application of the DMR methodology is further discussed in Chapter 7.

3.5.6 Far-field approximation

It has also been mentioned in the derivation of Equation 3.3.16 that this expression is a far-field approximation of the Rayleigh II integral with the near-field term being neglected for computational efficiency. Hence, Equation 3.4.40 underlying the DMR method is a far-field approximation, too. As stated in Appendix A, the approximation is valid if the distance between the source and receiver positions at the surface and at the new datum r is large compared to $\frac{v_1}{\omega}$. Assuming, for example, the maximum velocity of a datum layer to be approximately $2000\,\mathrm{m/s}$ and a minimum seismic frequency of $10\,\mathrm{Hz}$ yields $\frac{v_1}{\omega} = 35\,\mathrm{m}$. With datum layers usually being several hundreds of meters thick the far-field approximation should be valid. However, if the datum velocities are higher, the minimum seismic frequency is lower and a datum layer of relatively small thickness is treated, the far-field approximation might no longer be valid. In this case, the near-field term needs to be included, and Equation A.9 has to be utilized for the derivation of the integral expression describing the DMR method.
Furthermore, it should be investigated whether the chosen integral expression indeed converges to the AMO expression if the thickness of the datum layer converges to zero.

3.5.7 Converted waves

Finally, the issue of input data sets containing converted waves needs to be discussed. An example of such a converted wave is presented in Figure 3.10. The derivation of the KSR method, which is the basis of the DMR method, starts from the acoustic wave equation. This implies that only acoustic waves can be redatumed correctly by these methods. However, it can certainly be assumed that both methods redatum SH-waves correctly as well.
Furthermore, the KSR approach can be extended to handle converted waves kinematically correctly. The redatuming operators used to correct for the one-way wavepropagation between sources at the surface and at the datum and receivers at the

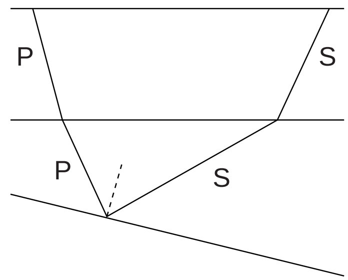

Figure 3.10: *Raypath of a converted wave with a down-going P-leg and an up-coming S-leg.*

surface and at the datum, respectively, have to be determined accordingly. If the data set consists of down-going P-waves and up-coming S-waves, a P-operator has to be used to correct the sources and a S-operator has to be used to correct the receivers. The redatumed result will be kinematically correct. Whether the amplitudes of the redatumed result are correct should be examined in detail, but is beyond the scope of this thesis.
The extension of the DMR approach to handle converted waves, at least, kinematically correctly requires little more effort, but can also be accomplished. This is discussed in greater detail in Chapter 7.
Note, that both the KSR and the DMR method can handle converted waves properly as long as the path through the datum layer can be associated with P-wave propagation (see Figure 3.11). What happens below the datum is of less importance. In case of the DMR method only a different, not fully correct velocity to describe the medium below the new datum is used. However, this yields only small errors in the amplitudes and the timing of the redatumed events.

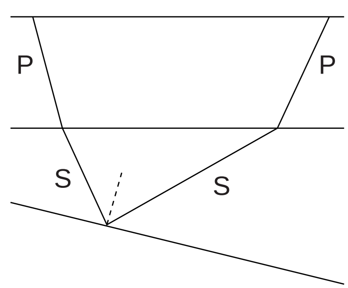

Figure 3.11: *Raypath of a converted wave with a down-going P-leg and an up-coming P-leg inside the datum layer.*

4

Evaluation of the DMR methodology with 2D data examples

Der Worte sind genug gewechselt,
Laßt mich endlich Taten sehen.

Johann Wolfgang von Goethe (1749 - 1832)

In this chapter results are presented for several tests of the DMR approach. At this stage, only the new redatuming method itself is assessed. That is, it is examined whether the proposed approach works, whether the assumed background medium describing the medium below the new datum level is sufficient, and whether the trace-selection parameters and the amplitude weights, which are needed for the weighted stack along the locus, have been derived correctly. The method can only be extended to sparse 3D data sets by combining it with the infill step, if these tests show correct results.
The set of experiments presented in this chapter is run on 2D data sets because of the ease of implementation and the low computational effort. In the following list, the objectives of the different experiments are named.

[1] The applicability of the proposed method and the derived trace-selection parameters need to be verified. To accomplish this, the new DMR approach is applied to seismic data from a velocity model with a constant velocity below and above the new datum level. In this situation the assumptions made about the background medium below the new datum layer are satisfied and, furthermore, the trace-selection parameters can be calculated analytically. As a result no numerical errors influence the trace-selection procedure.

[2] The sensitivity of the DMR method with respect to errors in the velocities describing the medium below the datum needs to be examined. Therefore, the DMR approach is applied, again, to seismic data from a velocity model with a constant velocity below and above the new datum level. In this situation the background medium below the new datum layer is well-known and, furthermore, the trace-selection parameters and amplitude weights can be calculated analytically. Hence, by assuming incorrect velocities below the new datum level and correct velocities above the datum the sensitivity of the new method with respect to these errors can clearly be identified.

[3] The applicability of the simplifying assumptions on the velocity model for the medium below the new datum level and the derived weighting parameters need to be tested. The DMR approach is therefore applied to seismic data from a velocity model with a constant velocity above the new datum level and a complex velocity structure below the datum. In this situation the weights can be calculated analytically and are not influenced by numerical errors.

[4] It needs to be examined whether the trace-selection parameters and the weighting factors can be extracted from given redatuming operators. To assess this the DMR method is applied to seismic data from two different velocity models. The first, and simpler velocity model consists of a complex datum layer and a constant velocity medium below the datum. The second, more realistic velocity model consists of a complex velocity model above and below the datum. Especially the latter experiment can be considered as a test under realistic conditions.

[5] The ultimate test of a newly developed methodology certainly is its application to real seismic data. This has been done as well for the DMR approach by applying it to a 2D data set acquired in the Middle-East. The data set has been acquired over a fairly complex near surface area, which is typical for this region.

It should be noted here, that the direct arrivals and reflections from the datum itself have been muted whenever possible, because, after redatuming, only events from below the datum level are of importance.
Once the 2D experiments are completed with a positive outcome, the method can be extended to and tested on 3D data sets (see Chapter 5 and Chapter 6).

4.1 Simple model – homogeneous datum layer; correct velocities

For the first test, a simple numerical model has been chosen, which satisfies the medium assumptions made for the DMR approach. In other words, the method is applied to seismic data obtained from a medium built of several layers with a constant velocity below the new datum. Reflections from below the new datum occur due to changes in the medium density. The model used for this first test is shown in Figure 4.1. The velocity of the datum layer is 2500 m/s, the velocity below the medium is 3500 m/s. The most distinct feature is the reflector below the new datum level, which has a sharp edge and a dip of 60°. This sharp edge will produce a reflection event showing characteristics of a diffraction. In other words, this event is especially suited to assess the amplitude weights, which have been derived assuming the potential reflectors not to be strongly curved.
A synthetic data set modeled with a moving spread geometry serves as input for this first test. Hereby, a 2D acoustic finite difference algorithm has been employed. The source positions are ranging from 2000 m to 6000 m with a sampling interval of 20 m. For the receivers, a split-spread geometry has been chosen with a maximum offset of 2000 m and a sampling interval of 20 m. This data set is utilized for the calculation of a redatumed shot gather with source and receivers both at the new datum level at a depth of 300 m. The source position at the new datum is 4000 m, the receivers range from 4000 m to 5500 m.
In Figure 4.2 two redatumed shot gathers are compared. The gather in Figure 4.2a has been computed with the conventional KSR method and, thus, represents the desired outcome. The gather in Figure 4.2b has been computed with the DMR

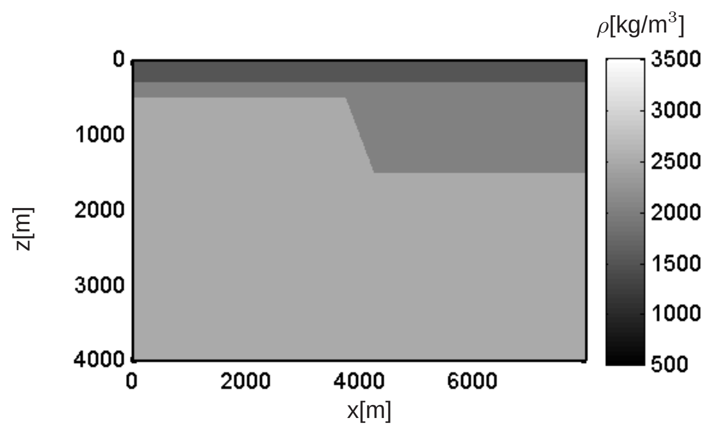

Figure 4.1: *Density model with a homogeneous datum layer and a simple subsurface below the datum. Note, that the velocity below the datum is homogeneous.*

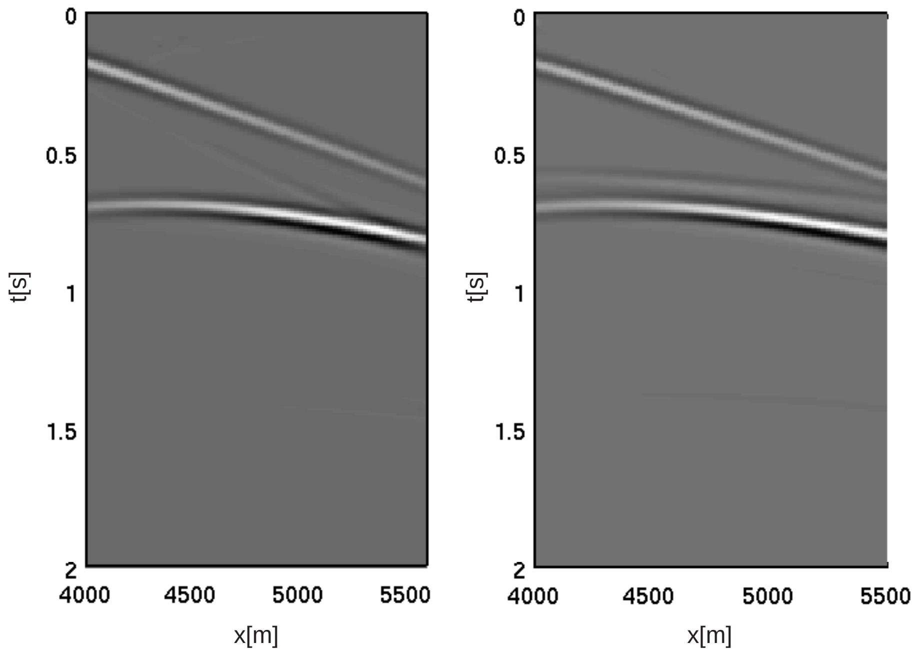

(a) *(b)*

Figure 4.2: *Comparison of (a) the redatumed shot gather computed by conventional redatuming and the redatumed shot gather computed by the DMR approach using (b) the correct velocity $v_2 = 3500$ m/s.*

approach assuming the correct velocity of 3500 m/s for the medium below the new datum.

At first glance, it can be concluded that the proposed method works well because the two events are reconstructed properly. However, to evaluate the output of the DMR approach the results need to be examined in detail, i.e. with respect to kinematic quantities like traveltimes as well as with respect to dynamic quantities like amplitudes. Therefore, the segments of the redatumed traces containing the two events, which have been computed with the DMR approach and the KSR approach, are compared. Figure 4.3 presents traces with an offset of 0 m, 200 m and 400 m.

It is apparent, that for a correct model assumption the redatumed traces using the DMR approach match the desired traces very well. There are neither timing errors nor significant errors in the absolute amplitudes. However, for the first event, corresponding to the reflection from the edge and the steeply dipping part of the reflector, small amplitude errors occur for small offsets. These errors decrease for larger offsets.

The appearance of these errors can be interpreted as a validation of the theory under-

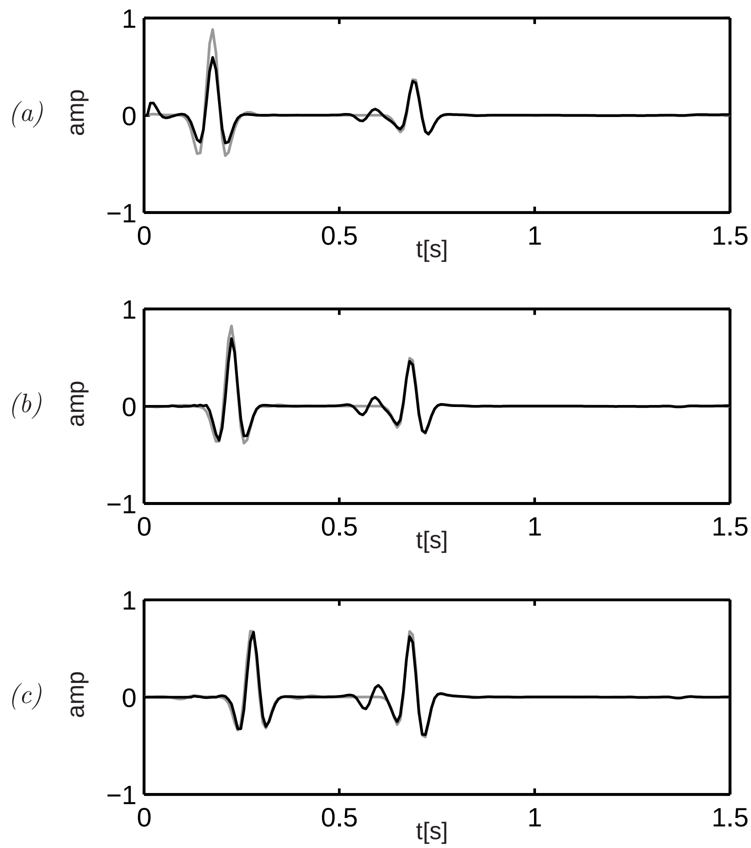

Figure 4.3: *Comparison of redatumed traces computed by the KSR approach (gray line) and by the DMR approach (black line) for an offset of (a) 0 m, (b) 200 m, and (c) 400 m.*

lying the DMR approach. For the derivation of the weighting factors, the potential reflectors below the new datum level are assumed not to have a strong curvature. As a consequence, incorrect amplitudes are to be expected for reflection events from strongly curved reflectors. In this experiment the first event is a diffraction event from the edge of the reflector for small offsets. Consequently, the amplitude of the first event shows a small error. However, with increasing offsets the characteristic of this event changes from a diffraction to a reflection of a steeply dipping, but flat reflector. In other words, for increasing offsets the assumptions made underlying the DMR approach are met. This is also confirmed by the results because the amplitude error of the first event decreases for increasing offsets. Note, that for the second event no amplitude errors are observed, as expected.

A second discrepancy between the two results is a small artifact, which appears

prior to the main events in the results of the DMR approach. Its occurrence can be explained by the limited aperture of the redatuming operators. For the new method, only dips of the ellipsoid between -90 ° and +90 ° are covered; i.e. the surface aperture of the redatuming operators is restricted to an area from which the considered source at the new datum and receiver at the new datum, respectively, are reached with an angle of incidence not exceeding the critical angle. This leads to a sharp cut-off of the corrected traces before the final Fresnel stack, which does not occur for the conventional method. The occurrence of this artifact does not pose a serious problem, because it could be removed by applying a taper before the stack. However, applying a taper in this situation also means that parts of the corrected traces could be tapered that actually contribute to the considered event. Since this would affect the absolute amplitude of the redatumed event, it was decided not to apply a taper.
In conclusion, this test on numerical data from a velocity model with a simple subsurface below the datum and a homogeneous datum layer can be summarized by the following statements:

- the DMR approach, whereby for 2D data a 2D integral is reduced to a 1D integral, works since it reproduces the desired results;
- small errors occur for strongly curved reflectors below the datum level; this was expected.

4.2 Simple model – homogeneous datum layer; erroneous velocities

As already mentioned, the sensitivity of the DMR approach with respect to an incorrect description of the background velocity model needs to be examined. For this purpose, two redatumed shot gathers have been calculated applying the DMR method to the input data set that has been described in the previous section. However, this time an incorrect velocity is assumed for the medium below the new datum level. For the result presented in Figure 4.4a this velocity has been assumed 500 m/s too low, and for the result presented in Figure 4.4b the velocity has been assumed 500 m/s too high. A comparison of these results with the desired result displayed in Figure 4.3a indicates a low sensitivity of the DMR approach to an incorrect background model. The results are kinematically and dynamically almost correct, even when a very wrong velocity is used. This can also be seen in Figure 4.5 and Figure 4.6, which provide a comparison of redatumed traces computed by the DMR approach for two offsets. Apparently only the amplitudes of the diffraction events are affected, while the amplitude of the reflection event stays unaffected.

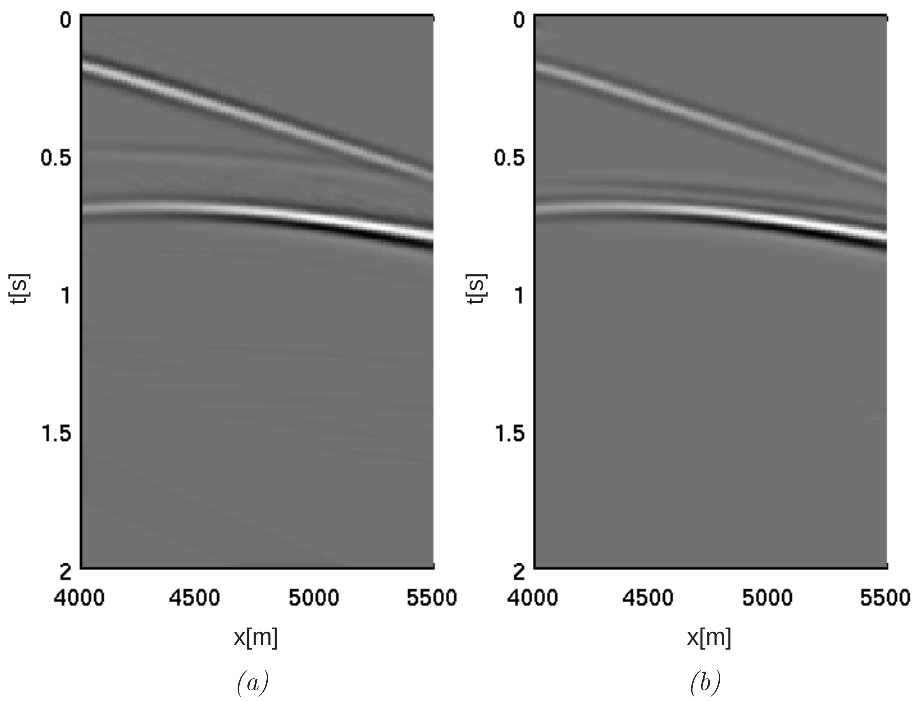

Figure 4.4: *Comparison of the redatumed shot gather computed by the DMR approach using (a) the incorrect velocity $v_2 = 3000$ m/s and (b) the incorrect velocity $v_2 = 4000$ m/s.*

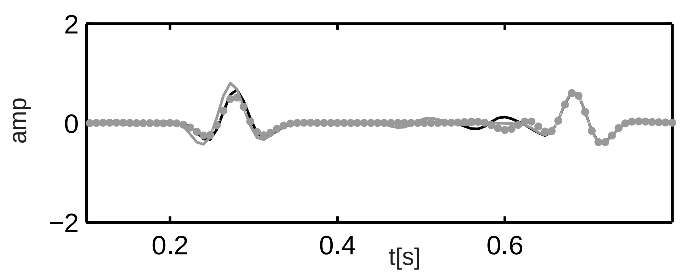

Figure 4.5: *Comparison of redatumed traces computed by the data mapping approach using the correct velocity (black line), the velocity $v_2 = 3000$ m/s (solid gray line) and the velocity $v_2 = 4000$ m/s (dotted gray line) for an offset of 400 m.*

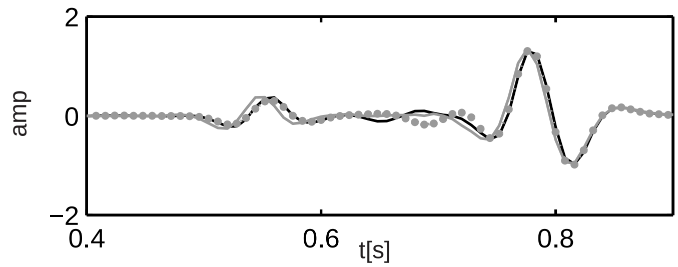

Figure 4.6: *Comparison of redatumed traces computed by the data mapping approach using the correct velocity (black line), the velocity $v_2 = 3000$ m/s (solid gray line) and the velocity $v_2 = 4000$ m/s (dotted gray line) for an offset of 1400 m.*

Besides this, the timing of both events is almost correct for the small offset. For larger offsets, the shallow event shows a small time shift while the timing of the deep event stays unaffected.
Hence, it has been learned from this second test that the DMR approach shows only a weak sensitivity to errors in the assumed background medium below the new datum. Even large errors in the assumed velocity produce only small errors in the amplitude and traveltime of the events.

4.3 Complex model – homogeneous datum layer

Next, the DMR approach is applied to synthetic data generated from a complex subsurface model below a homogeneous datum layer with a medium velocity of 1500 m/s. As indicated in the previous section, the expectation is that utilizing approximate RMS velocities to describe the velocity model below the new datum is sufficient to obtain kinematically and dynamically correct redatumed output traces.
The numerical model underlying this synthetic 2D data set is displayed in Figure 4.7. Unlike for the previous experiment this model is quite realistic. It contains a part of a salt dome, fault structures beneath the dome, turbidite structures with low velocities and vertical as well as lateral velocity gradients.
For this subsurface model a data set has been modeled with a moving spread geometry using a 2D acoustic finite difference code. The source positions are ranging from 4500 m to 10500 m with a sampling interval of 30 m. The receiver spread has a maximum offset of 4800 m at both sides of the source position and is sampled with an interval of 30 m. From this input data set a redatumed shot gather is calculated at a depth of 250 m. The source is positioned laterally at 6000 m, and the receivers range from 6000 m to 10000 m. To get the redatumed RMS velocity field used for redatuming a standard velocity analysis has been applied to the input data set.

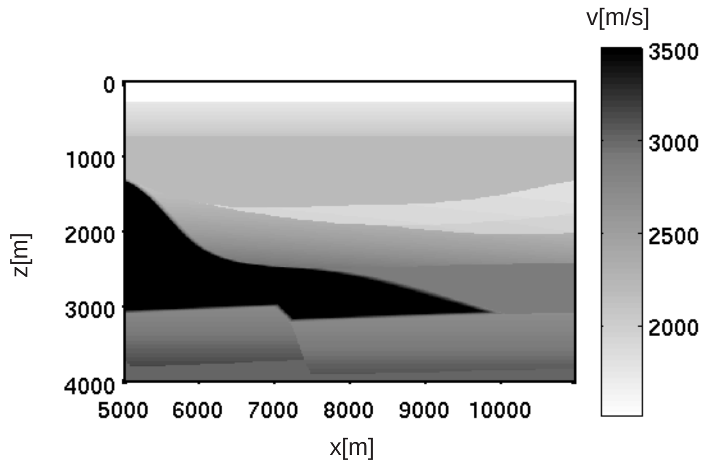

Figure 4.7: *Velocity model with a homogeneous datum layer and a complex subsurface below the datum.*

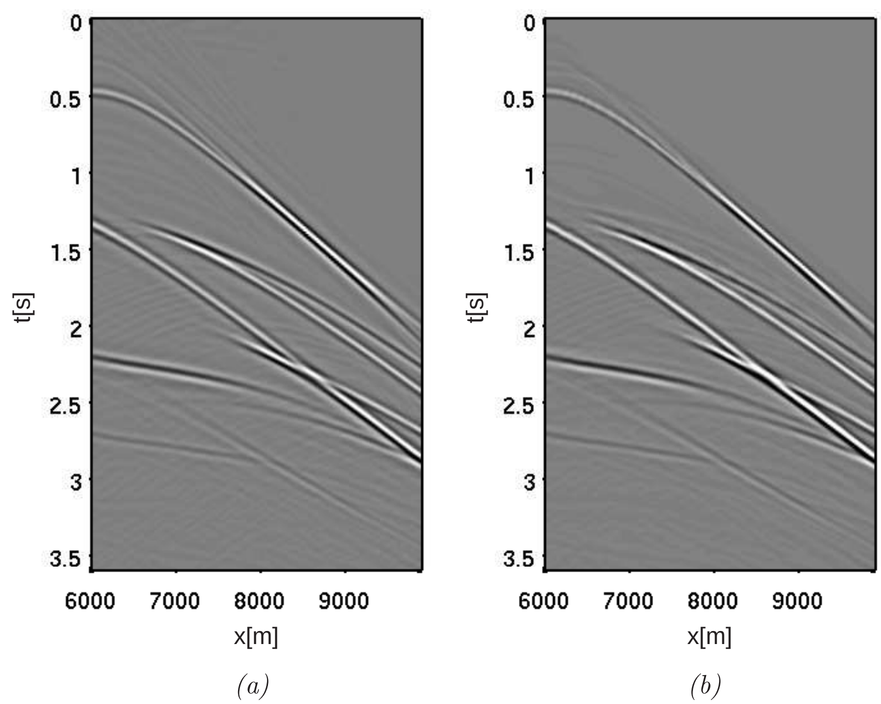

Figure 4.8: *Comparison of (a) the redatumed shot gather computed by the KSR method, and (b) the redatumed shot gather computed by the DMR approach.*

The resulting gather is displayed in Figure 4.8b. A comparison with the desired result (see Figure 4.8a), which has been computed by applying conventional redatuming, shows that the DMR approach produces very good results. Obviously all events are reconstructed and appear at a correct position in time. It should be remembered that, compared to conventional redatuming, in the new approach a 1D integral instead of a 2D integral has been applied to calculate one time sample. It should, furthermore, be noted that, for the DMR approach, only approximately 100 traces are needed for the calculation of one output sample.

(a) *(b)* *(c)*

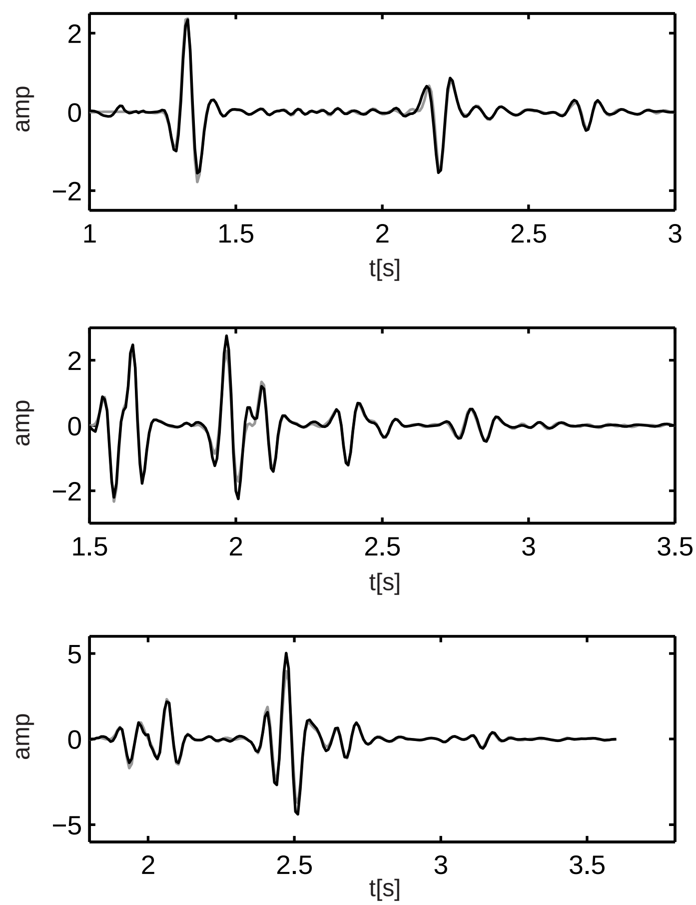

Figure 4.9: *Comparison of redatumed traces computed by conventional redatuming (gray line) and by the data mapping approach (black line) for an offset of (a) 30 m, (b) 1800 m, and (c) 3000 m.*

This considerable reduction of input data needed to calculate one time sample will be of special importance for the application to sparse 3D data since the number of traces to be infilled is strongly reduced then as well.
To evaluate the quality of the redatuming result more closely, again, traces representing the near-offset, the medium-offset and the far-offset range are selected.
In Figure 4.9 the traces are compared with the results of the KSR approach, which are obtained by calculating the full 2D integral. The redatumed events on these traces do not show any or only very minor errors in timing, and even the absolute amplitudes match very well.
It can thus be stated that the DMR method utilizing RMS velocities for the description of the medium below the new datum produces kinematically and dynamically correct results. Furthermore, these results prove that assuming a simple background medium below the new datum layer is indeed sufficient.

4.4 Simple model – complex datum layer

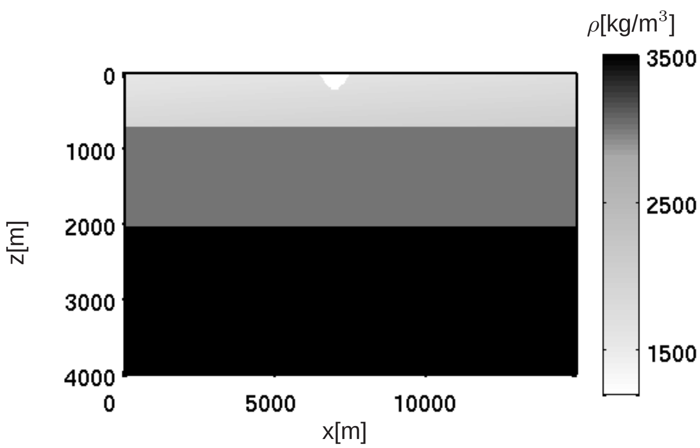

Figure 4.10: *Density model with a complex datum layer and a simple subsurface below the datum.*

For this test a complex near surface is included in the numerical model to create a more realistic situation than the ones considered before. Here, a constant velocity medium below the datum ($v_2 = 3000\,\mathrm{m/s}$) has been chosen. By doing this, it is assured that all occurring errors are resulting from errors made in the extraction of the trace-selection parameters and the weights from the redatuming operators. As illustrated in Figure 4.10 the datum layer is 700 m thick. This layer exhibits a velocity gradient with an increase of the velocity from top left ($v = 1500\,\mathrm{m/s}$) to bottom right ($v = 1700\,\mathrm{m/s}$). Furthermore, a low velocity zone ($v_{low} = 1200\ \mathrm{m/s}$) is present

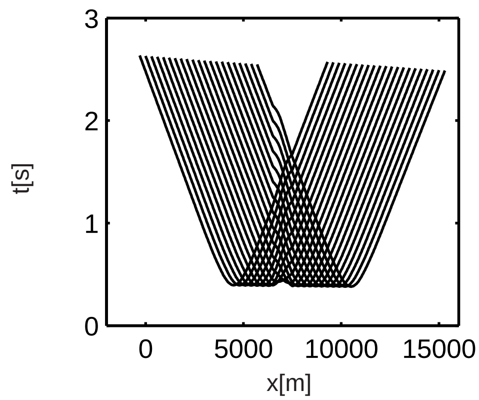

Figure 4.11: *Traveltimes of the redatuming operators for the complex datum layer.*

around $x = 7000$ m which corresponds to a wadi (dry riverbed) as often present in the Middle East. For this situation it is no longer possible to calculate the one-way traveltime operators including the time shifts, the ray parameters and the amplitude corrections analytically. Instead, an Eikonal solver has been used to calculate the traveltimes and the amplitudes of the one-way operators [see for example Vidale, 1988]. The traveltimes are presented in Figure 4.11. Note the imprint of the low velocity anomaly and the effect of the velocity gradient.

The ray parameters at the surface points were extracted from the traveltimes by sorting them into common receiver gathers and calculating the first derivative, as it has been described in Chapter 3.

For this numerical model a data set has been computed with a moving spread geometry utilizing a 2D acoustic finite difference code. Its sources are positioned between 4500 m to 10500 m with a sampling interval of 30 m. The receiver spread has a maximum offset of 4800 m at both sides of the source position and is sampled with an interval of 30 m. Again, a redatumed shot gather is calculated for this input data set at a depth of 700 m. The position of the redatumed source is 6000 m, the receivers range from 6000 m to 9500 m.

Figure 4.12a illustrates one shot gather of the input data set, which is clearly distorted by the low velocity infill. Four strong events can be identified. The two events with the apex positions at approximately x =6000 m represent the primary reflection from the reflector below the datum layer and the first-order surface-related multiple belonging to it. The two events whose apices are shifted to the right represent first-order multiples related to the low velocity zone. Here, the first event represents a reflection from the reflector below the datum, which has then been diffracted at the edges of the low velocity area; the second event represents a reflection from the reflector below the datum, which has then been reflected at the lower boundary of the low velocity area.

It should be noted here, that, in general, surface-related multiples are treated differently by the KSR and the DMR approach. The redatumed results will only be comparable if the stacking velocities used for the redatuming by means of the DMR approach are similar to the RMS velocities belonging to the paths the multiples took (see Chapter 3.5). However, this is not the case for the considered data set. Here, the velocity used for redatuming is 3000 m/s, whereas the surface-related multiples and the multiple events related to the low velocity zone mostly travel with a velocity that does not exceed 1700 m/s. Hence, errors in the timing of those events are to be expected. However, the redatuming of datum layer-related multiples is beyond the scope of this chapter. It will be discussed more thoroughly in Chapter 7.
The redatuming results are displayed in Figure 4.12. A comparison of the desired result (see Figure 4.12b), which has been computed by applying conventional full 2D integral redatuming, with the result of the DMR approach (see Figure 4.12c) is, again, positive. Obviously the primary reflection from the reflector below the datum has been reconstructed correctly. The distortions triggered by the low velocity zone within the datum layer have successfully been removed. Small errors can only be seen in the timing of the multiple events. This, however, was to be expected.
Amplitude comparisons of the desired result and the result of the DMR approach are presented in Figure 4.13 for two different offsets, again, showing that the primary event redatumed by means of the DMR method is dynamically correct.

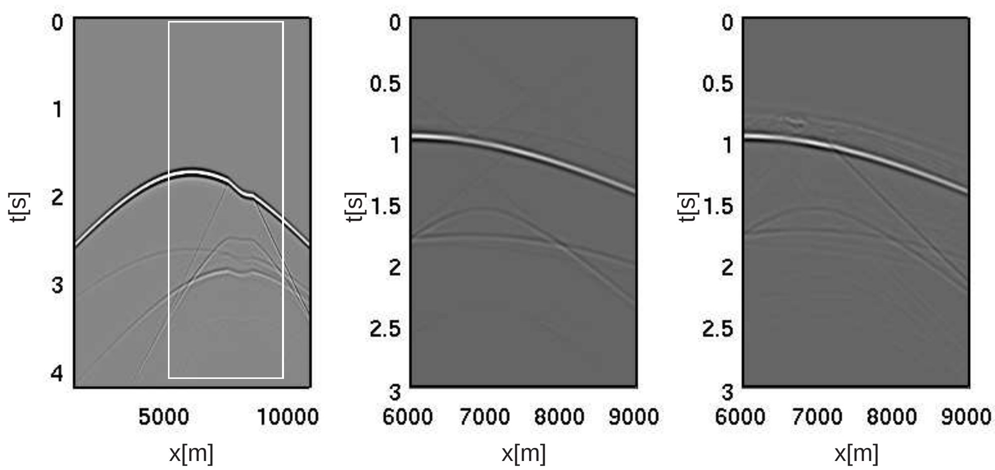

(a) *(b)* *(c)*

Figure 4.12: *Comparison of (a) a shot gather of the input data set, (b) the redatumed shot gather computed by conventional redatuming, and (c) the redatumed shot gather computed by the DMR approach.*

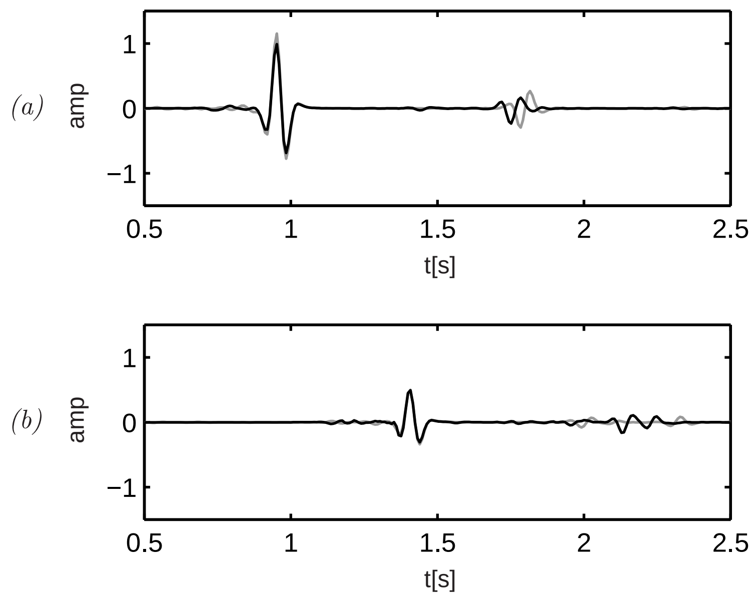

Figure 4.13: *Comparison of redatumed traces computed by conventional redatuming (gray line) and by the DMR approach (black line) for an offset of (a) 30 m and (b) 3000 m. Note that the earlier event is a primary reflection from below the datum layer, the later event is a multiple related to the low-velocity zone inside the datum layer.*

It can thus be concluded, that the results of the DMR method are kinematically and dynamically correct even if the amplitude weights and trace-selection parameters have to be extracted from redatuming operators.

4.5 Complex model – complex datum layer

For the next experiment a complex subsurface is included in the synthetic model. As illustrated in Figure 4.14 the datum layer is 700 m thick and includes exactly the same features as the datum layer included in the velocity model discussed before.
A synthetic data set has been produced for this numerical model using, again, an acoustic 2D finite difference code. The data set has a moving spread geometry with sources positioned between 4500 m to 10500 m with a sampling interval of 30 m. The receivers are arranged in a split-spread geometry with a maximum offset of 4800 m at both sides. They are sampled with 30 m, too. The redatumed shot gather being calculated from this input data set is positioned at a depth of 700 m with its lateral position at 6000 m. The receivers range from 6000 m to 9500 m.

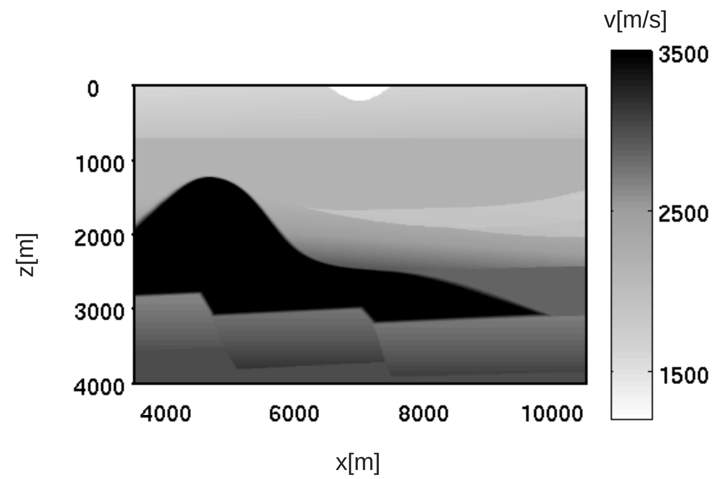

Figure 4.14: *Velocity model with a complex datum layer and a complex subsurface below the datum.*

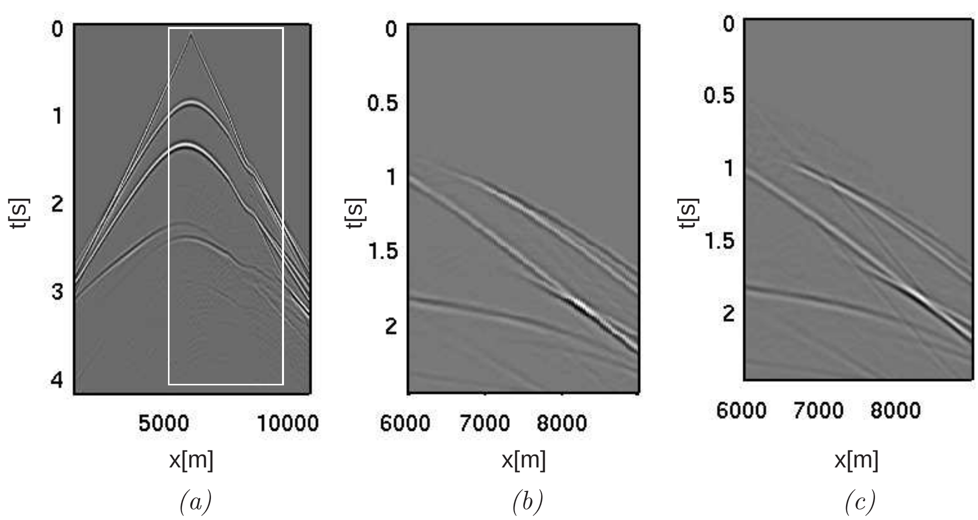

Figure 4.15: *Comparison of (a) a shot gather of the input data set, (b) the redatumed shot gather computed by conventional redatuming, and (c) the redatumed shot gather computed by the new data mapping approach.*

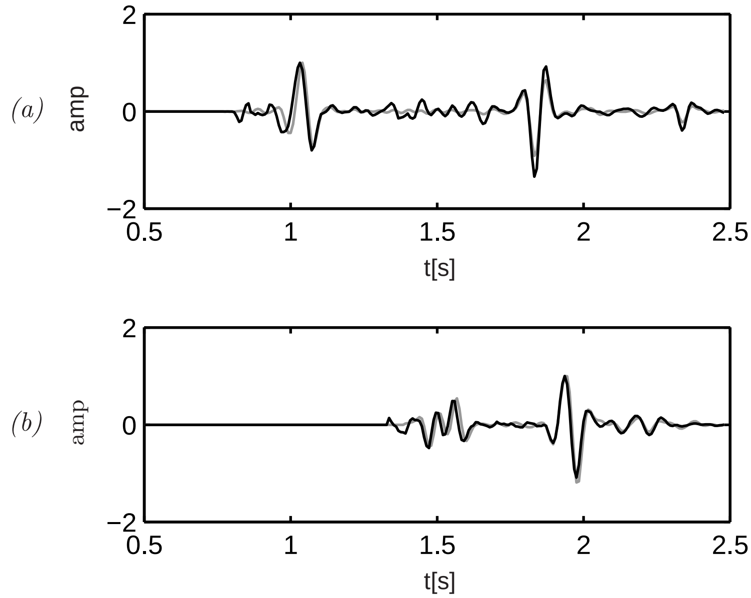

Figure 4.16: *Comparison of redatumed traces computed by conventional redatuming (gray line) and by the DMR approach (black line) for an offset of (a) 60 m and (c) 2400 m.*

Figure 4.15b and Figure 4.15c display the results of the redatuming. A comparison of them shows that the DMR method, again, produces good results, which are almost identical to the result of the KSR method. It can also be seen that the distortions of the near surface have been successfully removed. This can be observed when the redatumed shots are compared with a shot gather of the input data presented in Figure 4.15a.

The absolute amplitudes of the redatumed results can be examined in Figure 4.16 for traces at two different offsets. Here, the DMR result matches the desired result very well.

It can thus be concluded that even for this complex velocity model below and above the datum the DMR method produces satisfactory results, which kinematically and dynamically match the conventional redatuming results.

4.6 Real data example

The real 2D data set used here to test the DMR approach has been provided by Saudi Aramco. It is a land data set acquired over a complex near surface, which is typical for the Middle East. In Figure 4.17 a stacked section of the input data is presented, clearly showing this complexity.

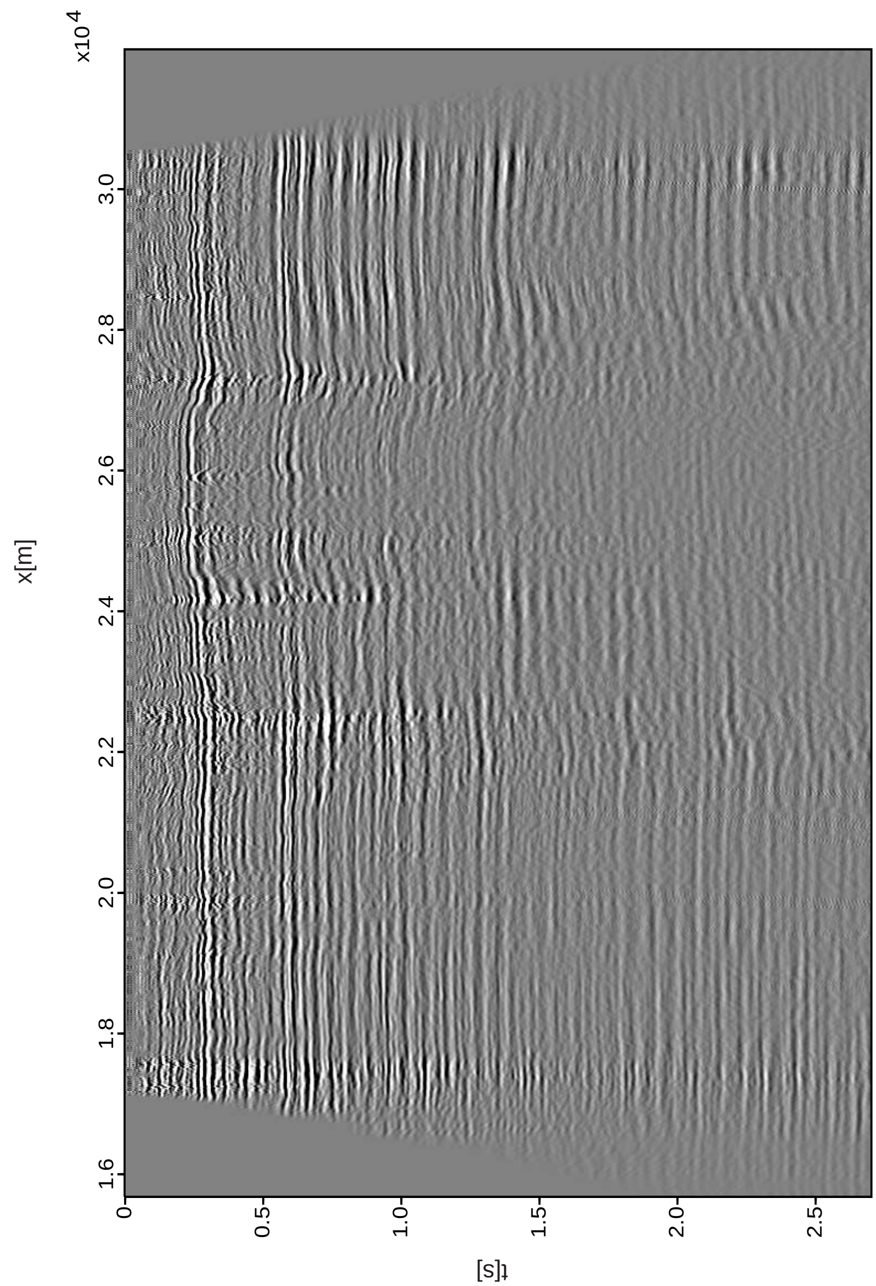

Figure 4.17: *A stack of the input data. Note that the reflection of the target reflector for redatuming occurs at approximately 0.59 s.*

For the first test on these data the redatuming operators have been estimated using the data-driven CFP technology employing the old iterative updating approach [see for example Kelamis et al., 1999; Hindriks and Verschuur, 2001; Al-Ali and Blacquiere, 2005]. The traveltimes of these operators are presented in Figure 4.18. It should be noted that the CFP location is equivalent to the source position of a one-way operator at the new datum level. The offset coordinates indicate the receiver offset at the surface with respect to the considered source (CFP) location at the new datum. It clearly can be seen that the traveltimes are inconsistent along the CFP

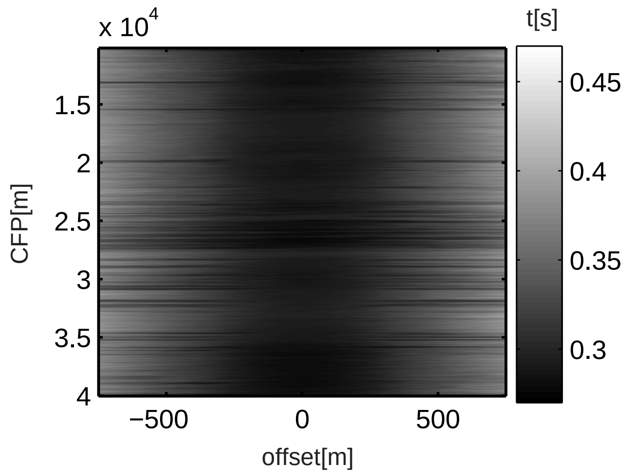

Figure 4.18: *Traveltimes of the first redatuming operators estimated for the real data set.*

location coordinate. In some areas neighboring operators exhibit large differences. It has to be noted here that these inconsistencies are a result of the applied iterative updating method, and that they are most likely not related to inhomogeneities in the datum layer itself. The reason for this is that neighboring operators are not included in the estimation of the traveltimes at a certain CFP position. The situation shown here is comparable to using different, slightly incorrect velocity models for the calculation of the redatuming operators at different CFP locations in the model-driven approach.

However, even though these operators are not fully correct, they still represent a realistic situation, because one usually cannot expect the estimated redatuming operators to be error-free. It is, therefore, interesting to see how the different redatuming methods handle these inconsistencies.

In Figure 4.19b the resulting redatumed shot gather using the conventional KSR method is displayed, and Figure 4.19c shows the result of the DMR approach. A comparison of these gathers with the same shot gather of the input data set (see Figure 4.19a), which has been shifted in time, reveals that, apparently, the KSR approach suffers more from the inconsistencies in the applied redatuming operators.

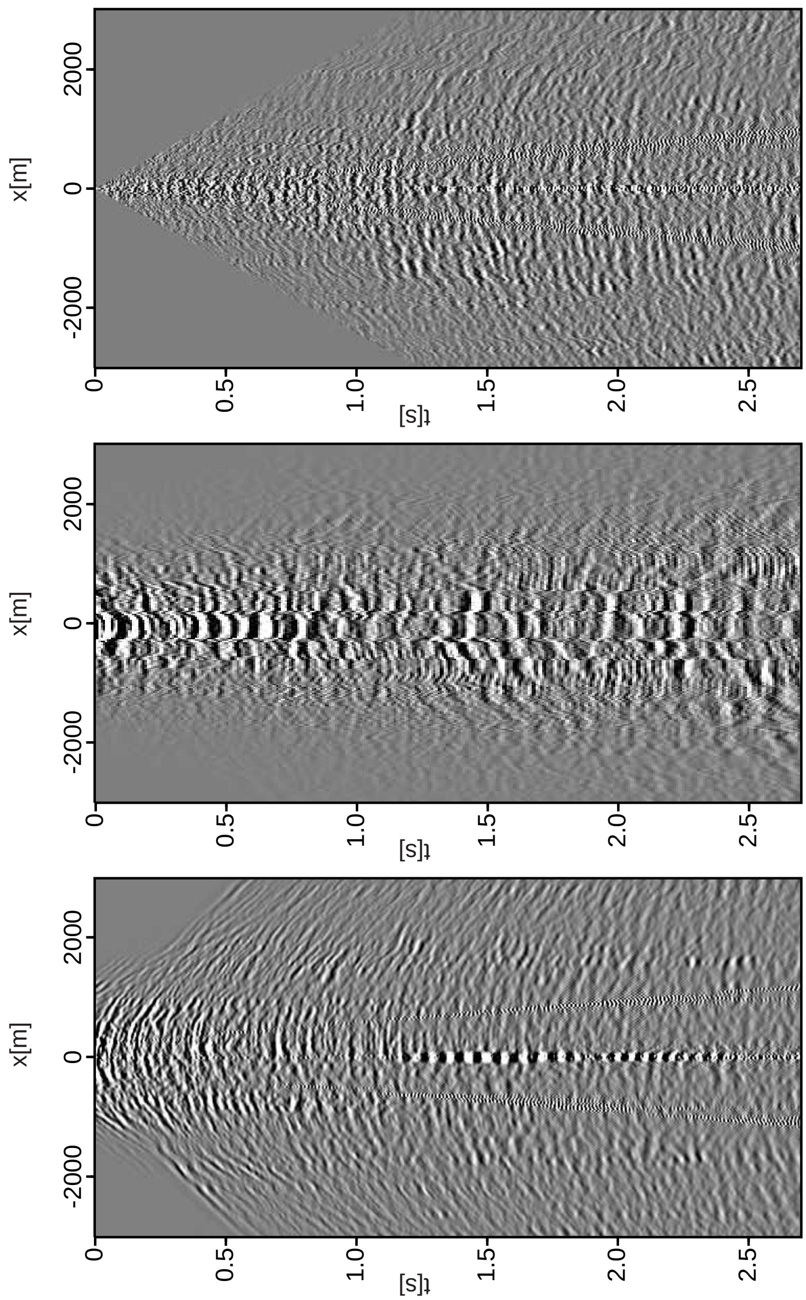

(c)

(b)

(a)

Figure 4.19: *(a) A shot gather of the input data shifted in time by approximately the amount redatuming shifts the data. (b) A redatumed shot gather computed by conventional redatuming using inconsistent operators. (c) A redatumed shot gather computed by the DMR approach using inconsistent operators.*

In the conventional approach the characteristics of the input data are less well preserved than by using the DMR approach. This can be explained by the fact that the inconsistent operators are applied twice to the data by the conventional approach. In contrast to this, the DMR method applies only one Fresnel stack, so that the error will be less pronounced in the final result.
A second test has been performed on this data set, this time using operators which have been estimated by an improved operator updating procedure. As one can see in Figure 4.20, these operators are more consistent. Again, the CFP location is equivalent to the source position of a one-way operator at the new datum level. The offset coordinates indicate the receiver offset at the surface with respect to the considered source (CFP) location at the new datum. They do not show as severe

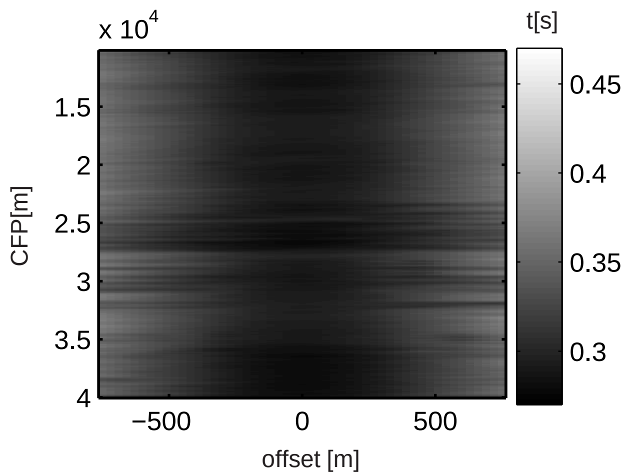

Figure 4.20: *Traveltimes of the second redatuming operators estimated for the real data set.*

inconsistencies of the traveltimes in CFP direction as the result of the old estimation method. Consequently, the result of the conventional redatuming improves (see Figure 4.21b). The reflection events are more continuous. However, also for this second experiment it is observed that the characteristics of the original data are preserved better by the DMR approach. This might not be apparent from a comparison of the redatumed shot gathers presented in Figure 4.21b and Figure 4.21c, but it becomes clear from the stacked sections of the redatumed data. In Figure 4.22 the stacked input data set shifted by the time of the reflection event from the new datum at zero offset is illustrated. Figure 4.23 presents the stack of the redatumed data using the conventional KSR approach. This stack shows more continuity than the stacked input data. However, this continuity has to be attributed to errors of the redatuming. It can be seen in Figure 4.19b and in Figure 4.21b that the inconsistency of the operators produces flat events in the redatumed shots using the KSR method.

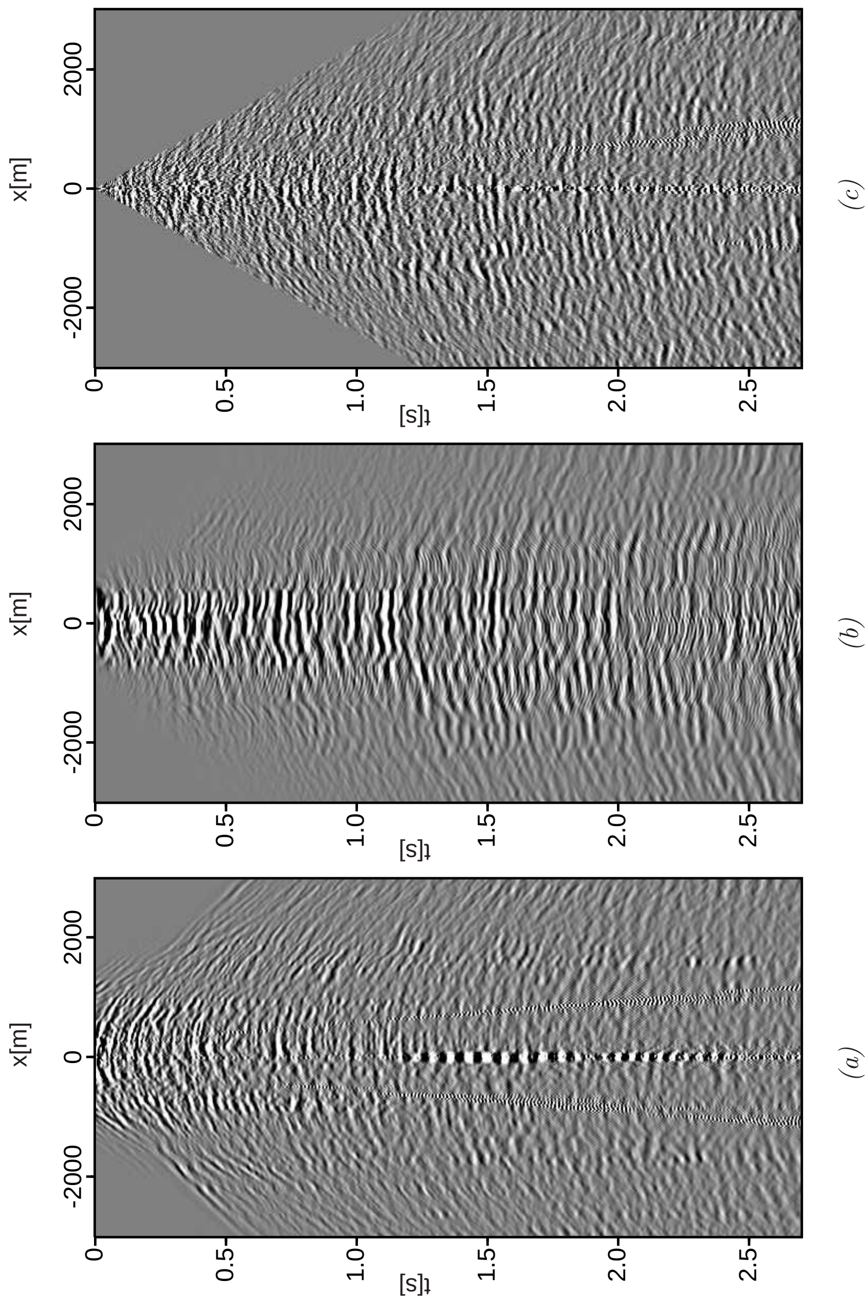

Figure 4.21: *(a) A shot gather of the input data shifted in time by approximately the amount redatuming shifts the data. (b) A redatumed shot gather computed by conventional redatuming using more consistent operators. (c) A redatumed shot gather computed by the DMR approach using more consistent operators.*

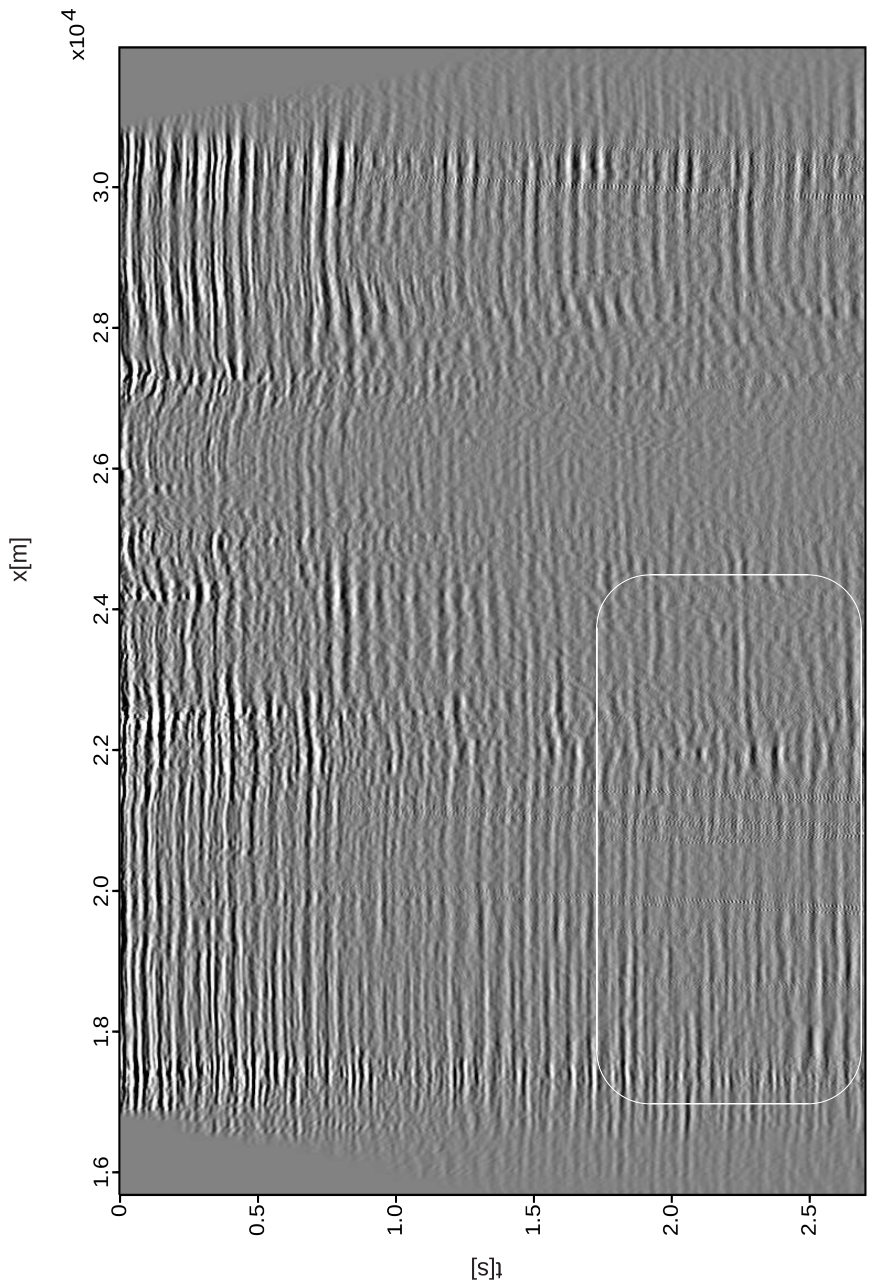

Figure 4.22: *A shifted stack of the input data. Here, the oval indicates an area where the data redatumed by the DMR approach show an improved continuity compared to the KSR result and the stacked input data.*

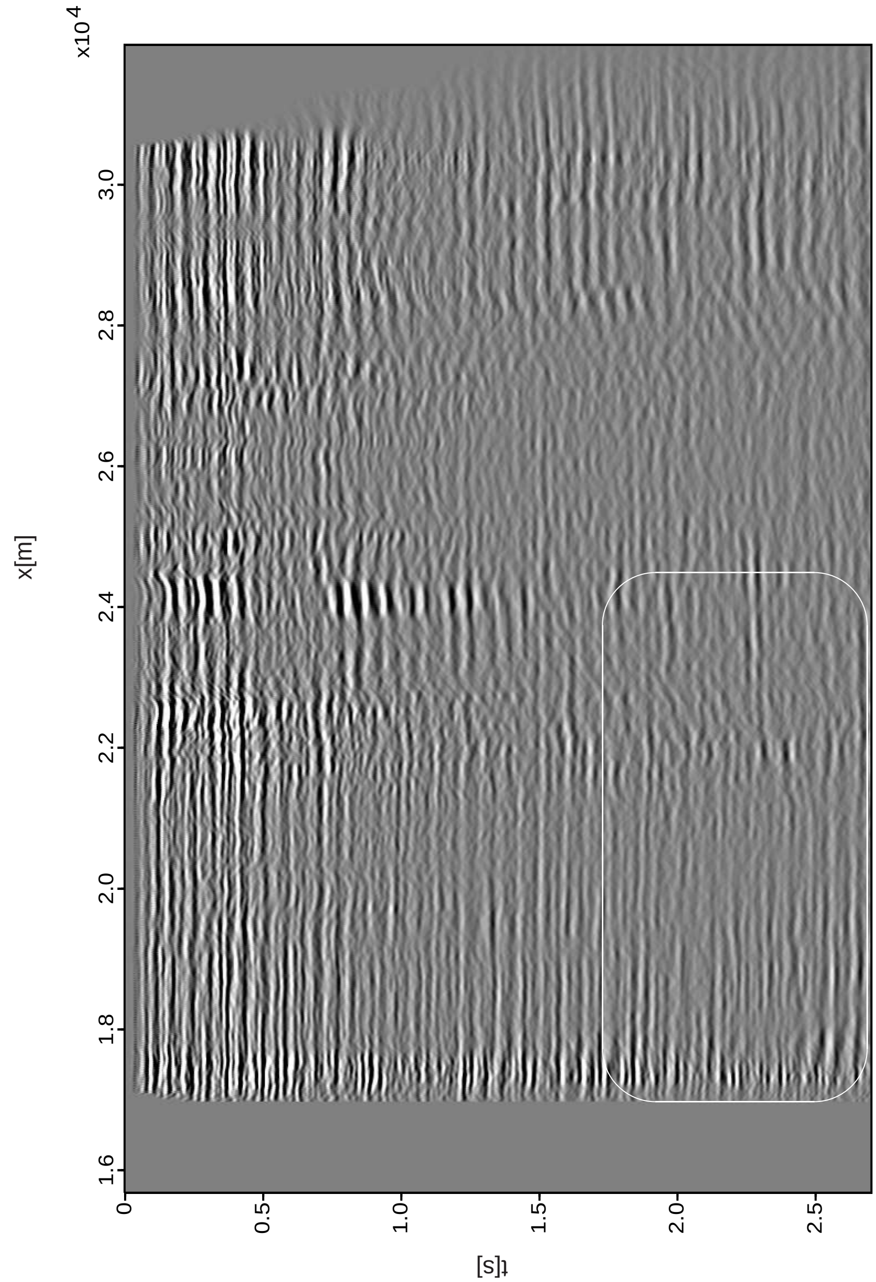

Figure 4.23: *A stack of the redatumed results computed by the KSR approach using more consistent operators. The oval indicates an area where the data redatumed by the DMR approach show an improved continuity compared to the KSR result shown here and the stacked input data.*

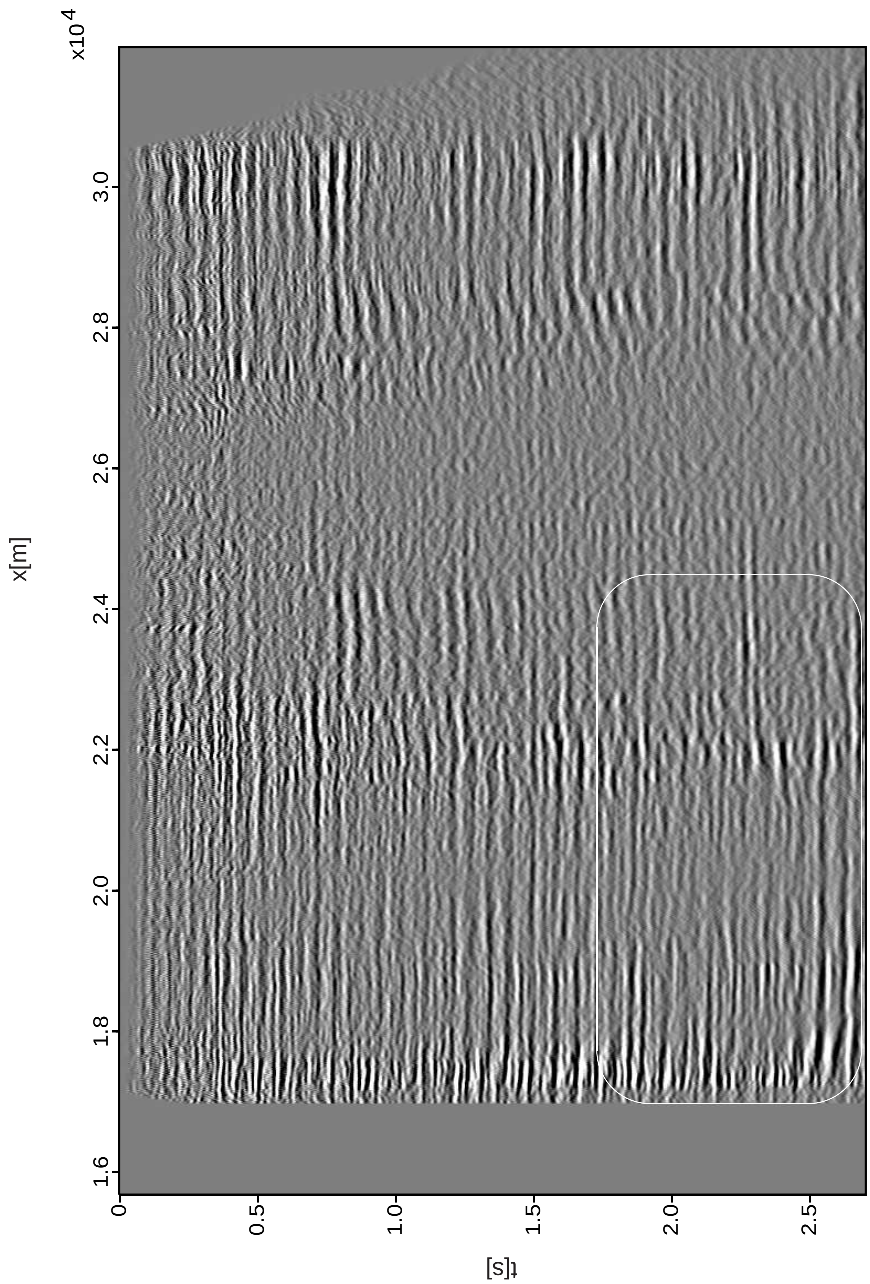

Figure 4.24: *A stack of the redatumed results computed by the DMR approach using more consistent operators. Here, the data inside the oval show a better continuity than the result of the KSR method and the stacked input data.*

(a)

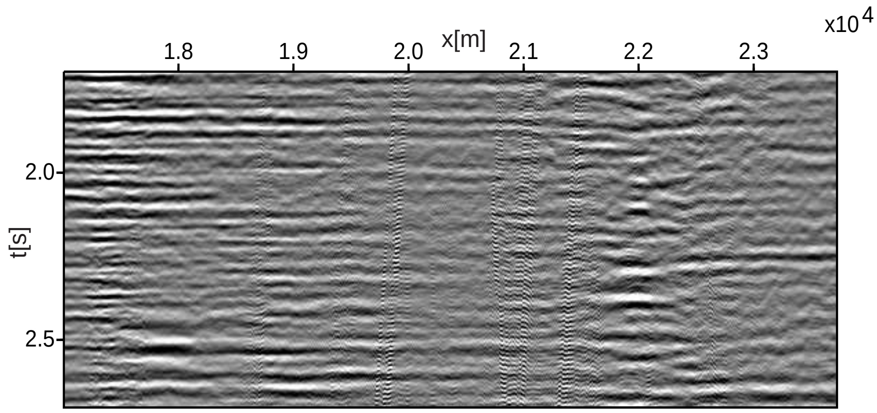

(b)

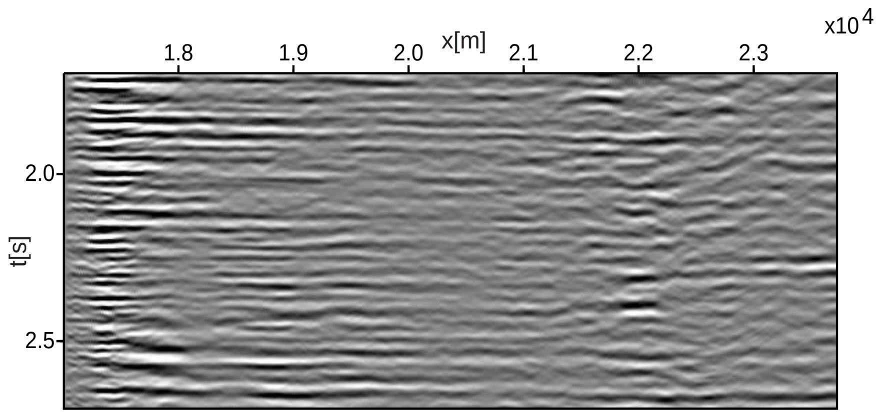

(c)

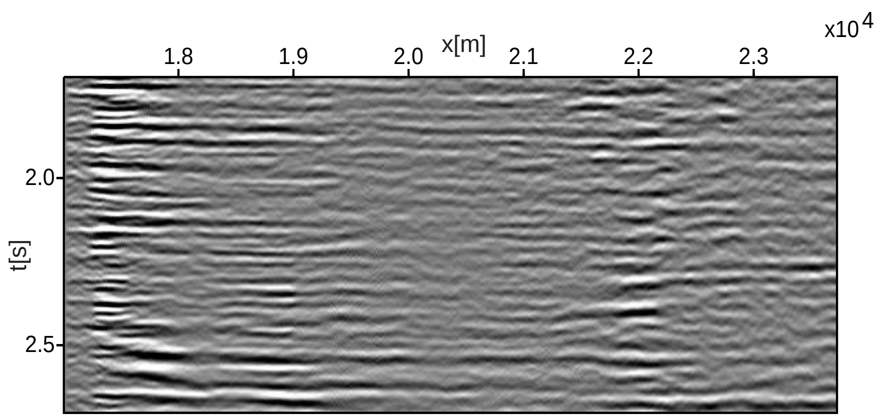

Figure 4.25: *A selected area of: (a) the stacked input data shifted in time by approximately the amount redatuming shifts the data, (b) the stack of the redatumed result computed by conventional redatuming and (c) the stack of the redatumed result computed by the DMR approach.*

A stack of these flat events certainly yields a strong continuous event, but it does not necessarily mean that this event exists. In opposite to this the DMR approach clearly preserves the characteristics of the original data better (see Figure 4.24). Furthermore, a slight improvement of the stacked result after DMR redatuming can be stated, because a better continuity has been achieved in some areas (see also Figure 4.25).
Hence, from these tests of the DMR approach on a real 2D data set it can be concluded that:

- the DMR approach produces satisfactory results for the application to complex real 2D data;
- the DMR approach preserves the characteristics of the input data better because only one Fresnel stack is applied, whereas the conventional redatuming approach uses two;
- the DMR approach is less sensitive to inconsistencies in the redatuming operators (e.g. due to an improper estimation of one-way travel times or the use of inaccurate velocities of the datum layer), which happened for this data set, compared to the conventional KSR method.

4.7 Conclusions and recommendations

The results of the tests on fully sampled 2D data can be summarized as follows:

[**1**] the DMR approach using RMS velocities for the description of the velocity model below the new datum level works very well;

[**2**] the redatumed traces are kinematically and dynamically correct;

[**3**] the absolute amplitudes are showing small errors for strongly curved reflectors below the new datum level;

[**4**] the number of traces needed to calculate one output sample is considerably reduced, only about 100 traces were enough to calculate one output time sample, whereas in the conventional approach this would be 10000;

[**5**] the dependency of the new approach on the assumed medium below the new datum level is weak because the assumption of a velocity medium where no ray bending occurs is already sufficient to produce correct results;

[**6**] the method is applicable to a complex near surface;

[**7**] the method has proved its applicability to real data.

With these tests showing satisfactory results the DMR approach can now be extended to, and tested on, 3D data sets. The proposed infill idea needs to be incorporated then.

5

The infill of missing data

So einfach wie möglich.
Aber nicht einfacher !

Albert Einstein (1879 - 1955)

In this chapter the problem of sparse 3D input data is addressed. The results of the DMR approach, which has been explained in Chapters 2 and 3, will suffer from aliasing if the loci of possibly contributing time samples in the input data set are not sampled sufficiently densely, i.e. if the weighted summation is performed on sparsely sampled data. To prevent this from happening, the DMR approach has to be combined with a data interpolation or data infill step prior to the application of the stack.

The first section of this chapter reviews the existing methods of data interpolation and regularization (Section 5.1) and evaluates their applicability to the problem at hand. Thereafter, the theory of the chosen 'DELPHI trace replacement'-method (DTR) is explained (see Section 5.2), and the implementation of this method as part of the DMR approach is described (see Section 5.3). In the end, assumptions being made for the DTR are discussed, and their implications with respect to the application in the DMR approach are listed (see Section 5.4).

5.1 Existing methods

A literature study on methods for the reconstruction, regularization and interpolation of seismic data reveals numerous approaches. In general, these approaches can be categorized in two classes:

- data mapping methods,
- signal processing methods.

A brief overview of these two categories is given here, followed by a discussion about which method is most appropriate for the application in the DMR approach.

5.1.1 Data reconstruction by data mapping approaches

This first class of methods to reconstruct missing seismic data bases on the principles of Kirchhoff data mapping (KDM) as explained in Chapter 2. They are utilized:

[**1**] to create zero-offset data from traces with non-zero offsets by applying a DMO operator [see Deregowski, 1986; Hale, 1991],

[**2**] to perform offset continuation by applying an offset move-out (OMO) operator [see Bagaini and Spagnolini, 1996; Spagnolini and Opreni, 1996],

[**3**] to reconstruct missing shot gathers by applying a shot continuation (SCO) operator [see Bagaini and Spagnolini, 1996],

[**4**] to create traces at arbitrary offsets and azimuths by applying the AMO operator [see Biondi et al., 1998].

It can be stated that the underlying principle of KDM methods utilized to reconstruct missing seismic data is to exploit their redundancy. A continuation operator is applied to the available input data set, and, thereafter, a weighted summation is performed on the corrected traces yielding the desired result. The application of this operator to the input data can be equated with the construction of a locus of possible contributing time samples. For the construction of the continuation operator all KDM approaches, including the DMR approach, assume some knowledge of the subsurface to be imaged. Usually, a constant medium is adopted for this purpose, whose velocity is related to the stacking velocity of the desired output sample.
Generally speaking, the DTR approach as described by Gisolf [2002] and van de Rijzen et al. [2003, 2004] can also be classified as a data mapping technique, although it has to be considered as a simplified version. As for the other KDM techniques, the DTR method utilizes the large redundancy of seismic data. However, all KDM techniques mentioned above make certain subsurface assumptions to create a surface

of possible contributing reflection points. They translate this information into continuation operators and, finally, calculate the desired output sample by applying a Kirchhoff summation to the input data, which have been corrected by the operators. For these techniques the exact location of the true reflection point belonging to the considered event is unknown. It is only implicitly determined by performing the Kirchhoff summation. In contrast to this, the DTR method assumes the position of the reflection point as well as the angle of incidence of the wave reflected at this point and recorded at the considered time sample to be known. If this information is available, the application of the Kirchhoff summation, i.e. the implicit determination of the position of the true reflection point, becomes superfluous. In fact, the a-priori information about the position of the reflection point and the angle of incidence is employed in the DTR approach to search the input data set for a trace that contains the reflection event from the considered reflection point reflected under the same angle of incidence as the event belonging to the desired output sample. Once this trace has been found, the time sample corresponding to the considered reflection event can be used for the reconstructed trace. It can thus be stated that the DTR approach is a simplified data mapping technique using a-priori information.

In conclusion, all data mapping approaches to reconstruct missing data employ the redundancy of seismic data based on the principles of wave propagation. However, they all need information about the subsurface and errors made in the assumed subsurface medium will have a deteriorating effect on the outcome of the data reconstruction. Besides this, all reconstruction techniques employing the KDM methodology, apart from the DTR approach, are computationally expensive, because they require the calculation of summations along multiple dimensions.

5.1.2 Data reconstruction by signal processing approaches

The second group of data reconstruction techniques is based on the principles of signal processing and not necessarily restricted to seismic data. They employ either transforms or a filter to the input data to create a regularly and densely sampled data set.

Transform-based methods

The methods of this class apply a cascade of transform and inverse transform. The forward transform is applied to an irregularly, sparsely sampled input data set yielding a regularly sampled data set in the transform domain. Thereby, the estimation of the transform coefficients is formulated as an inversion problem. Then, an inverse transformation is applied to compute the data on the desired grid. The transforms being used for these data reconstruction methods are, for example, the Fourier transform [see Hindriks et al., 1997; Duijndam et al., 1999; Zwartjes, 2005] or the Radon transform [see Thorson and Claerbout, 1985; Kabir and Verschuur, 1995].

All methods named here can be fast, if the transforms are implemented efficiently, and they are independent of information about the subsurface. However, as stated by Zwartjes [2005], they can produce incorrect results if the input data are non-bandlimited or aliased.

Filter-based methods

The second category of the signal processing approaches to data reconstruction are filter-based methods. Here, a filter is designed to interpolate the sparsely sampled spatial domain. Examples for the filter-based methods are Spitz [1991], who employed prediction-error filters in the $f-x$ domain to interpolate locally flat events, and Crawley et al. [1999], who applied prediction-error filters to interpolate non-stationary events. According to Zwartjes [2005], the first method mentioned here is limited by the assumptions made about the shape of the events and is restricted to relatively small gaps. The first problem has been fixed in the approach developed by Crawley et al. [1999]. However, this improvement is achieved at the costs of higher computational costs and a higher dependency on numerous parameters.

5.1.3 Reasons to chose the DELPHI trace replacement method

For the selection of a data reconstruction technique to be used in combination with the DMR method, the requirements of the DMR approach and the information provided by the DMR approach, that could facilitate certain reconstruction methods, have to be considered.
As mentioned previously, the DMR approach needs the locus of time samples possibly contributing to the desired output sample to be sampled sufficiently densely. Hence, missing time samples along this locus have to be filled in correctly. A complete and correct reconstruction of the traces belonging to the missing time samples is not necessary, however. This is, because the isochrones of possible reflection points in the subsurface defining the locus will be different for the calculation of every output sample. Consequently, the locus indicating the possibly contributing time samples of the input data set changes for the calculation of every output sample, and there will be different time samples belonging to different traces that are missing. The aim of the data reconstruction is, therefore, not to produce missing traces and to create a densely sampled input data set but to provide only the required time samples. This indicates already that the data mapping techniques for data reconstruction are particularly well suited for this situation. They are preferable to the signal processing methods, because these methods cannot be utilized for the reconstruction of single time samples due to their underlying principles.
Besides this, the information provided by the DMR approach, which is available as a-priori information for the data reconstruction, has to be taken into account. As explained in Chapters 2 and 3, the first step of the DMR methodology is to create an isochrone of possible reflection points belonging to the considered output sample. This information is then translated into a locus of possibly contributing time

samples in the input data set. In other words, during the application of the DMR approach, the reflection point positions belonging to the time samples along the locus are determined and can be used as a-priori information for the data reconstruction. Moreover, the angle of incidence at these reflection points can be determined easily. It can be calculated from the position of the reflection point belonging to the missing time sample and from the source and receiver position at the new datum by simple trigonometry. With this information being available the DTR method is the logical choice for the reconstruction of missing time samples in the DMR approach.

5.2 Theory of the DTR method

The Delphi trace replacement (DTR) method is based upon two basic assumptions:

- The reflectivity of a certain reflection point at a target reflector is independent of the azimuth.
- Two-way transmission losses can be ignored.

Both these assumptions are in concordance with the principles of modern 3D acquisition design. There, it is always aimed to achieve a large fold at the target reflector. However, a regular azimuthal illumination of the target points is not specifically aimed for. That is, data acquisition is carried out with the implicit understanding that the reflectivity of a reflection point is independent of the azimuth. Similarly, two-way transmission losses are ignored in all commonly used migration algorithms. The foregoing suggests that traces recorded at two different source/receiver pairs $(\mathbf{x}_s, \mathbf{x}_r)$ and $(\mathbf{x}_s^{'}, \mathbf{x}_r^{'})$ contain identical information regarding the target reflector if the rays belonging to the considered reflection event reach the same reflection point $\mathbf{x}_{iso}$ with an identical angle of incidence α (see Figure 5.1). Here, I use the subscript $_{iso}$ to describe the reflection points, because these points will be points on the elliptical isochrone if this method is applied to infill missing time samples in the DMR process. As a consequence, the time sample $p(\mathbf{x}_s, \mathbf{x}_r, t_e)$, which belongs to the considered reflection event, can be replaced by a time sample on the trace corresponding to $(\mathbf{x}_s^{'}, \mathbf{x}_r^{'})$:

$$p(\mathbf{x}_s, \mathbf{x}_r, t_e) \approx p(\mathbf{x}_s^{'}, \mathbf{x}_r^{'}, t_e - \Delta t_{DTR}). \qquad (5.2.1)$$

Δt_{DTR} is the difference in the two-way traveltimes of the reflection event considered at the missing source/receiver pair and the acquired source/receiver pair, which is used for the infill. Δt_{DTR} will only be zero if the reflector is horizontal and the medium between target point and acquisition surface is laterally homogeneous. This difference in two-way traveltime between the two samples at the locations $(\mathbf{x}_s, \mathbf{x}_r)$ and $(\mathbf{x}_s^{'}, \mathbf{x}_r^{'})$, that cover the same reflection point under the same angle of incidence, can be calculated from the one-way traveltimes from the locations $\mathbf{x}_s$, $\mathbf{x}_r$, $\mathbf{x}_s^{'}$, and

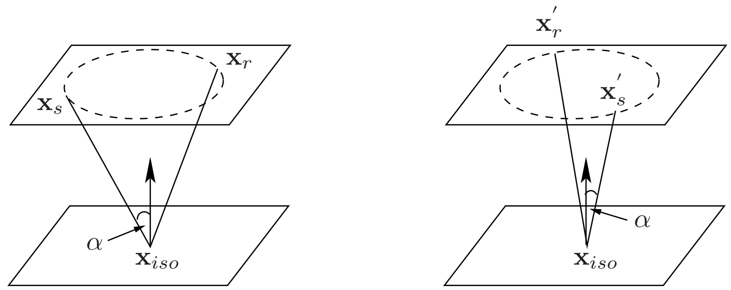

Figure 5.1: *Rays belonging to different source/receiver pairs reach the same reflection point with an identical angle of incidence.*

$\mathbf{x}_r^{'}$ to the reflection point.
As different traveltimes also mean different spherical spreading, one could apply an amplitude correction for these effects:

$$\begin{aligned} p(\mathbf{x}_s, \mathbf{x}_r, t_e) &= a_{DTR} p(\mathbf{x}_s^{'}, \mathbf{x}_r^{'}, t_e - \Delta t_{DTR}), \\ a_{DTR} &= \frac{a_{sr}}{a_{s'r'}}. \end{aligned} \tag{5.2.2}$$

Here, a_{sr} and $a_{s'r'}$ are the amplitudes belonging to the events at the different locations $(\mathbf{x}_s, \mathbf{x}_r)$ and $(\mathbf{x}_s^{'}, \mathbf{x}_r^{'})$. For the work presented in this thesis the choice has been made to apply the ratio of the different two-way traveltimes as amplitude correction. It should be stressed, again, that the position of the target point $\mathbf{x}_{iso}$ and the local dip δ_{iso} in this point need to be known to find the trace and the time shift that provide the missing information. Note, however, that this information is available for the DMR approach.
Furthermore, it should be noted that the given relationship is only valid for the primary reflection at the target point. It is not valid for reflections from other interfaces or multiples; i.e. if, for other applications than in DMR, it is intended to reconstruct traces the whole procedure has to be repeated for every single time sample.

5.3 Implementation of the DTR approach

An important aspect with respect to the application of the DTR approach is its implementation. The way of finding a source/receiver pair that contains the required time sample is crucial. Unfortunately, the search algorithm described by van de Rijzen et al. [2004] is not suited for the redatuming situation. This algorithm has been designed to replace missing traces in the estimation of 3D CFP gathers from sparsely sampled input data, using fully sampled 3D focusing operators. The focal

points of these focusing operators – one-way wave-propagation operators – are positioned along the target reflector of the considered event. Apart from the one-way traveltimes, these operators also contain information about their focal point position and the angles of incidence at these focal points. For their search routine they firstly regroup the operators from common focus point gathers to common surface point gathers, so-called transposed operators. Then they estimate the stationary reflection point for every source/receiver pair at the acquisition surface employing Fermat's principle of minimum two-way traveltime; the required two-way traveltimes are calculated from the transposed operators belonging to the considered source and receiver positions. Once this stationary reflection point is known, the reflection angle of the specular reflection at this point can be determined as well. The result of this procedure is a table containing the reflection point positions and reflection angles for all source/receiver pairs. This table can then be utilized to find an acquired source/receiver pair for every missing pair, which has an identical stationary reflection point and reflection angle.
Operators with focal points at the target reflector are not available for redatuming. This excludes the described search algorithm. Hence, a different approach to perform this search needs to be developed, and it has to be designed for the information available from the DMR method. This information, which is available for the DMR approach, or which becomes available during the application of the DMR approach, is the following. Fully sampled 3D redatuming operators are provided, whose focal points are located along the datum. The positions of the reflection points belonging to the considered time samples and the medium in-between those points and the new datum are known by the imposed assumptions of a velocity field below the datum and the scanning over all possible reflector dips inherent in the ellipsoid. This knowledge is utilized in a new search algorithm, which is solely based on geometrical considerations. The flowchart presented in Figure 5.2 describes this search routine for a certain time sample. As one can see, the following steps have to be performed:

[1] A contour at the new datum is determined indicating all source/receiver pairs $\tilde{\mathbf{x}}'_{s,r}$ with rays reaching the considered isochrone point under the same angle of incidence as the rays belonging to the missing time sample (see Appendix D). This contour constitutes the intersection of a cone and the new datum. The cone has its apex position at the considered isochrone point at the ellipsoid describing all possible reflection points, and it indicates all rays leaving this point under the considered angle of incidence.

[2] Redatuming operators are selected which have their focal points on or near this contour. The relative error ε_O of their focal point position with respect to the contour is recorded.

[3] All surface locations corresponding to the points along the contour on the new datum are determined by continuation to the surface of the rays from the isochrone point to the new datum. That is, all source/receiver pairs at a densely sampled acquisition surface are defined which correspond to the required pair. Traces acquired at these positions contain time samples which can be used to replace the missing one. The continuation of the rays of the cone from the datum to the acquisition surface is accomplished in exactly the same way as it has been done for the construction of the locus using the selected, fully sampled 3D redatuming operators (see Chapter 3). The relative error ε_ϱ of the ray parameter belonging to the selected surface position with respect to the ray parameter describing the considered ray on the cone is recorded.

[4] From all source/receiver locations at the surface that are found this way, one is selected that corresponds to a trace that has actually been acquired in the sparse data set. The relative error ε_S of the positions of the acquired pair with respect to the desired one is recorded.

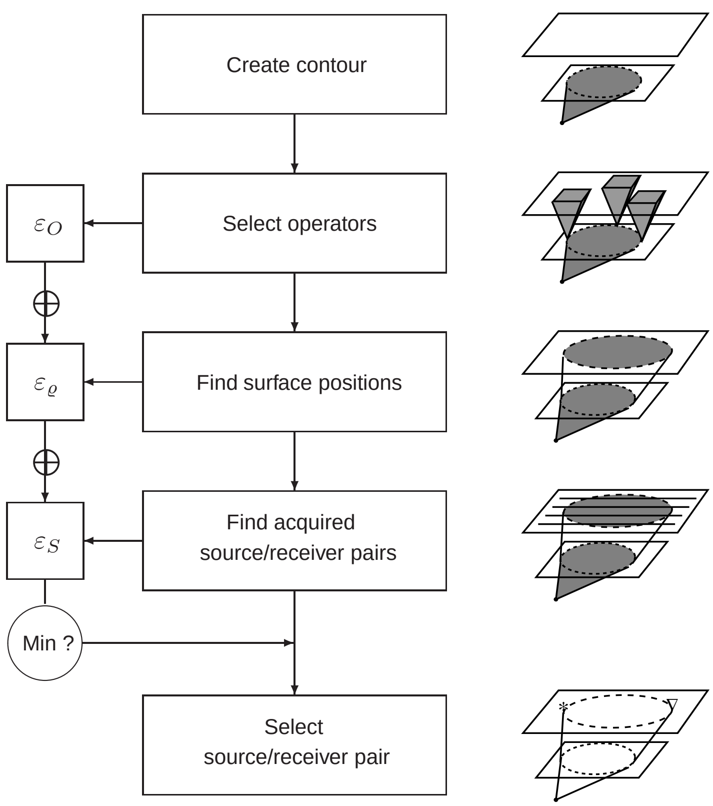

Figure 5.2: *Flowchart describing the search for an acquired source/receiver pair which is suitable to replace a missing pair if the DMR approach is applied to sparsely sampled data.*

[**5**] All relative errors are added and the source/receiver pair $\mathbf{x}'_{s,r}$ with the minimum relative error out of all selected pairs is chosen.

Once the trace has been selected, the desired time sample can be extracted according to Equation 5.2.2.

5.4 Assumptions and limitations

The DTR method has been chosen for the infill of missing time samples if the DMR approach is applied to sparsely sampled input data. As described above, the reconstruction of a time sample by means of the DTR methodology will only be correct if the isochrone point under consideration is an actual reflection point. For all other isochrone points the infill may not be correct, but since only the true reflection locations survive the isochrone stack, at least we can be sure that for that location the possible infill was correct. This is discussed further in Section 5.4.1. The search and infill, if the required trace is not in the data set, has to be repeated for every point on the isochrone.
As with so many things, the ultimate proof of a concept are experiments. We have proved the concept by the experiments presented in Chapter 6. It is recommended, however, to perform more detailed tests to evaluate further the assumptions and limitations discussed here.

5.4.1 Isochrone point is not a reflection point

The fact that the DTR method delivers correct results only if the considered isochrone point is an actual reflection point needs to be investigated further with respect to its application in the DMR approach. For our redatuming approach the isochrone is the locus of all possible reflection points belonging to the considered output sample. These possible reflection points are used to identify possibly contributing time samples in the input data set. Only very few of these points are true reflection points, even if the subsurface is complex. All other isochrone points are not positioned on a true reflector. Missing time samples due to sparseness of the input data, however, will not only be related to the true reflection points. They will also be related to points which are not true reflection points, and, as a consequence, their reconstruction will be incorrect. Hence, the influence of these errors in the reconstruction of missing time samples on the redatuming result needs to be evaluated.
Here, two situations need to be considered separately:

[**1**] the missing time sample belongs to an isochrone point in the vicinity of a true reflection point,

[**2**] the missing time sample belongs to an isochrone point further away from a true reflection point.

■ In the vicinity of a true reflection point

For the first case, it can be assumed that the error of the reconstruction is small, because the error in the position of the reflection point is negligible. This is similar to the situation described by van de Rijzen et al. [2004], where it was claimed that errors in the Green's functions have a negligible effect on the infill process.

■ Far away from a true reflection point

For the second case, the fact that the isochrone point is not near a true reflection point leads to errors in the selection of the source/receiver pair used in the reconstruction, and it leads to an incorrect calculation of the correction parameters Δt_{DTR} and a_{DTR}. However, the effect of these errors in the reconstruction depends on which of the following two situations applies:

[**1**] the azimuth difference between the missing source/receiver pair and the one selected for replacement is small,

[**2**] the azimuth between the missing source/receiver pair and the one selected for replacement is large.

○ Small azimuth between missing trace and selected trace

If the azimuth between the missing and the selected pair is small, the two raypaths belonging to those pairs, which have been constructed for the infill, will be very similar, unless the datum layer is very complex (see Figure 5.3).

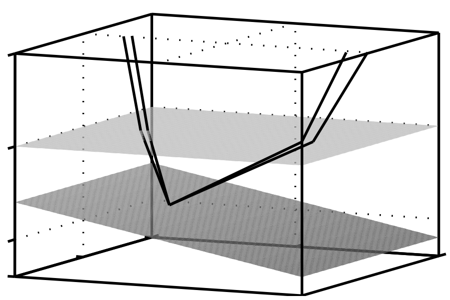

Figure 5.3: *Rays belonging to different source/receiver pairs reach the same reflection point with an identical angle of incidence. Here, the situation of a small azimuth between the missing trace and the selected trace is presented.*

This implies that the time-correction parameter Δt_{DTR} is close to zero. For traces acquired in the vicinity of each other (similar azimuth and offset) events recorded at similar traveltimes will belong to the same reflector if the subsurface is not very complex. These events can, therefore, be described by similar true raypaths. Because of this, the amplitude of the selected time sample is similar to the amplitude the missing time sample would have had, if it had been acquired. It can thus be assumed that the error of the reconstruction is small and, therefore, negligible for the redatumed result.

- **Large azimuth between missing trace and selected trace**

As already mentioned, the selection of the source/receiver pair as well as the calculated correction parameters are incorrect if the considered isochrone point position is not at a true reflection point. If the azimuth between the required and the selected source/receiver pair is large, it can no longer be assumed that this incorrectly selected time sample is similar to the time sample that would have been used if the missing trace had been acquired (see Figure 5.4). Consequently, the error made in this situation cannot be neglected.

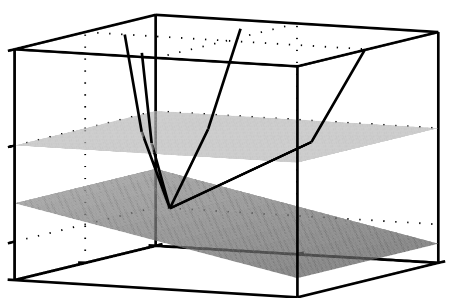

Figure 5.4: *Rays belonging to different source/receiver pairs reach the same reflection point with an identical angle of incidence. Here, the situation of a large azimuth between the missing trace and the selected trace is presented.*

In conclusion, it can be stated that the errors made in the data reconstruction, which cannot be neglected, occur only for missing time samples belonging to possible reflection points further away from the the true reflection point. The time samples in the vicinity of the apex of the locus are correct. Further away from the apex position of the locus the reconstructed time samples can occur at an incorrect position in time and/or with an incorrect amplitude. The redatumed time sample, which is the result of a weighted summation applied along the locus, is still correct, because all possible contributing time samples which interfere constructively (inside the Fresnel zone) are correct. However, if the errors in timing and/or amplitude lead to strong discontinuities, they can still have an effect. They can be interpreted as irregularities of the locus which destroy the destructive interference of the contributions outside the Fresnel zone. If that happens, artifacts can occur in the redatumed result. However, if the errors in the infill do not cause discontinuities along the locus but show a smooth behavior, no artifacts will be produced by the stack.

5.4.2 Discrete sampling of input data sets

It is assumed that at least one trace of the sparsely sampled input data set is available exactly at the infill contour pointing out all surface locations that could be used for the data reconstruction. However, seismic data acquisition yields a discrete sampling of the wavefield. It is likely, therefore, that no trace exists with source and receiver exactly on the infill contour. Instead, a trace closest to the contour is selected.

Furthermore, the sampling of the acquisition surface is not random. The data sets usually consist of several subsets, which all have the same geometry like marine parallel lines and cross-spread geometries at land. It is, therefore, likely that traces from a certain area are reconstructed by traces from one subset, and that the transition from one subset to another neighboring subset happens abruptly. This effect might cause the event on the set of corrected traces before the isochrone stack is applied to be discontinuous (see Figure 5.5). It is very clear, that the stack of such an event will produce artifacts in the redatumed result.

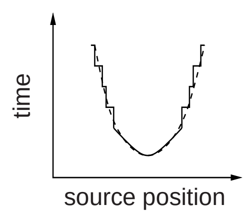

Figure 5.5: *Discontinuities of the considered event as it might appear in a very extreme case on the corrected traces before the final stack is applied. Abrupt changes from one subset of the 3D data set to the neighboring one could cause these kind of discontinuities.*

5.4.3 Recommendations

The occurrence of both artifacts, the one mentioned in Section 5.4.1 and the one mentioned in Section 5.4.2, could probably be suppressed if the requirements imposed on the selection of possibly contributing time samples for the DMR approach were eased. One could, for example, decide to use any trace belonging to a considered reflection point instead of restricting the search only to traces with a certain angle of incidence. By doing this, an incorrect amplitude of the selected time sample is accepted. However, the occurrence of unwanted artifacts due to an incorrect infill could be prevented as well. It is probably the best to develop an optimization strategy, that automatically decides whether to replace the missing time sample by means of the DTR method or to use a time sample of an acquired trace, which contains a reflection event from the considered reflection point but with a different angle of incidence at that point.

6

Evaluation of the DMR methodology with 3D data examples

Gibt es einen Unterschied zwischen Theorie und Praxis ?
Es gibt ihn. In der Tat.
Werner Mitsch (1936 -)

In this chapter the DMR approach is evaluated on fully sampled and sparsely sampled 3D data sets. The intention is to examine whether the DMR amplitude corrections have been extended correctly to the 3D situation. Besides this, it needs to be tested whether the infill by means of the DTR methodology, which is needed in case of sparsely sampled input data sets, has been implemented correctly.
Below, the objectives of the different experiments are listed.

[**1**] The trace-selection parameters and amplitude weights need to be verified for the 3D situation. As for the 2D situation, the DMR approach is applied to fully sampled seismic data from a velocity model using a constant velocity below and above the new datum level. In this situation the assumptions made about the background medium below the new datum layer are satisfied and the trace-selection parameters and amplitude weights can be calculated analytically. Consequently, no numerical errors influence the result.

[**2**] The applicability of the proposed infill method needs to be tested. The DMR

approach is, therefore, applied to a sparsely sampled input data set using the velocity model which has been used for the first test. In this situation the infill contour needed for the trace selection as well as the time shifts and amplitude corrections belonging to the selected trace can be calculated analytically. As a consequence, the infill is not influenced by numerical errors.

[**3**] The applicability of the DMR approach for a more realistic medium below the new datum level needs to be tested. The DMR approach is, therefore, applied to a fully sampled 3D data set using a velocity model with a constant velocity above the new datum level and a complex velocity structure below the datum.

[4] It needs to be examined whether the proposed DTR approach to infilling missing data works if the medium below the new datum level is complex. The DMR approach combined with the infill step is, therefore, applied to a sparsely sampled 3D data set using the velocity model which has also been used for test 3.

[**5**] The ultimate test of a newly developed methodology certainly is its application to realistic seismic data. This has been done by applying the DMR approach to a sparsely sampled 3D data set, which has been acquired over a scale model.

6.1 Simple model – homogeneous datum layer; fully sampled input data

In this test the DMR approach is applied to a very simple input data set. The purpose of this test is to examine whether the method has been extended correctly to the 3D situation. The model used to create the synthetic 3D data is presented in Figure 6.1. It consists of a homogeneous velocity layer ($v_1 = 1500\,{}^{\mathrm{m}}\!/\!{}_{\mathrm{s}}$) above the new datum at 300 m. Below the datum the velocity is constant ($v_2 = 2500\,{}^{\mathrm{m}}\!/\!{}_{\mathrm{s}}$) as well. Reflections from this area are caused by differences in the densities. Note, that the reflectors below the datum are dipping in both in-line and cross-line direction. A synthetic data set modeled with a moving spread geometry serves as input for this first test. Hereby, 3D ray tracing has been employed. As shown in Figure 6.2 the source layout is 0 m to 900 m in the in-line direction and -300 m to +300 m in the cross-line direction. The source spacing in either direction is 15 m. The maximum receiver offsets are ± 1500 m in the in-line direction and ± 300 m in the cross-line direction. The receiver spacing is 15 m in both directions.
For this fully sampled 3D data set a 2D line at the new datum level is computed. The source position at the new datum is (300 m,0 m), the receivers range from 300 m to 900 m in in-line direction with a cross-line offset of 100 m; i.e. a truly 3D problem is handled.

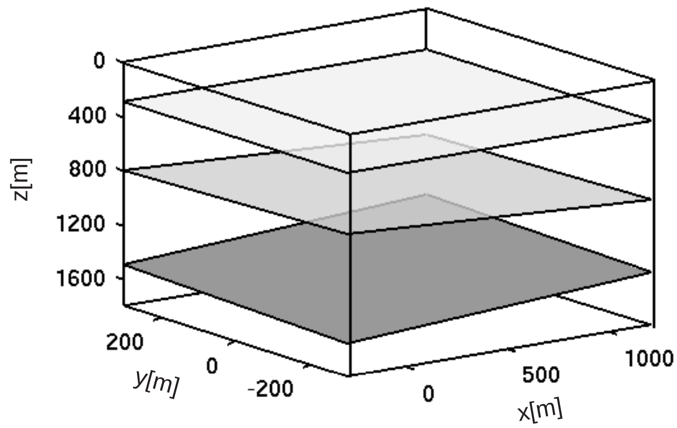

Figure 6.1: *3D velocity model with a homogeneous datum layer and a simple subsurface below the datum.*

It is important to note that for the calculation of one output sample by means of the DMR approach only about 900 traces of the full data set were used. This is a tremendous reduction of data used in the redatuming process and gives an idea about the potential of this DMR approach with respect to the reduction of computational costs.
In Figure 6.3 the desired result computed by the KSR method applied to the fully sampled 3D data set and the result of the DMR method are compared. Apparently, the reflection events have been reconstructed correctly. They appear at a correct position in time and the phase of the redatumed events is correct as well.

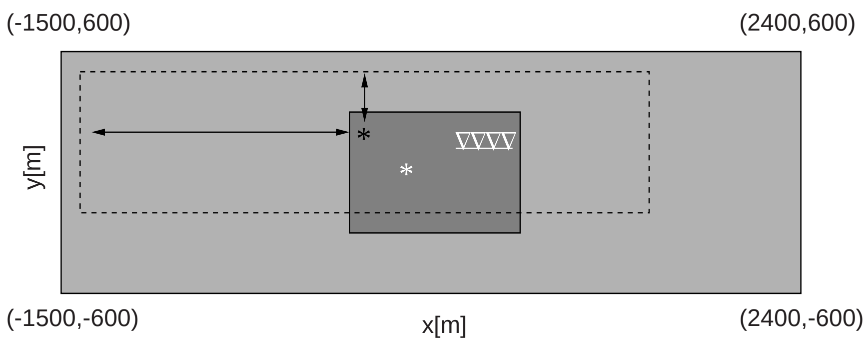

Figure 6.2: *Acquisition geometry of the data set computed for the simple velocity model. The receivers are distributed with dense sampling all over the light gray area. The sources are distributed with dense sampling all over the dark gray area. The dashed line indicates the receiver spread for one particular source position. The geometry of the redatumed shot gather is indicated by the white symbols.*

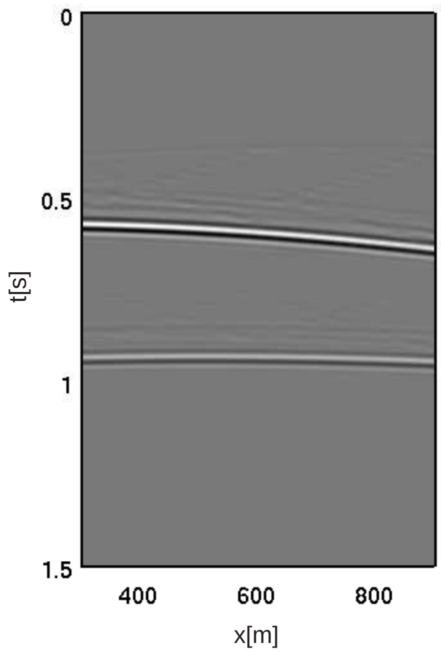

(a)

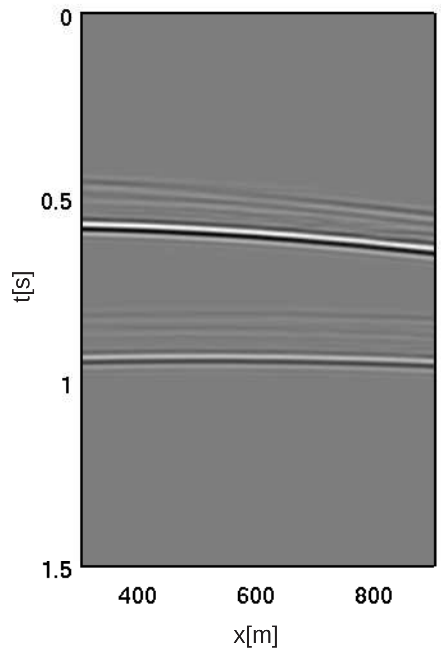

(b)

Figure 6.3: *Comparison of (a) the redatumed shot gather computed by conventional redatuming and (b) the redatumed shot gather computed by the DMR approach.*

However, to evaluate the quality of the redatuming result more closely traces representing the near-offset and the medium-offset range are selected. In Figure 6.4a and Figure 6.4b the traces with absolute amplitudes are compared with the results of the KSR approach, which were obtained by calculating the full 4D integral. The redatumed events on these traces show no errors in the timing, and the absolute amplitudes match very well. The events have been reconstructed dynamically and kinematically correct.

The results of this first test on fully sampled 3D data imply, therefore, that the DMR method has been extended correctly to the 3D situation.

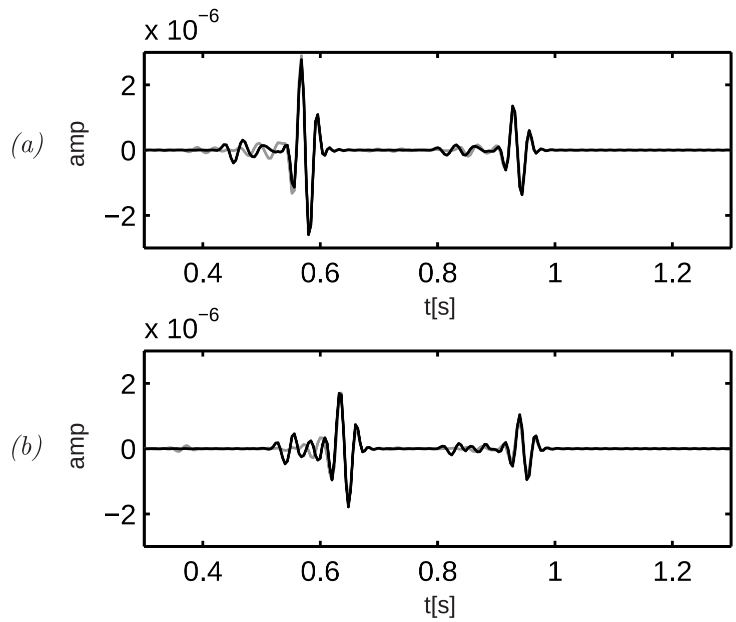

Figure 6.4: *Comparison of redatumed traces computed by the DMR approach (black line) and the KSR approach (gray line) for an in-line offset of (a) 0 m and (b) 600 m.*

6.2 Simple model – homogeneous datum layer; sparsely sampled input data

Next, the applicability of the proposed DTR approach to infilling missing data needs to be examined. For this purpose, a redatumed shot gather is computed for a sparsely sampled input data set utilizing the DMR method combined with the proposed infill approach. The velocity model underlying this data set has been described in the previous section.

This time the input data set consists of 2D lines (see Figure 6.5). The sources are ranging from 0 m to 900 m in the in-line direction. The source spacing in in-line direction is 15 m. For every 2D line a split-spread geometry has been chosen with a maximum receiver offset of 1500 m and a receiver spacing of 15 m. The cross-line spacing between the 2D lines is 50 m.

In Figure 6.6a the desired result is presented, which is, this time, a redatumed shot gather computed by means of the DMR approach applied to a fully sampled input data set. Figure 6.6b shows the redatuming result for sparsely sampled input data. It has been calculated using the DMR method in combination with the proposed infill approach.

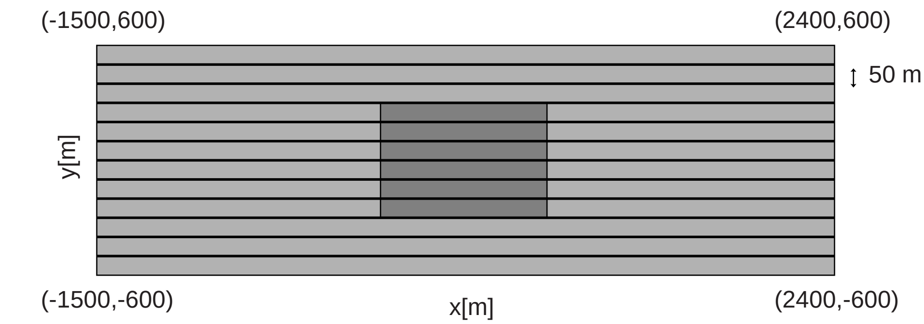

Figure 6.5: *Acquisition geometry of the data set computed for the simple velocity model. For the fully sampled data set the receivers were distributed with a dense sampling all over the light gray area; the sources were distributed with a dense sampling all over the dark gray area. For the sparse input data set sources and receivers were distributed only along the lines.*

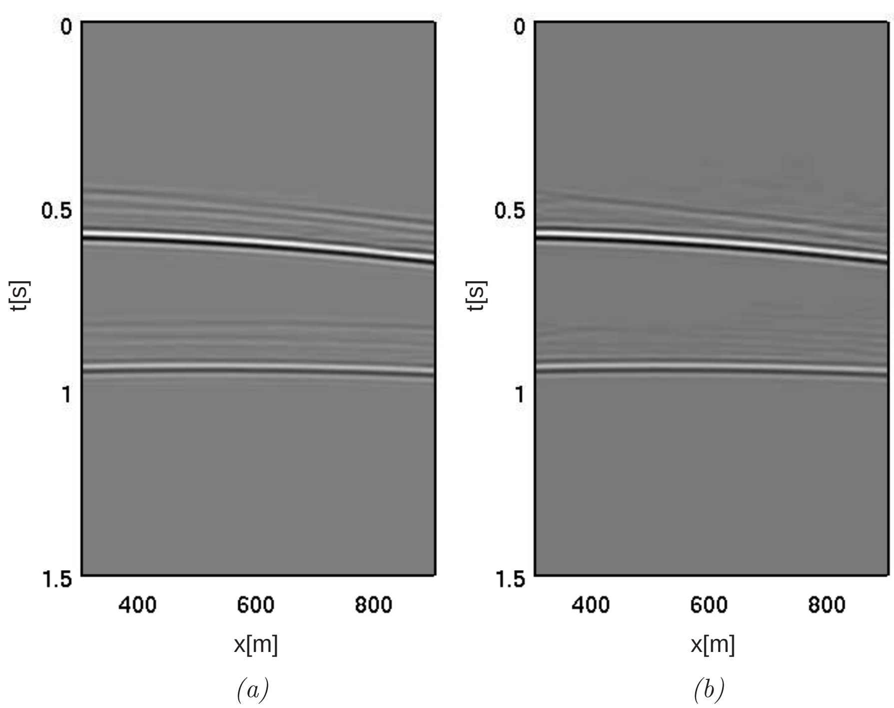

Figure 6.6: *Comparison of (a) the redatumed shot gather computed by the DMR method for fully sampled input data (same as Figure 6.3b) and (b) the redatumed shot gather computed by the DMR approach combined with the infill for sparsely sampled input data.*

(a)
(b)

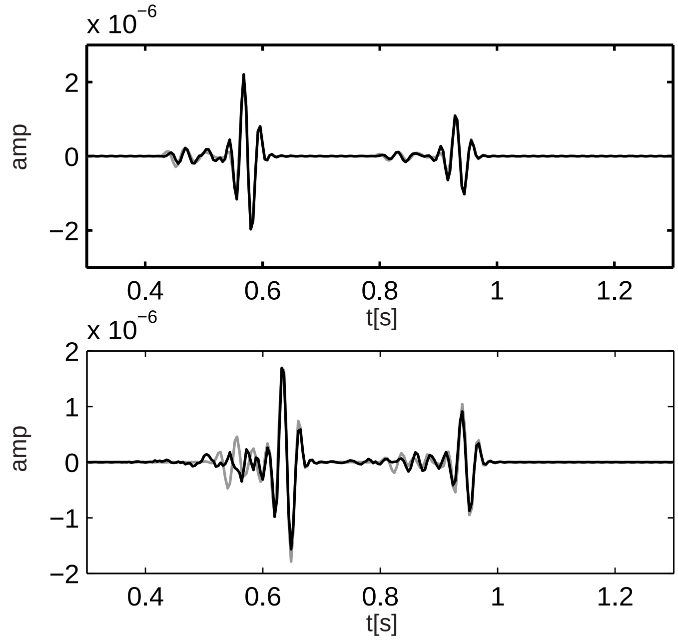

Figure 6.7: *Comparison of redatumed traces computed by the DMR approach for fully sampled data (gray line) and for sparsely sampled data (black line) for an in-line offset of (a) 0 m and (b) 600 m.*

A comparison of these redatumed shot gathers reveals that the proposed infill approach works. The results are kinematically and dynamically correct. This can also be seen in Figure 6.7a and Figure 6.7b, which provide a comparison of redatumed traces for two offsets.
Hence, it can be concluded that the DMR method combined with the proposed infill approach produces kinematically and dynamically correct results for sparsely sampled 3D input data.

6.3 Complex model – homogeneous datum layer; fully sampled input data

The purpose of the experiments presented in this and in the following section is to assess whether correct redatuming results can be obtained from fully and sparsely sampled 3D data sets by means of the DMR approach if the subsurface model is complex. The velocity model used to compute the synthetic data sets is displayed in Figure 6.8. It is the so-called EAGE/SEG Overthrust model combined with a homogeneous datum layer of 500 m thickness and a velocity of 2000 $^{m}/_{s}$ [see Aminzadeh et

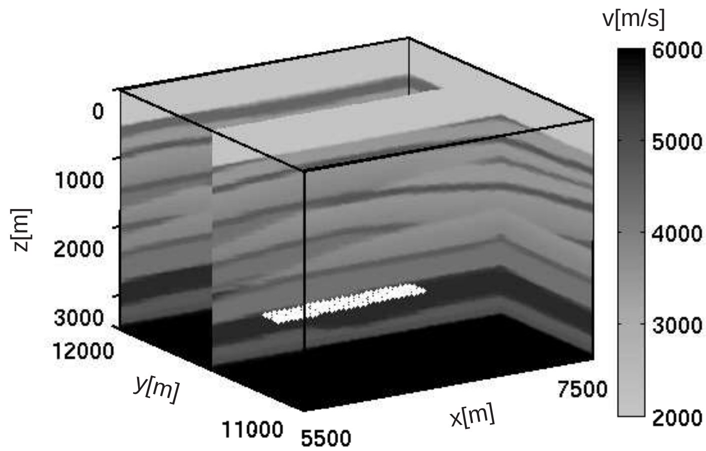

Figure 6.8: *3D velocity model with a homogeneous datum layer and a complex subsurface below the datum. The target points are indicated by the white dots.*

al., 1994, 1996]. Since the modeling of a full 3D data set would have taken too long, it was decided to create the input data by target-oriented modeling; i.e., reflection points were distributed along a target reflector and one-way operators were modeled between these points and the acquisition surface. All required traces of the input data set were composed from these operators. One major drawback of this fast modeling approach for the 3D situation is that the resulting data set contains only one reflection event. However, this reflection event is part of a complex subsurface, and, therefore, the data are considered adequate for the intended experiments.
The target points at the reflector are positioned between 5775 m and 6525 m in the in-line direction and from 11375 m to 11625 m in the cross-line direction. They are sampled with 25 m in both directions. The surface positions range from 25 m to

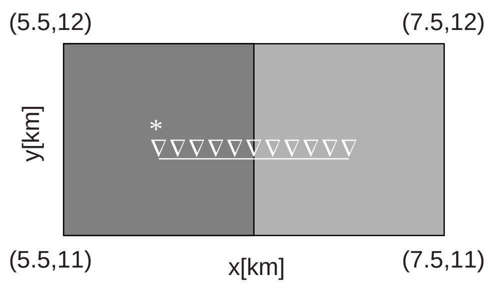

Figure 6.9: *Acquisition geometry of the data set computed for the complex velocity model. The receivers used for the KSR approach were distributed with a dense sampling over the whole area; the sources are distributed with a dense sampling all over the dark gray area. The geometry of the redatumed shot gather is indicated by the white symbols.*

12975 m in the in-line direction and from 9025 m to 13975 m in the cross-line direction with a sampling of 25 m in both directions.
From these operators all traces that were required during the DMR process were built. For the calculation of the desired result by means of the KSR method the possible input traces were restricted beforehand to a maximum aperture of 500 m with respect to the positions of the redatumed source and receivers. This was done to reduce the computation time for this method. However, the critical angle at the datum level, which limits the aperture of the possible contributing sources and receivers, is expected to be smaller than 45°. Hence, all contributing sources and receivers are expected to lie well inside this maximum aperture. The surface positions used for the KSR approach are shown in Figure 6.9. The source and receiver positions of the possibly contributing traces for the DMR approach will be inside this area as well.
In Figure 6.10 one modeled shot gather and two redatumed shot gathers are compared. The source is positioned at (6000 m,11625 m), the modeled receivers range from 5000 m to 7500 m in the in-line direction and the redatumed receivers range from 6000 m to 7500 m. The cross-line offset between source and receiver line is 250 m.
Figure 6.10a illustrates the shot gather, which has been modeled with the source and the receivers at the new datum level. Here, another effect of the technique

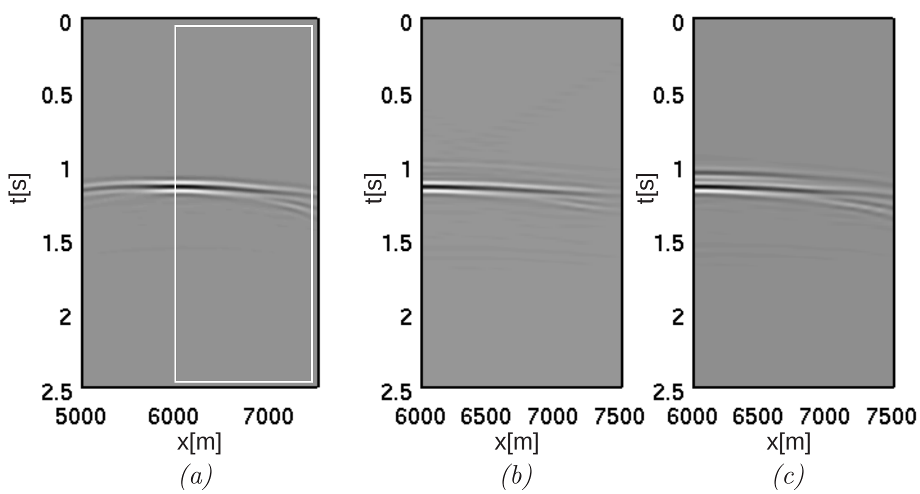

Figure 6.10: *Comparison of (a) a modeled shot gather referenced to the new datum level, (b) the redatumed shot gather computed by the KSR approach and (c) the redatumed shot gather computed by the DMR approach. The box in (a) refers to the reconstructed offsets in (b) and (c).*

used to build the data set becomes obvious. The constructed event shows only in the area directly above the target points the characteristics of a reflection event. Towards the edges of this area the event becomes more diffuse. This is, because it no longer resembles a reflection event; instead it has to be considered a diffraction event. However, the DMR approach has been implemented such that reflections from reflectors that are not strongly curved are reconstructed correctly. Redatumed diffractions exhibit small errors of the absolute amplitudes (see Chapter 4). Therefore, this experiment can also be interpreted as a test on 3D diffracted events.
In Figure 6.10b and Figure 6.10c the redatumed shot gathers are presented, which show the desired result computed by means of the KSR approach and the result of the DMR method, respectively. Again, it can be concluded, that the DMR approach delivers satisfying results. The reflection event occurs at the correct position in time, and the phase has been reconstructed correctly. Even the diffraction, which occurs for offsets larger than 7000 m as second event, has been reconstructed correctly. Only an artifact occurring prior to the reflection event is treated differently by the two approaches.
The occurrence of this artifact can, again, be related to the limited aperture of the input data set. This can also be seen in Figure 6.11. It shows all selected and corrected traces prior to the final stack for the calculation of the redatumed time sample $t_{red} = 1.2\,\mathrm{s}$ of a trace with the source at (6000 m,11625 m) and the receiver at (6500 m,11375 m) by means of the DMR approach. Note here, that this is a 2D display of a cube. Every panel of 20 traces belongs to a certain position in y-direction

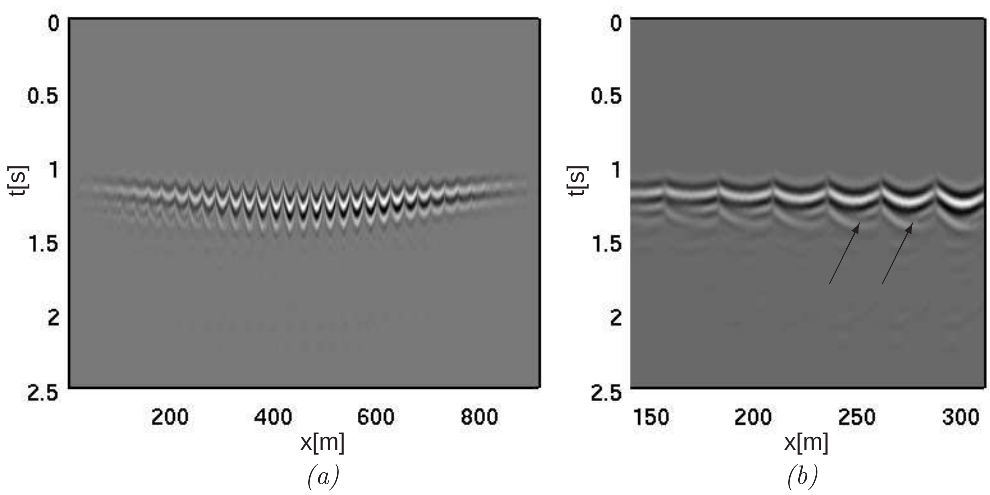

Figure 6.11: *(a) Selected and corrected traces prior to the final stack for the calculation of one redatumed time sample by means of the DMR approach. (b) Subset of these traces. The arrows indicate the contributions to the diffraction event.*

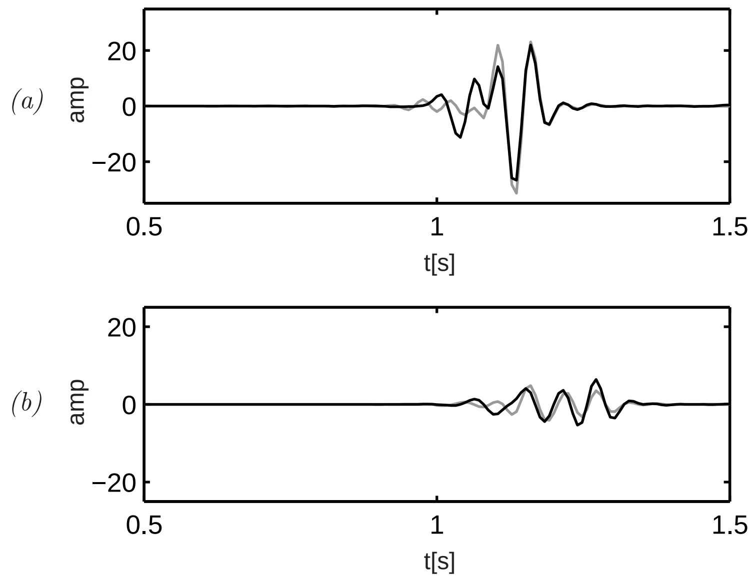

Figure 6.12: *Comparison of redatumed traces computed by the DMR approach (black line) and the KSR approach (gray line) for an offset of (a) 0 m and (b) 1300 m in in-line direction. The cross-line offset is 250 m.*

of the underlying isochrone. It can clearly be seen that that the global shape of the corrected event flattens further away from the global apex position. This explains the occurrence of the artifact. One can also see that traces further away from the global apex position clearly contain two events (see Figure 6.11b). These are the contributions for the diffraction event.

Figure 6.12 provides a comparison of redatumed traces for two different offsets. It can be seen that the absolute amplitudes of the redatumed event are correct as well. It can thus be stated that the DMR method produces kinematically and dynamically correct results for fully sampled 3D input data even over a complex subsurface.

6.4 Complex model – homogeneous datum layer; sparsely sampled input data

Next, the applicability of the proposed infill approach needs to be assessed. For this purpose a redatumed shot gather is computed for a sparsely sampled input data set utilizing the DMR method combined with the proposed infill approach. The velocity

model underlying this data set has been described in the previous section.
Again, the input data set consists of 2D lines (see Figure 6.13). The sources are ranging from 4000 m to 8000 m in the in-line direction. The source spacing in in-line direction is 25 m. For every 2D line a split-spread geometry has been chosen with a maximum receiver offset of ±1975 m and a receiver spacing of 25 m. The cross-line spacing between the 2D lines is 50 m.
From these input data, again, a redatumed shot gather is computed with the source and the receivers at exactly the same positions as for the experiment on fully sampled data. Figure 6.14a displays a redatumed shot gather computed by means of the DMR approach for a fully sampled input data set. This is considered the desired result. Figure 6.14b shows the redatuming result for sparsely sampled input data. This shot gather has been calculated using the DMR method in combination with the infill approach. No significant differences can be found between these two results.
Even a detailed comparison of traces does not reveal any errors in the absolute amplitudes (see Figure 6.15). Errors in the traveltimes of the traces computed from the sparsely sampled input data cannot be found.
The findings of this experiment suggest, therefore, that the DMR method combined with the infill approach produces kinematically and dynamically correct results for sparsely sampled 3D input data even over a complex subsurface. However, it is recommended for future research to repeat this experiment on synthetic data sets which have been modeled with full reflector responses. Then the traces will contain more than only one event. In this case, the amplitude behavior can be examined more thoroughly than it was possible for this data set. Especially the relative behavior of many reflections should be looked at.

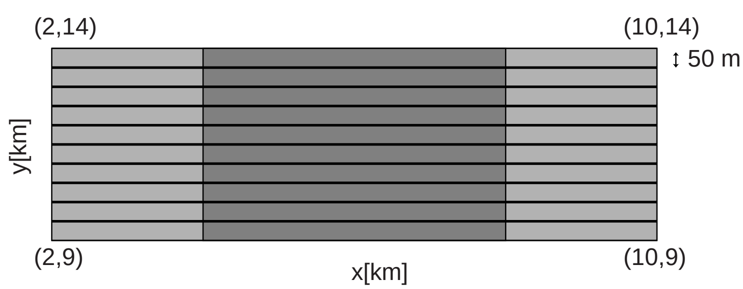

Figure 6.13: *Acquisition geometry of the data set computed for the complex velocity model. The receivers used for the KSR approach were distributed with a dense sampling all over dark and the light gray area; the sources are distributed with a dense sampling all over the dark gray area. For the sparse input data set sources and receivers are distributed along the lines.*

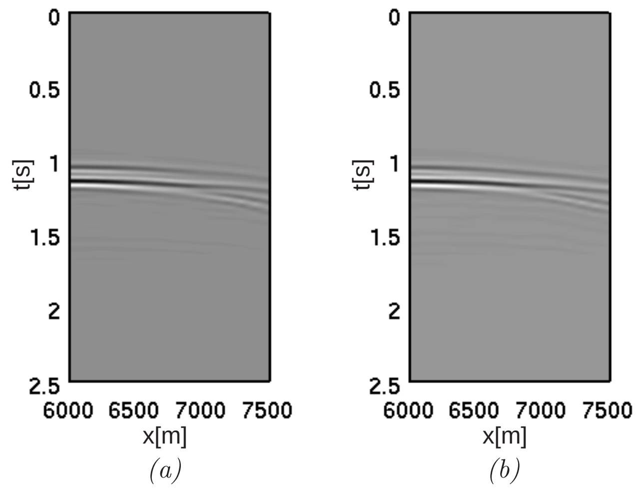

Figure 6.14: *Comparison of (a) the redatumed shot gather computed by the DMR method for fully sampled input data (same as Figure 6.10c) and (b) the redatumed shot gather computed by the DMR approach combined with the infill for sparsely sampled input data.*

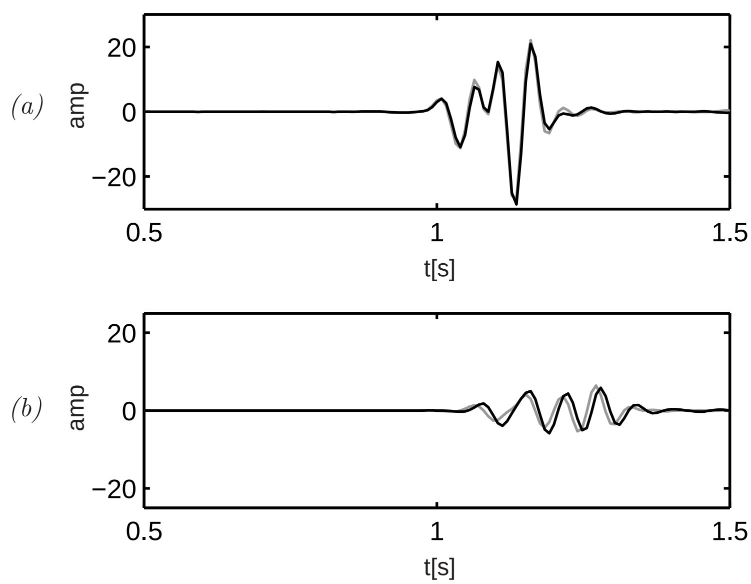

Figure 6.15: *Comparison of redatumed traces computed by the DMR approach for fully sampled data (gray line) and for sparsely sampled data (black line) for an in-line offset of (a) 0 m and (b) 1300 m. The cross-line offset is 250 m.*

6.5 Realistic data example

The realistic 3D data set used to test the DMR approach has been acquired over a scale model in the Experimental Facility for Imaging (EFI) of the TU Delft [see for example Blacquiere and Koek, 1997]. For this experiment the so-called Ziggy model, which is also being used for the ZMAART[1] project, has been chosen. This model is described in detail by van Veldhuizen and Blacquiere [2005]. It was placed inside the water tank with a silicon hemisphere (v =1000 m/s) on top, to simulate a low velocity zone inside the homogeneous water layer (v =1480 m/s). Data were acquired over an area around this hemisphere, with a water depth of approximately 1000 m. The relevant part of the Ziggy model as well as a picture of the silicon hemisphere are presented in Figure 6.16.
The acquired data set consists of 2D lines. The sources are ranging from 24000 m to 30000 m in the in-line direction and from 11000 m to 14000 m in the cross-line direction. The source spacing in the in-line direction is 25 m. For every 2D line end-on shooting has been chosen with a minimum receiver offset of -425 m and a maximum offset of -1900 m. The receiver spacing is 25 m. The cross-line spacing between the 2D lines is 50 m.
Figure 6.17 shows two common-offset gathers of the input data set, which clearly show the influence of the low velocity zone. The events of gather 6.17a, which has been acquired at y =11000 m with an offset of -850 m, are undistorted because this 2D line has been acquired well away from the hemisphere. This hemisphere

[1] Ziggy Model Acquisition and the ART of physical modeling

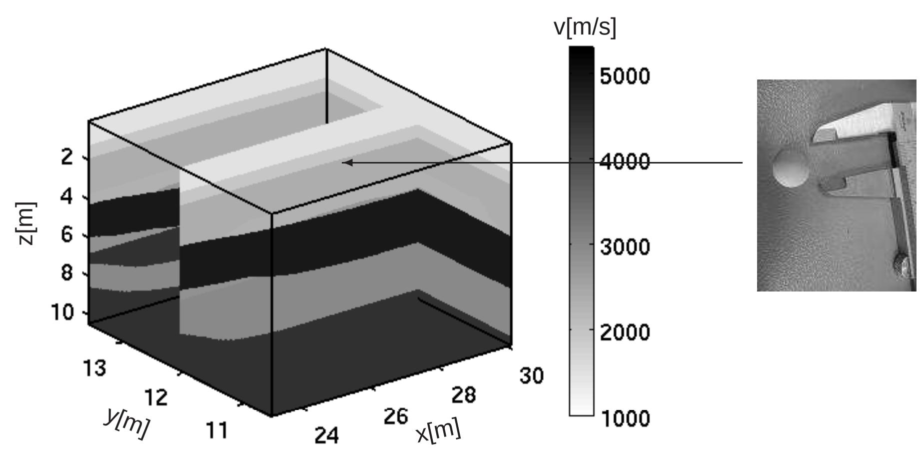

Figure 6.16: *Part of the Ziggy model that has been utilized for the acquisition of the water tank data. Furthermore, a picture of the silicon hemisphere – the low velocity area – is presented.*

is centered approximately at (27450 m,12150 m) with an approximate diameter of 1000 m and an approximate height of 240 m. The events of gather 6.17b are clearly distorted. This gather has been acquired at $y = 12150$ m with an offset of -850 m. It is the aim of redatuming to remove these distortions as well as possible.
In a first attempt to redatum the data, operators have been estimated from the input data set employing the technology developed by Verschuur and Marhfoul [2005]. This data-driven technique is based on an iterative updating scheme as well. For

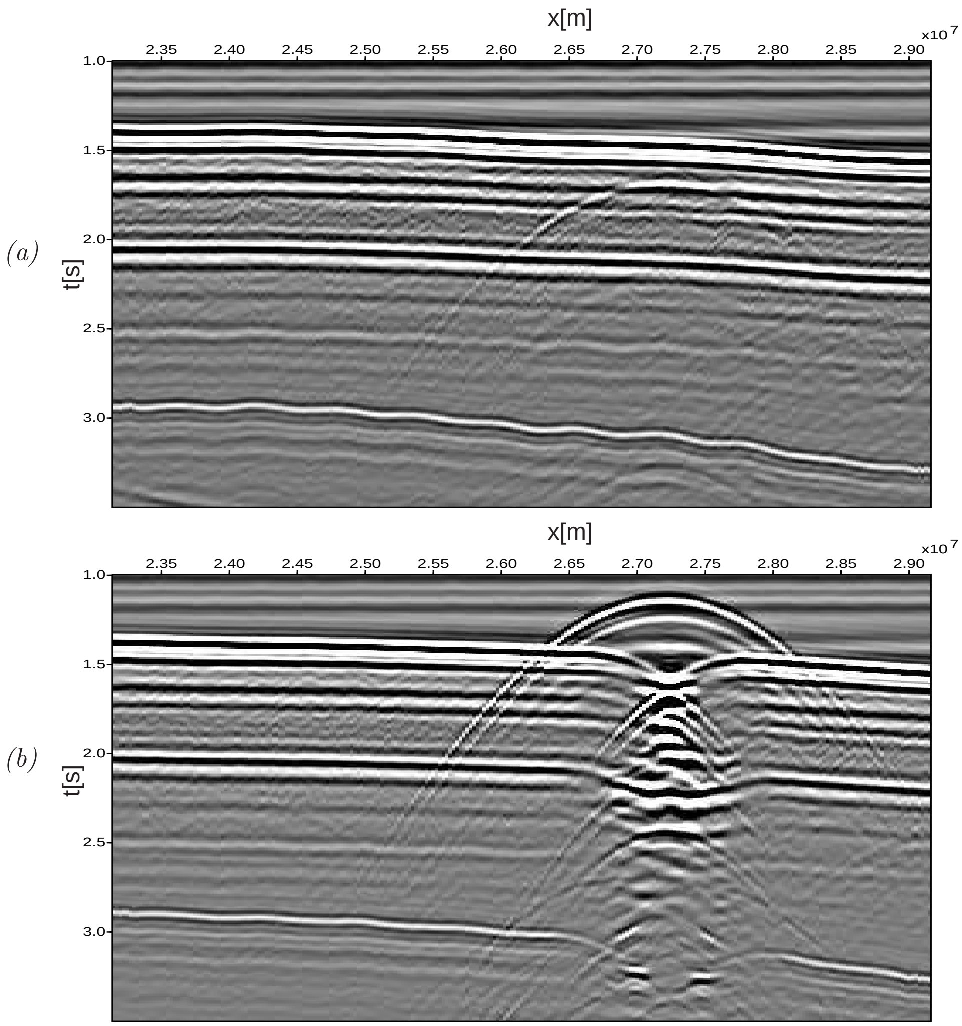

Figure 6.17: *Common offset gathers of the input data set with an offset of -850 m. (a) is recorded at $y = 11000$ m, and (b) is recorded at $y = 12150$ m.*

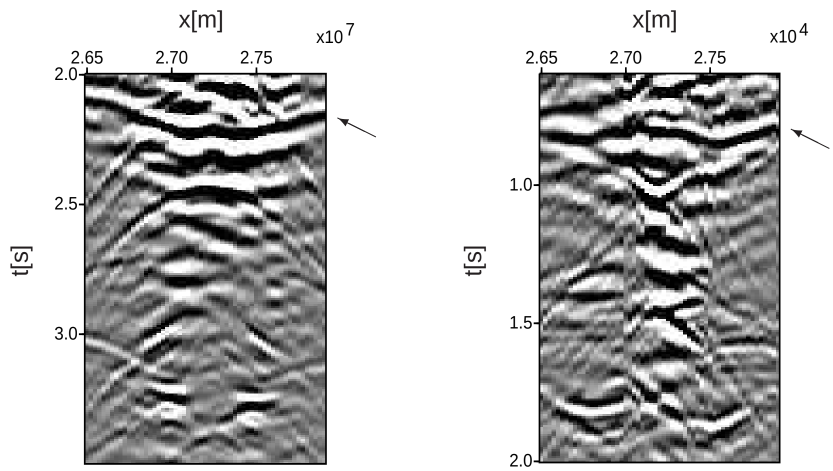

(a) *(b)*

Figure 6.18: *(a) Common offset gather with offset -850 m before redatuming showing the area right below the low-velocity anomaly. (b) Common offset gather after redatuming using the DMR approach combined with the DTR methodology to infill missing data.*

the estimation of the operators used in this experiment only very few updating steps have been performed. I.e. it is very likely that the scheme had not yet converged to the final result and inaccurate operators are being used. This is, again, comparable to using an incorrect velocity model in the model-driven operator estimation.

In Figure 6.18 the redatumed common offset gather at y =12150 m with an offset of -850 m (see Figure 6.18b) is compared to the relevant part of the common offset gather of the input data set (see Figure 6.18a). Here, the event marked by the arrow is important. This event is the reflection from the first reflector below the water bottom. As one can see in Figure 6.18b this event has clearly been improved by applying the redatuming. However, it is obvious that the presented result is not yet perfect. There are still discontinuities left. This probably has to be attributed to the use of incorrect redatuming operators.

The findings of this test suggest that the DMR approach handles sparsely sampled realistic 3D data correctly. However, it is strongly recommended to repeat this experiment with correct redatuming operators.

6.6 Conclusions and recommendations

The results of the tests on fully and sparsely sampled 3D data can be summarized as follows:

[**1**] The DMR method has been extended correctly to the 3D situation; the tests on fully sampled 3D synthetic data sets from simple and complex subsurface models show satisfactory results, which are kinematically and dynamically correct.

[**2**] The DMR method combined with the proposed infill approach produces satisfying results; the redatumed traces for sparsely sampled 3D synthetic data sets from simple and complex subsurface models are kinematically and dynamically correct.

[**3**] The number of traces needed to calculate one output sample is considerably reduced, already about 900 traces were enough to calculate one output time sample.

[**4**] The results for a sparsely sampled realistic 3D data set are promising. However, these results suffer from errors of the employed redatuming operators.

For further research the following recommendations are made:

[**1**] The experiments on synthetic data from a numerical model with a homogeneous datum layer and a complex subsurface below the datum should be repeated. Thereby, a finite difference code should be employed to model the data. In this way, the amplitudes of the input data set are reliable, and the considered traces contain more than only one reflection event. As a consequence, errors in the absolute amplitudes of the redatumed events can easily be identified.

[**2**] The experiments on the realistic data should be repeated with correct redatuming operators. These operators could either be estimated directly from the input data set, or they could be computed for a correct velocity model of the datum layer.

[**3**] The proposed DTR approach for the infill of missing data should be evaluated more thoroughly. Here, it has only been applied in combination with the DMR approach. It is worthwhile, however, to set up tests that concentrate exclusively on the evaluation of the proposed infill method to examine its applicability and its limitations in detail.

7

Further applications of the DMR methodology

Die Klugheit ist sehr geeignet zu bewahren, was man besitzt
doch allein die Kühnheit versteht zu erwerben.

Friedrich der Große (1712 - 1786)

The DMR methodology, as it has been described in the previous chapters, primarily aims at the redatuming of P-wave data consisting of primary reflections. However, in this chapter the possibilities for a modification of this methodology are explored with respect to:

[**1**] its application to PS-data,

[**2**] its applicability for the prediction of datum layer-related multiples in the redatumed result.

The modification of the DMR method for PS-data is described (see Section 7.1) and evaluated on a synthetic 2D data set (see Section 7.2). Furthermore, a new concept for the prediction of datum layer-related multiples based on the DMR methodology is developed (see Section 7.3) and tested on numerical 2D data (see Section 7.4).

7.1 Redatuming of PS-data using the DMR technology – Theory

The derivation of the KSR method, which is the basis of the DMR method, starts from the acoustic wave equation. This implies that only acoustic waves can be redatumed correctly by these methods. However, the KSR approach can be extended to handle converted waves as well. The redatuming operators used to correct for the one-way wave-propagation between sources at the surface and at the datum and receivers at the surface and at the datum have to be determined accordingly. If, as

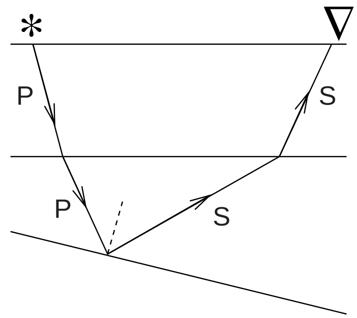

Figure 7.1: *Raypath of a converted wave with a down-going P-leg and an up-coming S-leg.*

illustrated in Figure 7.1, the data set consists of down-going P-waves and up-coming S-waves, a P-operator has to be used to redatum the sources and a S-operator has to be used to redatum the receivers. The redatumed result will be kinematically correct. Whether the amplitudes of the redatumed result are correct should be examined in detail, but this is beyond the scope of this thesis.
The extension of the DMR approach to handle converted waves, at least kinematically, correctly requires only little more effort. The methodology, as explained in Chapter 2, remains unchanged. Still, for the calculation of one output sample the four steps described there have to be executed (see Figure 2.2). Only the implementation of these steps has to be modified.

7.1.1 The isochrone

First, the surface of possible reflection points belonging to the considered time sample t_{red}, the so-called isochrone, needs to be determined. In case of converted waves this can no longer be achieved in an analytical manner assuming a constant velocity for the medium below the datum. Instead, two velocities are necessary. The velocity belonging to the down-going P-wave and the velocity belonging to the up-going S-wave. The possible reflection points along the isochrone all have to satisfy the following requirement: the sum of the P-traveltime t_s from the source at the new datum to the isochrone point and the S-traveltime t_r from the same point to the receiver at the new datum has to equal the traveltime of the considered output sample t_{red}:

$$\{(x_{iso}, y_{iso}, z_{iso}) \,|\, t_{red} = t_r + t_s\} \,. \tag{7.1.1}$$

Hence, an isochrone point $\mathbf{x}_{iso}$ belonging to the emergence angle β and the azimuth θ_s at the redatumed source position has to lie on a straight line $\mathbf{x}_{\beta,\theta_s}$ which intersects the datum with these angles, and it has to satisfy Equation 7.1.1. In the search for this point, firstly, the intersection points of $\mathbf{x}_{\beta,\theta_s}$ and a number of straight lines $\mathbf{x}_{\gamma,\theta_r}$, which cross the datum at the receiver position with an emergence angle $\gamma \in [-\frac{\pi}{2}, \frac{\pi}{2}]$ and azimuth $\theta_r \in [0, 2\pi)$ are determined and the traveltimes t_s and t_r are calculated accordingly. Then, the point which satisfies Equation 7.1.1 is selected from this set of points.

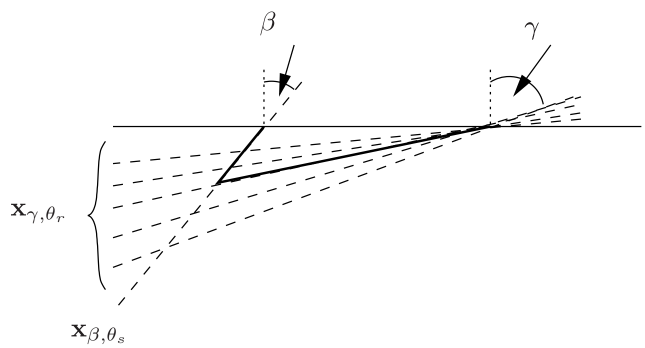

Figure 7.2: *Search for an isochrone point in case of converted-wave redatuming. The raypath belonging to the selected point is indicated with a bold line.*

Figure 7.2 illustrates this search routine for the 2D situation, which is equivalent for the search of all points with $\theta_s = 0$ and $\theta_s = \pi$. As shown in Figure 7.3, this procedure has to be repeated for all $\beta \in [-\frac{\pi}{2}, \frac{\pi}{2}]$ and $\theta_s \in [0, 2\pi)$ to create the entire isochrone.

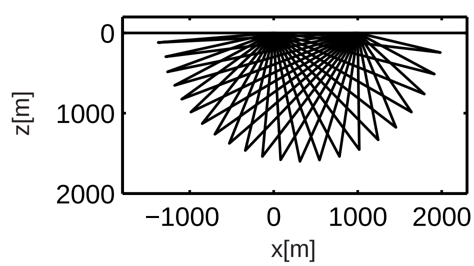

Figure 7.3: *Isochrone points for the redatuming of PS-waves. Note the asymmetry due to the different wave types at source and receiver side.*

7.1.2 The locus

The estimation of the locus for the redatuming of PS-data is conducted in exactly the same way as it has been described in Chapter 2 and Chapter 3. For every possible reflection point on the isochrone, ray tracing is performed towards the acquisition surface. Again, straight rays are employed below the new datum level and the ray parameters at the datum are calculated by means of Snell's law. This time, the P-wave velocity $v_{p,2}$ for the medium below the new datum is utilized to determine the ray parameter at the source position and the S-wave velocity $v_{s,2}$ is utilized to determine the ray parameter at the receiver position. Finally, the raypaths are continued upwards to the acquisition surface. The information about the ray parameter needed is extracted from the traveltimes of the redatuming operators. These operators have to be selected accordingly. In case of a down-going P-wave and a up-going S-wave, a P-operator, which describes the one-way wave-propagation of a P-wave, is employed for the source side, and a S-operator is utilized for the receiver side. In the end, all possibly contributing time samples can be determined by calculating the traveltimes along the different raypaths.

7.1.3 The infill

The infill step remains unchanged as well. Its implementation is outlined in Chapter 5. Firstly, a contour at the new datum is determined indicating all source/receiver pairs with rays reaching the considered isochrone point under the same angle of incidence as the rays belonging to the missing source/receiver pair. The size and position of this contour depends only on the position of the isochrone point, on the source position at the new datum level and on the receiver position at the new datum level (see Appendix D). Once this contour is known, the source/receiver pairs at the acquisition surface are determined by an upward continuation of the rays from the contour points at the datum to the surface. This is accomplished in exactly the same way as it has been done for the construction of the locus. Again, a P-operator is utilized for upward continuation at the source side, and a S-operator is used for the receiver side. At last, the time sample which is used to replace the missing one is taken from a trace that has been acquired at one of the selected source/receiver pairs.

7.1.4 The weighted summation

For the application of the DMR approach to PS-data, as far as it is considered in this thesis, a straightforward application of the integral expression for P-wave data to the situation of converted-wave data has been chosen. In fact, only the redatuming operators, which are needed for the calculation of the time shifts and the amplitude corrections are selected accordingly. The expression for the DMR approach for P-data is repeated here:

$$p(\tilde{\mathbf{x}}_s, \tilde{\mathbf{x}}_r, t_{red}) = \left[\int \sqrt{\frac{\mathcal{A}_{DMR}}{\mathcal{A}_{KSR}}} \frac{a_{pp}}{\sqrt{\mathcal{A}}} \frac{\partial}{\partial t} p(\mathbf{x}_s, \hat{\mathbf{x}}_r, t + \tau_r + \tau_s) d\mathbf{x}_s \right]_{t=t_{red}}, \tag{7.1.2}$$

with:

$$a_{pp} = -\frac{1}{2\pi v_1^2} \frac{\cos\alpha_r \cos\alpha_s}{r_r r_s}.$$

It has to be noted that this equation has been derived from the scalar wave equation for the acoustic pressure p. For the elastic case, however, the surface displacement $\mathbf{u}$ is measured. Unfortunately, the wave equation for the displacement is more complex than the scalar wave equation for the acoustic case. Therefore, often the choice is made to formulate the problem in terms of the displacement potentials Φ and $\mathbf{\Psi}$, with Φ being referred to as the P-wave potential and $\mathbf{\Psi}$ being referred to as the S-wave potential [see Aki and Richards, 2002]. The relationship between the potentials and the displacement $\mathbf{u}$ is described by the Helmholtz theorem:

$$\mathbf{u} = \nabla\Phi + \nabla \times \mathbf{\Psi}. \tag{7.1.3}$$

The wave equation for the scalar potential Φ is:

$$\frac{\partial^2 \Phi}{\partial t^2} = v_p^2 \nabla^2 \Phi. \tag{7.1.4}$$

The wave equation for the vector potential $\mathbf{\Psi}$ is:

$$\frac{\partial^2 \mathbf{\Psi}}{\partial t^2} = v_s^2 \nabla^2 \mathbf{\Psi}. \tag{7.1.5}$$

They are comparable to the wave equation for the acoustic pressure:

$$\frac{\partial^2 p}{\partial t^2} = v_p^2 \nabla^2 p. \tag{7.1.6}$$

Assuming 2D wave propagation in the $x - z$ plane, the SV-waves are fully governed by the y-component Ψ_y of the shear potential $\mathbf{\Psi}$. Hence, in the 2D situation a scalar wave equation for Ψ_y can be found to describe the wave propagation of the SV-wave. I.e., the redatuming of converted waves assuming 2D wave propagation can be formulated as:

$$\Psi_y(\tilde{x}_s, \tilde{x}_r, t_{red}) = \left[\int \sqrt{\frac{\mathcal{A}_{DMR}}{\mathcal{A}_{KSR}}} \frac{a_{ps}}{\sqrt{\mathcal{A}}} \frac{\partial}{\partial t} \Psi_y(x_s, \hat{x}_r, t + \tau_r + \tau_s) dx_s \right]_{t=t_{red}}, \tag{7.1.7}$$

with:

$$a_{ps} = -\frac{1}{2\pi v_{p,1} v_{s,1}} \frac{\cos\alpha_r \cos\alpha_s}{r_r r_s}.$$

It has to be noted here, that the decomposition of converted-wave data into two scalar potentials has been performed successfully for 2D data [see for example Schalkwijk et al., 2003].
If it was possible to decompose the measured displacement $\mathbf{u}$ into two scalar potentials Φ and Ψ for the 3D situation as well, the redatuming of converted PS-waves in 3D could be formulated as:

$$\Psi(\tilde{\mathbf{x}}_s, \tilde{\mathbf{x}}_r, t_{red}) = \left[\int \sqrt{\frac{\mathcal{A}_{DMR}}{\mathcal{A}_{KSR}}} \frac{a_{ps}}{\sqrt{\mathcal{A}}} \frac{\partial}{\partial t} \Psi(\mathbf{x}_s, \hat{\mathbf{x}}_r, t + \tau_r + \tau_s) d\mathbf{x}_s \right]_{t=t_{red}} . \qquad (7.1.8)$$

However, 3D wavefield decomposition into two scalar potentials is by no means a trivial thing. It is being researched within DELPHI right now whether this is, at all, possible. However, this is beyond the scope of this thesis.
If Equation 7.1.7 or Equation 7.1.8 are applied, the calculation of the amplitude weights $\mathcal{A}$, $\mathcal{A}_{DMR}$, $\mathcal{A}_{KSR}$ and the time shifts τ_r, τ_s has to be adapted to the respective situation. For an input data set with down-going P-waves and up-going S-waves, the time shifts related to the source side, which are also utilized for the calculation of $\mathcal{A}_{DMR}$ and $\mathcal{A}_{KSR}$, have to be extracted from the P-operators. The time shifts related to the receiver side, which are also utilized for the calculation of $\mathcal{A}$ and $\mathcal{A}_{DMR}$, have to be extracted from the S-operators.

7.2 Redatuming of PS-data using the DMR technology – Evaluation

The DMR methodology for converted-wave data for the 2D situation is evaluated on a synthetic data set, which has been modeled for the subsurface model displayed in Figure 7.4. Due to the lack of an elastic modeling tool, the data set had to be generated by conventional ray tracing [Cerveny, 2001] in an alternative acoustic model with mirrored sources (see Figure 7.5). By doing this, it is ensured that the traveltimes of the modeled events are correct. However, their amplitudes will not be correct. The modeled events represent transmission events through interfaces of an acoustical model, whereas the reflection of converted waves in an elastic model is aimed for. The source positions of the input data set are ranging from -1500 m to 1500 m with a sampling interval of 15 m. For the receivers a split-spread geometry has been chosen with a maximum offset of 1500 m and a sampling interval of 15 m. This data set serves as input for the calculation of a redatumed shot gather with source and receivers both at the new datum level at a depth of 300 m. The source position at the new datum is 0 m, the receivers range from 15 m to 1185 m.
In Figure 7.6a and Figure 7.6b the redatumed shot gathers are compared. Gather 7.6a has been computed with the conventional KSR method modified for PS-data. Gather 7.6b has been computed with the modified DMR approach assuming the correct P- and S-velocities for the medium below the new datum.

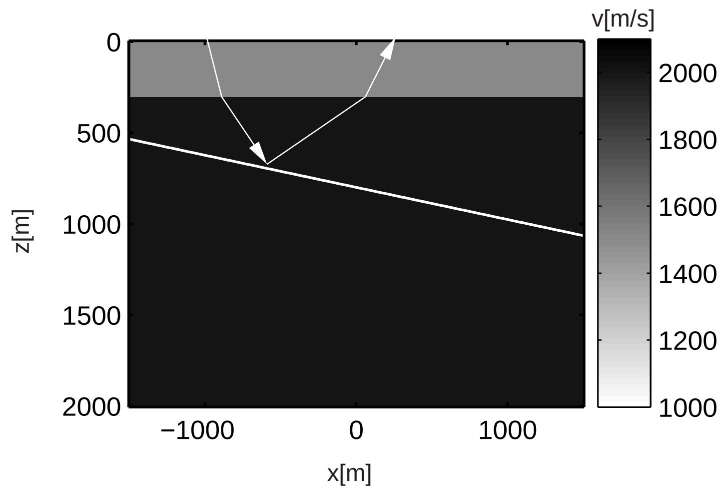

Figure 7.4: *Velocity model of the subsurface for the PS-data set showing P-wave velocities. Note, that the reflection below the datum is caused by an inhomogeneity of the density. The S-wave velocities can be derived from this model by applying the scaling factor of 0.67.*

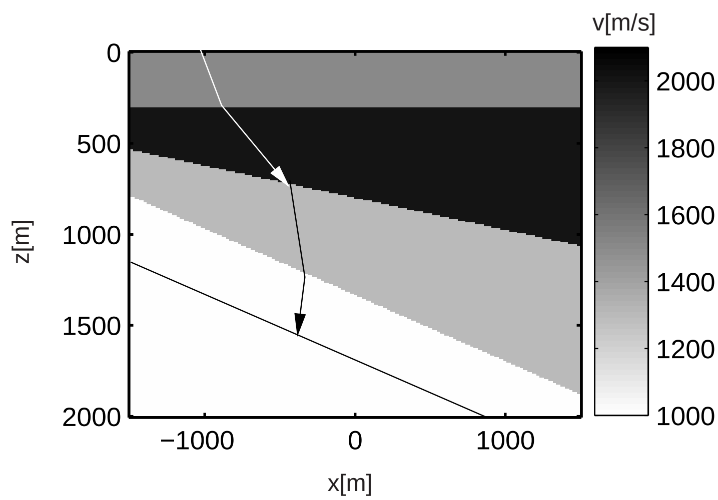

Figure 7.5: *Alternative velocity model used for the modeling of the PS data. All computed events are transmission events recorded at the dipping line. The traveltimes of these events are identical to the traveltimes of reflected PS-data of the model presented in Figure 7.4.*

From these results, it can be concluded that the proposed method works well for the redatuming of PS-data, because the event has been reconstructed properly.
For an evaluation of the presented results with respect to the kinematic quantities like traveltimes as well as with respect to dynamic quantities like amplitudes the segments of the redatumed traces containing this event, which have been computed with the DMR approach and the KSR approach, are compared. Figure 7.7 displays traces with an offset of 15 m and 900 m. A comparison of the two results reveals that the redatumed PS-events have been reconstructed at identical traveltimes but with small differences in the absolute amplitudes. The occurrence of these amplitude errors could possibly be explained with errors made in the derivation of the factors $\mathcal{A}$ and $\frac{\mathcal{A}_{DMR}}{\mathcal{A}_{KSR}}$. However, it has not been examined in detail. This is recommended for future research.

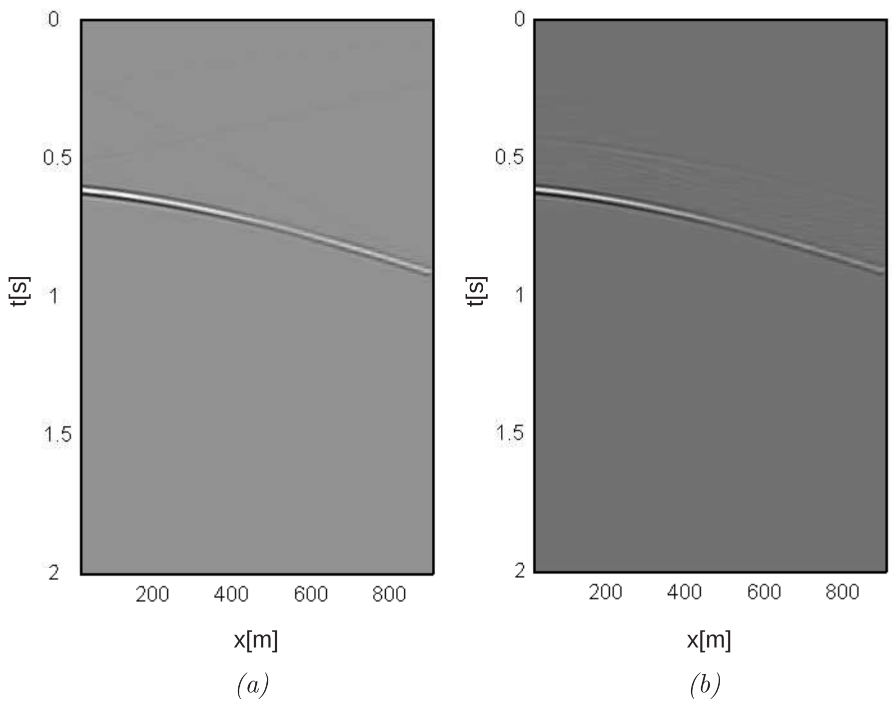

Figure 7.6: *Comparison of (a) the redatumed shot gather computed by the KSR method, and (b) the redatumed shot gather computed by the DMR approach.*

(a)

(b)

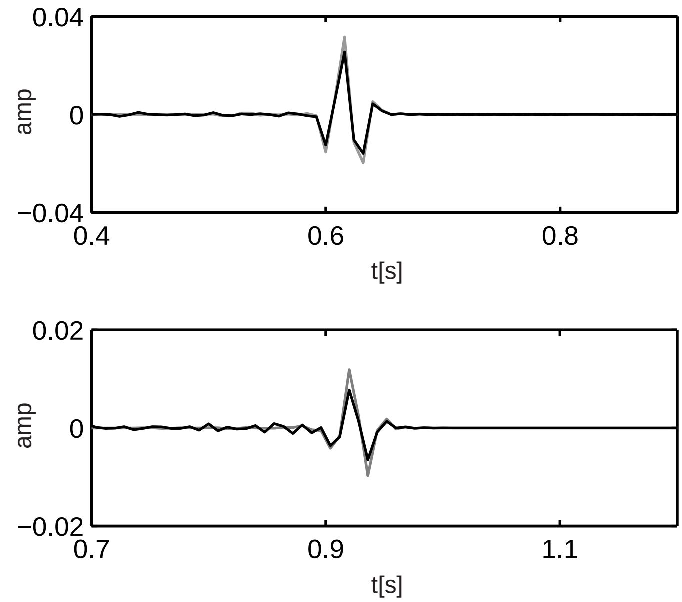

Figure 7.7: *Comparison of redatumed traces computed by conventional redatuming (gray line) and by the DMR approach (black line) for an offset of (a) 15 m and (b) 900 m.*

In the end, this test on numerical converted-wave data can be summarized by the following statements:

- the modification of the DMR approach for converted-wave data has been done correctly;
- it reproduces the desired results kinematically correct;
- small errors occur for the amplitudes of the events.

Furthermore, the following recommendations can be made for future research:

- the integral expression describing the weighted summation of the DMR approach for converted-wave data should be checked by deriving it from the integral expression underlying the KSR approach for elastic waves based on a proper decomposition of the Φ and the Ψ potential;
- the DMR methodology should be evaluated on synthetic and real input data; the synthetic input data sets should be computed with an elastic modeling algorithm.

7.3 Prediction of datum layer-related multiples based on the DMR technology – Theory

Redatuming, as it is usually performed and as it is presented in this thesis, considers and corrects only one-way wave-propagation inside the datum layer; i.e. of the events recorded at the acquisition surface only one down-going source leg and one up-going receiver leg is removed. Hence, after redatuming for primaries and internal multiples with the multiple reflection occurring below the datum all contributions inside the datum layer have been removed. For datum layer-related multiples with the multiple reflection occurring at the surface one source leg and one receiver leg inside the datum layer are removed correctly, all other up- and down-going legs of the event inside the datum layer cannot be removed.
The aim of all redatuming approaches, however, is to produce events that are only traveling below the datum layer. Consequently, a new method needs to be developed to predict and remove the remainings of the datum layer-related multiples from the redatumed data set.
The development of the new concept for the prediction of datum layer-related multiples in a redatumed data set by means of the DMR methodology is explained here step by step. Firstly, the characteristics of the events that are to be predicted are analyzed, and it is discussed how similar events could be constructed. Thereafter, the new concept for the prediction of datum layer-related multiples is explained. This new DMR-based concept for multiple prediction is very well suited for the situation of sparsely sampled 3D input data.

7.3.1 Datum layer-related multiples

Figure 7.8 illustrates the redatuming process for a datum layer-related multiple in the input data set. As one can see in Figure 7.8a, prior to redatuming the event consists of one leg inside the datum layer on the source side and three legs inside the datum layer at the receiver side. During redatuming, one source leg and one receiver leg is removed (see Figure 7.8b). Figure 7.8c shows that for the redatumed

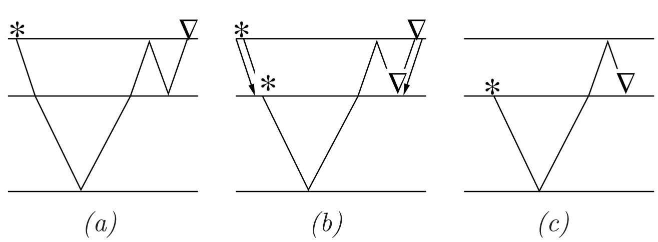

Figure 7.8: *Correction of a datum layer-related multiple during redatuming.*

datum layer-related multiple two legs remain inside the datum layer. They have not been removed. These are the events to be predicted by the new approach.
Note, that this example is also representative for events with multiple reflections at the source side.

7.3.2 Transforming primaries into datum layer-related multiples

The basic idea underlying the new concept for the prediction of redatumed datum layer-related multiples is simple:

> *If it is possible to remove the source and the receivers legs inside the datum layer, it is also be possible to remove one leg and add one leg.*

Figure 7.9 illustrates this for a primary event in the input data set. From the event presented in Figure 7.9a the source leg inside the datum layer is removed and one leg inside the datum is added at the receiver side (see Figure 7.9b). The resulting event shown in Figure 7.9c resembles the desired redatumed datum layer-related multiple shown in Figure 7.8c. Note again, that this example is also representative for events with multiple reflections at the source side.
Hence, primaries in the input data set can be used to predict first-order multiples in the redatumed data set, first-order multiples in the input data set can be used to predict second-order multiples, etc..
This idea of removing one source leg and adding a receiver leg is not new. Kirchhoff summation based method have been developed and successfully applied to fully sampled 2D data sets [see for example Berryhill and Kim, 1986; Wiggins, 1988]. In the method described by Wiggins [1988] one down-going leg is removed by applying an inverse extrapolation step to the input data, and one down-going leg is added by applying a forward extrapolation step to the data. Next, the predicted multiples are subtracted, after which the result is forward extrapolated to the surface.
However, as the KSR method, these methods suffer from the sparseness of 3D input data sets and can, therefore, not be applied directly to 3D data sets from conventional acquisition geometries. Pica et al. [2005] tried to overcome the problem of sparsely

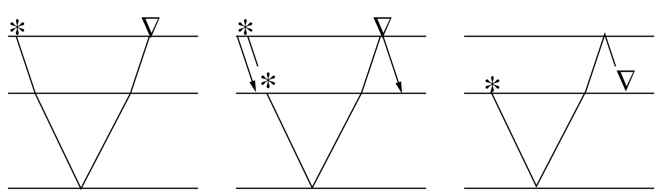

(a) *(b)* *(c)*

Figure 7.9: *Estimation of a datum layer-related multiple from a primary reflection.*

sampled input data by performing a data interpolation step prior to the multiple prediction. This is computationally very expensive.
A new concept for the prediction of datum layer-related multiples based on the DMR methodology can, however, easily be combined with the DTR method to infill missing data. By doing this, an additional interpolation of the data set prior to the multiple prediction is no longer necessary.

7.3.3 A new concept for the prediction of datum layer-related multiples

In the previous section the basic idea for the prediction of datum layer-related multiples has been described. For the description of the new concept, a multiple reflection at the receiver side is considered. It should be noted that the same derivation also holds for a multiple at the source side.
The applied redatuming approach needs to be modified such that it removes one leg inside the datum layer from the events of the input data set and that it adds one leg inside the datum layer. Furthermore, it needs to be taken into account that a number of multiples with different angles of incidence could be recorded at the considered trace location at the new datum (see Figure 7.10). Every one of these possible multiples needs to be computed. This is done by applying the modified DMR approach. The modification of the DMR approach, such that it removes one leg inside the datum layer from the considered possible event and adds one leg inside the datum layer, is straightforward. As already mentioned, the inverse extrapolation of the receivers is replaced by a forward extrapolation.
A crucial point with respect to the calculation of the possible multiples at the considered source/receiver pair at the new datum for a certain angle of incidence is the selection of the focal points for the ellipsoidal isochrones used in the modified DMR approach. Unlike for redatuming, they are not identical to the considered source/receiver locations at the new datum. If, as for this example, a multiple reflection at the receiver side is to be predicted, the focal points for the isochrones are located at the source position considered and at a location in-between the source position and the receiver position. The position of this second focal point is depen-

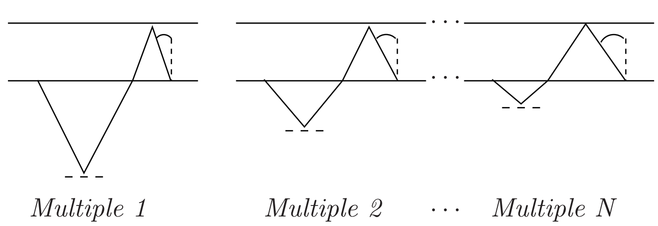

Figure 7.10: *Datum layer-related multiples which are possibly contributing to the considered redatumed trace.*

dent on the considered angle of incidence.
Furthermore, it should be noted that, if it is intended to compute the time sample t_{red} of the possible multiple event at the considered source/receiver pair, the time t_{red} cannot be used to create the isochrone. Actually, the isochrone has to be calculated using $t_{red} - \Delta t_M$, with Δt_M being the two-way traveltime of a primary event between the second focal point of the isochrone and the receiver location considered, which is reflected at the surface.
Hence, a for every possible angle of incidence at the receiver position considered a trace is computed using as focal points the redatumed source location and and the second focal point whose position is dependent of the considered angle of incidence. This trace is shifted by Δt_M. In the end, a weighted summation is applied to the traces, which contain the possible multiple events. The result is one trace with the predicted datum layer-related multiples.
Until now, only a concept for the prediction of datum layer-related multiples in a redatumed data set has been developed. The amplitude weights needed for the weighted stack of all possible multiples have not been derived yet. This is, however, recommended for future research.
In the following section it is evaluated whether the proposed procedure for the prediction of datum layer-related multiples delivers kinematically correct results.

7.4 Prediction of datum layer-related multiples based on the DMR technology – Evaluation

The concept for the prediction of datum layer-related multiples based on the DMR methodology is assessed on a synthetic 2D data set. A simple numerical model has been chosen, which is built of several layers with a constant velocity below the new datum. Reflections from below the new datum occur due to changes in the medium density. The model used for this test is shown in Figure 7.11.
For this numerical model a data set has been computed with a moving spread geometry. Its sources are positioned between -1500 m to 1500 m with a sampling interval of 15 m. The receiver spread has a maximum offset of 1500 m at both sides of the source position and is sampled with an interval of 15 m. The input data set, which has been modeled by ray tracing, consists of the two primary reflections from the reflectors below the datum and of the first- and second-order multiples belonging to these primaries. Note here, that only the multiples with the receiver-side peg-legs have been modeled.
For this input data set redatumed shot gathers are calculated using the conventional KSR method and the DMR method. The position of the redatumed source is 0 m at a depth of 300 m, the receivers range from 150 m to 900 m. Furthermore, the datum layer-related multiples for the considered shot gather are predicted by means of the modified DMR methodology as described in Section 7.3.

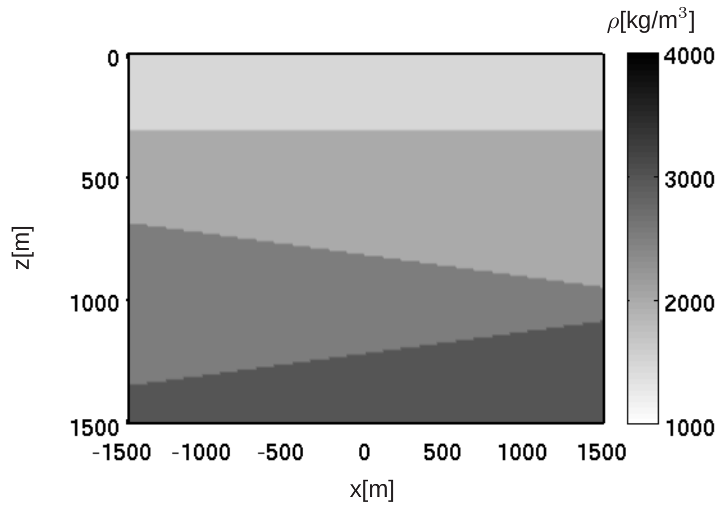

Figure 7.11: *Density model of the subsurface underlying the data set with datum layer-related multiples. Note, that the velocity below the datum is homogeneous.*

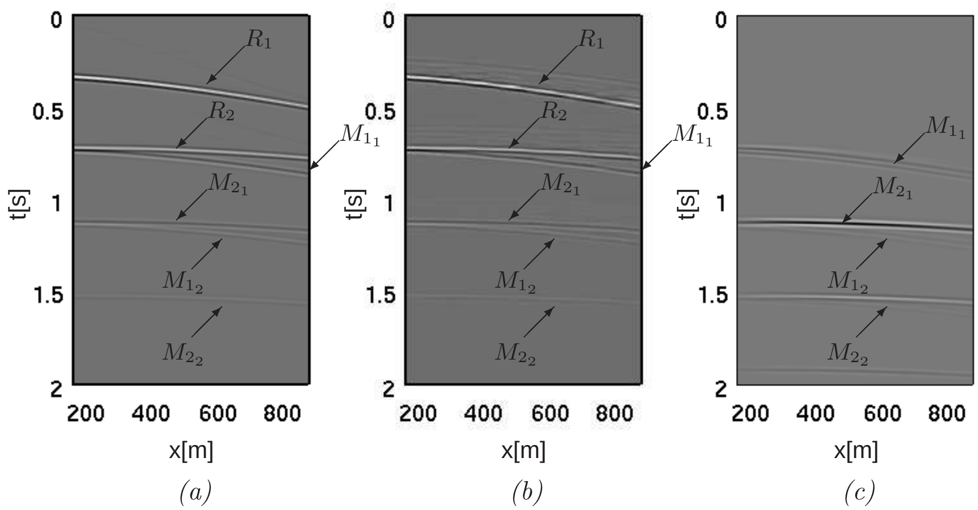

Figure 7.12: *(a) The redatumed shot gather with multiples computed by conventional redatuming, (b) the redatumed shot gather with multiples computed by the DMR approach, and (c) the predicted multiples in the redatumed shot gather computed by the modified DMR approach. The events marked with R_1 and R_2 are the primary reflections of the two reflectors, the events marked with M_{1_1} and M_{1_2} are the first- and second-order multiple belonging to the reflection from the shallow reflector, and the events marked with M_{2_1} and M_{2_2} are the first- and second-order multiple belonging to the reflection from the deeper reflector.*

The redatumed gathers are displayed in Figure 7.12a and Figure 7.12b. Figure 7.12c illustrates the predicted multiples. A comparison of Figure 7.12a and Figure 7.12b reveals that the DMR approach constructs the datum layer-related multiples accurately. Moreover, it can be stated that the new concept for the prediction of datum layer-related multiples delivers satisfying results. This can be seen from a comparison of a redatumed shot gather (see Figure 7.12a or b) and the predicted multiples presented in Figure 7.12c. Obviously all multiples have been constructed and appear at a correct position in time. For a detailed evaluation of the presented results the segments of the redatumed traces containing the multiple events, which have been computed with the DMR approach, are compared to the predicted multiples. Figure 7.13 displays the computed traces normalized with respect to their maximum amplitude for an offset of 450 m and 870 m. A comparison of the two results shows that the predicted multiples have been reconstructed kinematically correctly. They occur at the desired traveltimes. In contrast to this, the reconstruction of the amplitudes has not been done correctly. However, this was to be expected because the amplitude weights used for the modified DMR approach have not yet been derived properly.

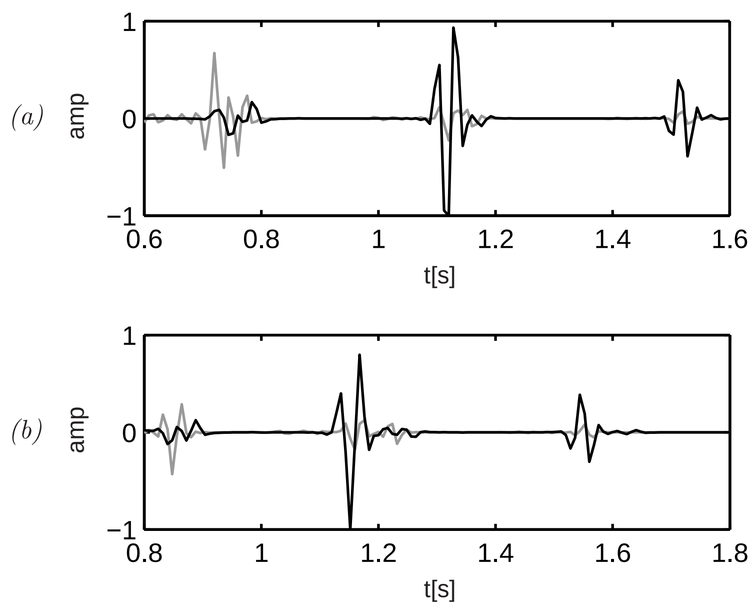

Figure 7.13: *Comparison of redatumed traces computed by the DMR approach (gray line) and the predicted multiples computed by the modified DMR approach (black line) for an offset of (a) 450 m and (b) 870 m.*

Finally, this test can be summarized as follows:

- a new concept for the prediction of datum layer-related multiples in a redatumed data set has been developed;
- this new concept for the prediction of datum layer-related multiples is based on the DMR technology;
- it reproduces the desired results kinematically correct;
- the amplitudes of the predicted events are erroneous; this is due to the fact that the proper amplitude weights have not yet been derived.

Furthermore, the following recommendations can be made for future research:

- the amplitude weights needed for the prediction of the datum layer-related multiples have to be derived;
- the proposed concept should be evaluated on synthetic and real input data.

7.5 Conclusions and recommendations

In this chapter the modification of the DMR approach for PS-data has been described and evaluated on a synthetic 2D data set. From this test the following conclusions can be drawn:

[**1**] the events are reconstructed kinematically correct by the modified DMR approach;

[**2**] small errors occur for the amplitudes of the events; this needs to be examined.

In addition to this, a new concept for the prediction of datum layer-related multiples based on the DMR methodology has been developed and tested on numerical 2D data. The results from this test can be summarized as follows:

[**1**] the predicted multiples are kinematically correct;

[**2**] the amplitudes of the predicted events are not correct; this is due to the fact that the proper amplitude weights have not yet been derived.

On the basis of these results it is recommended to:

[**1**] derive the integral expression describing the weighted summation of the DMR approach for converted-wave data from the integral expression underlying the KSR approach based on elastic wave propagation and to check the derived weights;

[**2**] derive the amplitude weights needed for the prediction of the datum layer-related multiples properly;

[**3**] evaluate both approaches, the DMR approach for converted-wave data and the proposed concept for the prediction of datum layer-related multiples, on synthetic and real input data; the synthetic input data sets should be computed with an appropriate modeling algorithm which delivers reliable amplitudes.

8

Conclusions and recommendations

Der Abschied von einer langen und wichtigen Arbeit
ist immer mehr traurig als erfreulich.

Friedrich von Schiller (1759 - 1805)

In this thesis a new methodology for redatuming has been presented. The aim of redatuming is to reconstruct new seismic traces with sources and receivers positioned at a user-defined datum level, which is different from the acquisition surface. This new datum level is typically located below a complex overburden, such that redatuming will remove the imprint of this complexity on the seismic data. For a successful application of the redatuming process full knowledge of the one-way wave-propagation between the sources at the surface and at the new datum and the receivers at the surface and at the new datum is required; i.e. it is assumed that so-called redatuming operators are available, which contain amplitudes and traveltimes accounting for this one-way wave-propagation. These redatuming operators can be determined either in a model-driven way from a given velocity model of the datum layer, or they can be extracted in a data-driven way from the input data set. For the redatuming method described in this thesis they are assumed to be known. The methodology most commonly used for redatuming is the so-called Kirchhoff summation redatuming (KSR). There, the redatuming is performed in two separate steps, one to redatum the receivers and one to redatum the sources. Each step requires the computation of an integral over the coordinates of the considered sources and receivers. Hence, the KSR method requires the input data set to have a dense sampling in both sources and receivers at the acquisition surface. It should also be

noted that a 4D integral has to be computed for the redatuming of 3D pre-stack data.
Nowadays, the amount of 3D data increases, which makes it more and more important to develop a feasible method for the redatuming of 3D pre-stack data. However, the conventionally used KSR approach is not only computationally demanding, it also requires the input data set to be densely sampled. Unfortunately, all commonly used 3D acquisition geometries deliver data sets that are sparse in at least one of the coordinates. Hence, a new redatuming methodology needed to be developed, which is also applicable to sparsely sampled 3D data.
In this thesis, the data mapping redatuming (DMR) methodology was presented. The research objectives underlying the development of this new methodology to redatuming were:

[**1**] The method should be applicable to sparse 3D data, acquired with conventionally used 3D acquisition geometries.

[**2**] The results should be comparable to the results the application of the Kirchhoff summation method would have delivered if applied to a densely sampled input data set.

[**3**] A reduction of the amount of data needed to calculate one output sample should be achieved.

The choice has been made to formulate the redatuming process in terms of a data mapping problem. Thereby, firstly all time samples of the input data set are identified which are possibly contributing to the considered output sample. Then, a weighted stack is applied to the possibly contributing time samples, which yields the required time sample of the redatumed trace to be calculated. To achieve this certain assumptions about the velocity model below the new datum level have to be made. This is different from the conventional methods. However, in this new DMR approach, the number of traces involved in the calculation of one output sample is reduced considerably as well as the dimensionality of the integral expression describing the process. Only a 2D integral needs to be calculated to compute one output sample compared to a 4D integral for the conventional KSR approach. The DMR methodology and the theory underlying it have been explained in Chapter 2 and Chapter 3.
The DMR approach is in general applicable to all sorts of input data sets, but, as already mentioned, the primary interest of this work was to develop an approach applicable to data sets that do not have a dense areal coverage of sources and receivers at the acquisition surface. For the DMR approach it can still happen that the required traces have not been acquired, even if it uses considerably fewer traces per output sample. In case this happens, the DMR approach needs to be combined with a data infill procedure. Fortunately, the DMR approach provides exactly the information that is needed in order to be able to apply the DELPHI trace replacement (DTR) method to infill missing data. This DTR method can be categorized

as a simplified data mapping technique, whose application in combination with the DMR approach gets facilitated by certain information provided by the DMR approach itself. By combining the DMR approach with the proposed infill method the new approach to redatuming becomes applicable to 3D data sets from conventionally used acquisition geometries. The DTR method has been described in Chapter 5.

The newly developed approach for redatuming has also been evaluated on several data examples. The applicability of the proposed DMR methodology has been tested with positive outcome on fully sampled synthetic 2D and 3D data sets and on a 2D field data set (see Chapter 4 and Chapter 6). The objective of producing results that are comparable to the results of the conventional KSR approach was achieved. Furthermore, the applicability of the DMR method combined with the proposed DTR approach to infill missing data has been investigated. The method has been applied to sparsely sampled synthetic and realistic 3D data sets. The results of these tests were very satisfactory too (see again Chapter 6). It can thus be stated that all research objectives have been achieved.

Together with the exposition of the DMR and the DTR methodologies and the derivation of their theoretical principles, the advantages and limitations of these approaches have been discussed extensively. In this chapter, the most important findings for these two methods will be summarized. Furthermore, recommendations for future research will be made (see Section 8.1 and Section 8.2).

Additionally, further applications of the DMR approach have been examined. The methodology has been modified such that it can be applied for the redatuming of PS-data, and a new concept for the prediction of datum layer-related multiples by means of the DMR methodology has been developed (see Chapter 7.1 and Chapter 7.3). The applicability of the modified redatuming approach and the new concept for multiple prediction, both, have been evaluated on numerical 2D data sets with a positive outcome (see Chapter 7.2 and Chapter 7.4). The most important advantages and limitations of these approaches as well as recommendations for future research will be given in Section 8.3.

8.1 The DMR methodology

■ Advantages

- The DMR technology utilizes RMS velocities to describe the medium below the new datum level, which can be extracted from the input data set. Due to this, the redatuming procedure can be expressed as a data mapping technique, similar to DMO and AMO. Instead of a 4D integral, as for the conventional KSR approach, only a 2D integral has to be computed. Hence, the computational demand of the new approach is reduced compared to the KSR approach.

- In the application of the DMR methodology certain information becomes available that is required for the DTR methodology to infill missing data. In fact, the DMR technology can easily be combined with an infill step employing the DTR approach and can, therefore, handle sparsely sampled 3D data sets. All a-priori information required for a successful application of the DTR methodology to infill missing time samples is computed during the application of the DMR approach anyway.

■ Limitations

- The DMR approach has been derived from the Rayleigh II integral for inverse wavefield extrapolation. However, the application of Rayleigh II integral yields dynamically and kinematically correct results only if (1) the acquisition surface is flat, (2) the employed redatuming operators – the Green's functions – describe the wave propagation inside the datum layer correctly. For a curved acquisition surface, the redatumed results will be dynamically incorrect. For a complex datum layer the redatumed result will dynamically be correct within the approximations where transmission effects, internal reflections and multipathing inside the datum layer are ignored.

- Different from conventional redatuming, the DMR approach relies on certain knowledge of the subsurface below the datum layer. It has been shown that this dependence is insensitive and that the use of a redatumed RMS velocity field extracted from the input data set is already sufficient. However, if these velocities are greatly incorrect, errors in the traveltimes of the reconstructed events have to be expected.

- For the implementation of the DMR approach a flat new datum level has been assumed.

■ Recommendations

- It is recommended to adjust the implementation of the DMR approach such that traces with sources and receivers at a different depth level can be handled correctly. Therefore, a small modification of the code is necessary. Only the axes of the ellipsoid indicating the positions of all possible reflection points belonging to the considered time sample have to be rotated.

- There is a lot of scope to improve the efficiency of the current implementation of the DMR approach. The current algorithm strictly follows the flowchart presented in Chapter 2 and treats every output sample separately. It is, for example, advisable to treat several time samples simultaneously. The problem is very well suited for parallel implementation; i.e. the calculation of different time samples or groups of time samples, respectively, could be performed simultaneously on different nodes of a parallel machine.

- For dynamically correct redatuming results from curved acquisition surfaces it is recommended to derive the DMR integral from the Kirchhoff-Helmholtz integral equation, which handles these cases correctly [see Wapenaar, 1993].

- For dynamically correct redatuming results from complex datum layers with several interfaces it is recommended to perform the redatuming as an iterative procedure between the different interfaces. Furthermore, it is strongly advised to estimate the redatuming operators such that multipathing occurring inside the datum layer is handled correctly.

- For a dynamically correct result from relatively thin datum layers it is recommended to include the near-field term in the derivation of the DMR integral.

- The DMR methodology should be extended such that anisotropy can be handled correctly.

8.2 The DTR method

■ Advantages

- Different from the signal processing approaches to data reconstruction, the DELPHI trace replacement (DTR) method does not make any assumptions about the shape of the considered events. It purely utilizes the redundancy of seismic data sets, as every other data mapping technique, which generally scan for all possible dips for the reconstruction of a missing time sample. Hence, the result is not biased by the assumptions made about the shape of the events occurring in the reconstructed data set.

- As mentioned above, data mapping techniques usually scan all possible reflection points belonging to the considered output sample. In contrast to this, the DTR method assumes the position of the reflection point and its local dip belonging to missing time sample to be known. In fact, this information becomes available during the application of the DMR approach. It is then used by the DTR approach as a-priori knowledge. Due to this, the missing time sample no longer has to be reconstructed by means of a weighted stack along possibly contributing time samples. Instead, the missing time sample is replaced by a suitable (amplitude-corrected) time sample. This process is computationally less intensive.

- The a-priori knowledge needed for the DTR approach becomes available during the application of the DMR method. For this reason, the combination of the DMR technology and the DTR approach is ideal for the redatuming of sparsely sampled 3D seismic data.

■ Limitations

- Missing time samples can only be reconstructed correctly if the reflection point positions and their local dips are correct. If the current isochrone point is far away from the true reflection point and if the azimuth difference between the missing source/receiver pair and the source/receiver pair selected for the reconstruction are both large, the reconstruction will be incorrect. This can lead to artifacts in the redatumed result.

- In theory at least one trace of the sparsely sampled input data is assumed to be available exactly at the infill contour indicating all surface source and receiver locations that could be used for the data reconstruction. However, seismic data acquisition yields a discrete sampling of the wavefield. It is, therefore, likely that no trace exists with source and receiver exactly on the infill contour. Instead, a trace closest to the contour is selected.
  Furthermore, the sampling of the acquisition surface is not random. The data sets usually consist of several subsets, which all have the same geometry like marine parallel lines and cross-spread geometries at land. It is, therefore, likely that traces from a certain area are reconstructed by traces from one subset, and that the transition from one subset to another neighboring subset happens abruptly. This effect might as well cause artifacts in the redatumed result.

■ Recommendations

- Until now the DTR methodology has only been evaluated in combination with redatuming. For a more thorough evaluation it is recommended to test it separately.

- Until now only parallel line geometries have been considered to test the proposed sparse data redatuming approach. These tests should be extended to all commonly used 3D acquisition geometries, such as cross-spread geometries for land data.

- It is recommended to ease the requirements imposed on the selection of possibly contributing time samples for the DMR approach. One could, for example, opt to use any trace belonging to a considered reflection point instead of restricting the search only to traces with a certain angle of incidence. By doing this, an incorrect amplitude of the selected time sample is accepted. However, the occurrence of unwanted artifacts due to an incorrect infill could be prevented this way.

8.3 Further applications of the DMR methodology

■ Advantages

- The DMR approach can easily be extended to the redatuming of converted-wave data. Only the construction of the isochrone of possible reflection points belonging to the desired output sample has to be adjusted and the redatuming operators have to be selected accordingly.
- The DMR method can be modified such that redatumed datum layer-related multiples can be predicted and removed.

■ Limitations

- The integral expression of the DMR approach for converted-wave data has been derived from the integral expression underlying the KSR approach based on scalar wave equations. This assumes that the reconstructed pressure and velocity data has been decomposed in scalar P-wave and SV-wave potentials. For 3D data sets, this is by no means a trivial process, that is researched right now.
- The amplitude weights needed for the prediction of the datum layer-related multiples have not been derived yet. Hence, the amplitudes of the predicted multiples will not be correct.

■ Recommendations

- The DMR methodology for converted-wave data should be evaluated more thoroughly on synthetic and real input data.
- The amplitude weights needed for the prediction of the datum layer-related multiples by means of the modified DMR technology have to be derived.
- The proposed methodology for the prediction of datum layer-related multiples should be examined more detailed on synthetic and real input data.

A

Theory of the Kirchhoff summation approach to redatuming

In this appendix a derivation of the conventional KSR approach for 3D pre-stack data is presented.
Starting point for the derivation of the integral expression underlying the KSR method is the well-known Kirchhoff-Helmholtz integral [see for example Wapenaar, 1993]. This equation states that for any point A with the coordinates $\tilde{\mathbf{x}}_A = (\tilde{x}_A, \tilde{y}_A, \tilde{z}_A)$ inside the volume V with surface S and the inward pointing normal vector $\mathbf{n}$ (see Figure A.1) the acoustic pressure $P(\tilde{\mathbf{x}}_A, \omega)$ can be expressed as:

$$P(\tilde{\mathbf{x}}_A, \omega) = \frac{1}{4\pi} \int_S [G\nabla P - P\nabla G] \cdot \mathbf{n} dS + \int_V GQdV, \tag{A.1}$$

or, alternatively:

$$P(\tilde{\mathbf{x}}_A, \omega) = \frac{1}{4\pi} \int_S [G^*\nabla P - P\nabla G^*] \cdot \mathbf{n} dS + \int_V G^*QdV. \tag{A.2}$$

Here, $Q(\mathbf{x}, \omega)$ describes the source distribution inside V, $G(\mathbf{x}, \tilde{\mathbf{x}}_A, \omega)$ represents the forward-propagating Green's wavefield, and $G^*(\mathbf{x}, \tilde{\mathbf{x}}_A, \omega)$ represents the backward-propagating Green's wavefield.
At this point, it needs to be decided whether a two-way wavefield-extrapolation or a one-way wavefield-extrapolation should be applied. For a two-way – or full – wavefield-extrapolation full Green's functions are required including single scattered

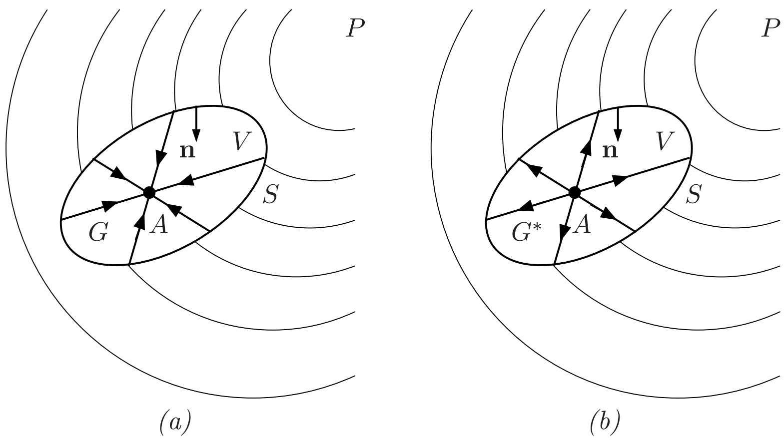

Figure A.1: *Point A inside V enclosed by S to which the wavefield should be extrapolated using the Kirchhoff-Helmholtz integral. (a) shows the situation for forward extrapolation with the causal Green's function G. (b) represents the backward extrapolation with the anti-causal Green's function G^*. [Figures according to Wapenaar et al., 1989]*

events (primaries) as well as multiply scattered events (multiples). To calculate such a Green's function correctly, an accurate velocity model of the probed subsurface is required and, additionally, a correct description of the sources. Thereby, the multiple events are very sensitive to the position of the reflectors.

In opposite to this, one-way extrapolation schemes consider primary events only. They are, therefore, more robust to errors of the subsurface model being used. In most cases an accurate velocity model of the probed subsurface is not available, since the estimation of such a model is usually the aim of seismic processing. Hence, inverse wavefield extrapolation, or redatuming, is mostly formulated as one-way extrapolation. Thereby, the input data set is assumed to contain only primaries; i.e. it is assumed that strong surface-related multiples have been removed by preprocessing and internal multiples are negligible. The latter assumption is true if the reflectivities of the probed subsurface are small.

Next, the Kirchhoff-Helmholtz integral needs to be modified for seismic data. In this situation the volume V and the surface S can be defined as presented in Figure A.2a. Here, the volume V around A is surrounded by the acquisition surface S_0 and by the surface S_h of a hemisphere with radius R. Hence, if V is assumed source-free and the radius R goes to infinity:

$$P(\tilde{\mathbf{x}}_A, \omega) = \frac{1}{4\pi} \int_{S_0} [G\nabla P - P\nabla G] \cdot \mathbf{n}\, dS_0. \tag{A.3}$$

According to the Sommerfeld radiation condition, the contribution over the hemisphere vanishes for the forward extrapolation case [Bleistein, 1984]. However, this radiation condition requires the Green's wavefield inside V to travel in the same

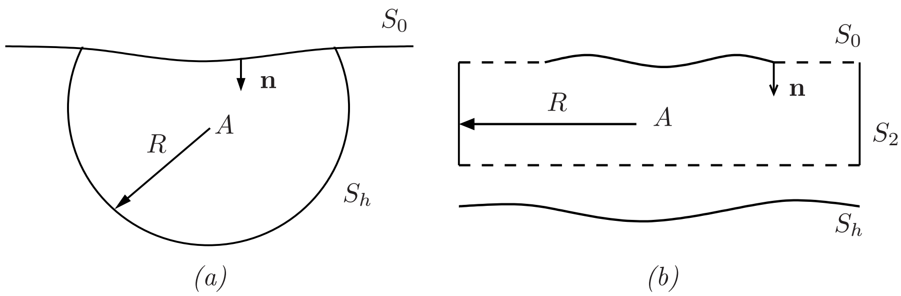

Figure A.2: *Volume V modified for the seismic situation for (a) forward extrapolation and (b) backward extrapolation. [Figures according to Wapenaar et al., 1989]*

direction as P. Unfortunately, this requirement is not met in case of backward extrapolation, which is applied for redatuming. In order to derive an expression similar to Equation A.3 for inverse extrapolation, the representation of the seismic data is changed. As displayed in Figure A.2b, the volume V is now enclosed by the acquisition surface S_0, a surface S_h between A and the reflector and by the cylindrical surface S_2 with radius R. If R goes to infinity, the contribution of S_2 vanishes, however, the contribution of S_h does not. It has been shown by Wapenaar et al. [1989] that this part is approximately zero if, for a constant velocity inside V, the evanescent waves at S_h are neglected, or, for an inhomogeneous velocity inside V, evanescent waves and multiply reflected waves inside V are neglected. These approximations for the inverse extrapolation of P yield:

$$P(\tilde{\mathbf{x}}_A, \omega) \approx \frac{1}{4\pi} \int_{S_0} [G^* \nabla P - P \nabla G^*] \cdot \mathbf{n} dS_0. \tag{A.4}$$

Here, $P(\tilde{\mathbf{x}}_A, \omega)$ is the up-going wavefield at A, while P represents the total wavefield at S_0. Furthermore, the Kirchhoff-Helmholtz integral can be replaced by the Rayleigh II integral if the seismic data are acquired at a plane acquisition surface S_0:

$$P(\tilde{\mathbf{x}}_A, \omega) = \frac{1}{2\pi} \int [P(\mathbf{x}, \omega) \frac{\partial G^*}{\partial n_0}] dS_0, \tag{A.5}$$

Note, that $\nabla G^* \cdot \mathbf{n}$ is now expressed as $\frac{\partial G^*}{\partial n_0}$, and that $P(\tilde{\mathbf{x}}_A, \omega)$ and $P(\mathbf{x}, \omega)$ both represent up-going wavefields. Furthermore, $\approx$ has been replaced by $=$ keeping the approximation in mind.

For a constant velocity v_1 between the surface S_0 and point A at the new datum the free space solution can be used for the Green's function:

$$G^* = \frac{e^{ikr}}{r}, \tag{A.6}$$

with $r = \sqrt{(\tilde{x}_A - x)^2 - (\tilde{y}_A - y)^2 - \tilde{z}_A^2}$ and the wavenumber k. This yields the following for the derivative of G^* with respect to $\mathbf{n}$:

$$\frac{\partial G^*}{\partial n_0} = \cos\alpha(\frac{ikr - 1}{r^2})e^{ikr}, \tag{A.7}$$

with:

$$\frac{\partial r}{\partial n_0} = \cos\alpha. \tag{A.8}$$

As shown in Figure A.3, α is the emergence angle.
Substituting Equation A.7 into A.5 results in:

$$P(\tilde{\mathbf{x}}_A, \omega) \quad = \quad \frac{1}{2\pi}\int P(\mathbf{x}, \omega)\cos\alpha\left[\frac{i\omega}{v_1 r} - \frac{1}{r^2}\right] e^{i\omega\tau} dS_0, \tag{A.9}$$

with the time shift $\tau = r/v_1$ given by the traveltime along the raypath from $\mathbf{x}$ to $\tilde{\mathbf{x}}_A$.
To save computation time, the near field term decaying with $1/r^2$ can be neglected when r is large with respect to v_1/ω:

$$P(\tilde{\mathbf{x}}_A, \omega) = \frac{1}{2\pi}\int P(\mathbf{x}, \omega)\cos\alpha\frac{i\omega}{v_1 r}\, e^{i\omega\tau} d\mathbf{x}. \tag{A.10}$$

This integral expression, the far-field approximation of the Rayleigh II integral assuming a constant medium between the acquisition surface and the new datum level, is commonly used for the conventional KSR approach. Note, that the surface integration $\int dS_0$ has been replaced by the equivalent expression $\int d\mathbf{x}$; i.e. the integration is formulated in terms of the x- and y-coordinates on S_0.
A seismic survey usually consists of sources and receivers both at S_0. In other words, both, sources and receivers, have to be moved from S_0 to the new datum S_1. Equation A.10 describes how the wavefield in point A on some surface S_1 can be

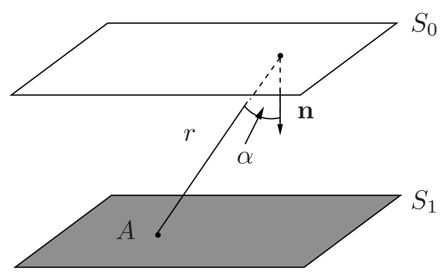

Figure A.3: *Geometry for the downward extrapolation.*

calculated from the observations on S_0. It can thus be used to calculate the result of having sources on S_0 and receivers on S_1:

$$P(\tilde{\mathbf{x}}_r, \mathbf{x}_s, \omega) = \frac{1}{2\pi} \int P(\mathbf{x}_r, \mathbf{x}_s, \omega) \cos \alpha_r \frac{i\omega}{v_1 r_r} e^{i\omega\tau_r} d\mathbf{x}_r, \tag{A.11}$$

with $r_r = |\tilde{\mathbf{x}}_r - \mathbf{x}_r|$, α_r being the emergence angle between the inward pointing normal vector of S_0 and the local raypath at $\mathbf{x}_r$, and $\tau_r = \frac{r_r}{v_1}$.
As stated by Wiggins [1984], Equation A.11 cannot be applied to move the sources to S_1, because this integral describes the backward extrapolation of a received signal. To move the sources, the principle of reciprocity is utilized. It states that a signal received at $\tilde{\mathbf{x}}_r$ from a source at $\mathbf{x}_s$ is equal to a signal that is received at $\mathbf{x}_s$ from a source at $\tilde{\mathbf{x}}_r$. Therefore, Equation A.10 can be applied to $P(\tilde{\mathbf{x}}_r, \mathbf{x}_s, \omega)$ to move the sources to S_1 as well:

$$P(\tilde{\mathbf{x}}_r, \tilde{\mathbf{x}}_s, \omega) = \frac{1}{2\pi} \int P(\tilde{\mathbf{x}}_r, \mathbf{x}_s, \omega) \cos \alpha_s \frac{i\omega}{v_1 r_s} e^{i\omega\tau_s} d\mathbf{x}_s. \tag{A.12}$$

Substituting A.11 into A.12 yields:

$$P(\tilde{\mathbf{x}}_r, \tilde{\mathbf{x}}_s, \omega) = \int\int \frac{\cos \alpha_r \cos \alpha_s}{(2\pi v_1)^2\, r_r r_s} (i\omega)^2 P(\mathbf{x}_r, \mathbf{x}_s, \omega)\, e^{i\omega(\tau_r + \tau_s)} d\mathbf{x}_r d\mathbf{x}_s, \tag{A.13}$$

with $\tau_s = \frac{r_s}{v_1}$.
Wiggins [1984] refers to Equation A.13 as the KRK integral. As one can see, it describes a double extrapolation of sources and receivers and is applicable to prestack data. This equation actually forms the basis of the KSR approach.

B

The estimation of ray parameters from the traveltimes of redatuming operators

The aim of this appendix is to explain how the ray parameters needed for the trace selection of the DMR approach can be estimated from the traveltimes of the given redatuming operators.
It is well known that the ray parameter ϱ of a certain ray can be expressed in terms of its angle of incidence α with respect to a surface and the medium velocity v:

$$\varrho = \frac{\sin\alpha}{v}. \tag{B.1}$$

However, it has been shown by for example Bleistein [1984] that this relation can easily be reformulated in terms of the traveltimes of the considered wave using the geometrical relations illustrated in Figure B.1. There, a wavefront is depicted at two different points in time belonging to the wave described by a ray with ray parameter ϱ. These wavefronts impinge on the reflector under the angle α. The sine of this angle of incidence can be expressed as:

$$\sin\alpha = \frac{vdt}{dx}, \tag{B.2}$$

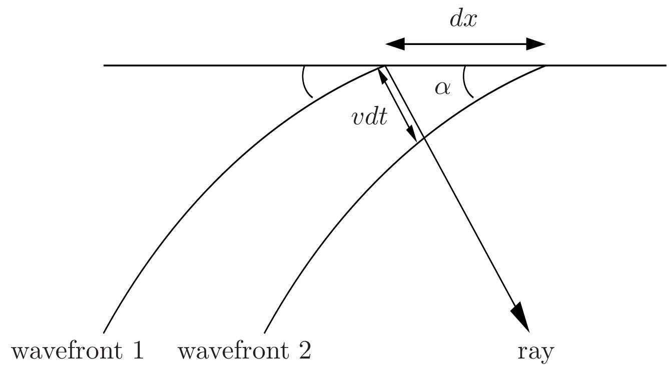

Figure B.1: *Derivation of the ray parameter ϱ. [Figure according to Bleistein, 1984]*

with dt being the difference in time and dx as depicted in Figure B.1. Substituting B.2 into B.1 yields:

$$\varrho = \frac{vdt}{vdx} = \frac{dt}{dx}. \tag{B.3}$$

Hence, the ray parameter ϱ of a certain ray reaching a surface can be estimated by taking the spatial derivative of the traveltimes measured at this surface.
For the DMR method the redatuming operators are utilized as common shot responses with sources at the new datum and receivers at the acquisition surface (see Figure B.2a). Taking the spatial derivatives here means calculating ray parameters at the acquisition surface. However, what is needed are ray parameters at the new datum layer in order to continue the estimated ray from the datum upwards. This can be achieved by rearranging the operators from common source gathers to common receiver gathers and taking the spatial derivatives at the datum location (see Figure B.2b). Note, that this requires the redatuming operators to be available for a dense grid of locations along the datum.
Furthermore, it needs to be taken into account that a 3D situation is considered; i.e.

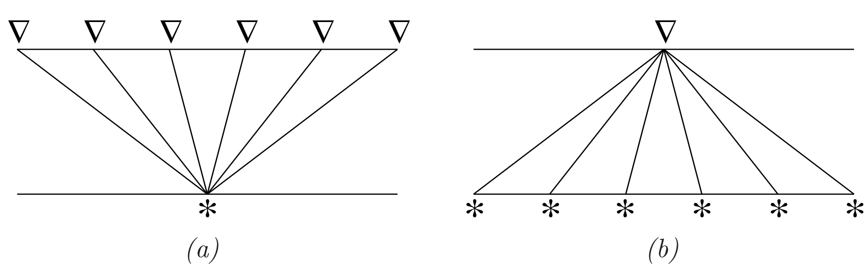

Figure B.2: *Redatuming operators (a) grouped as common source gathers and (b) grouped as common receiver gathers.*

the ray parameters:

$$\varrho_x = \frac{\sin\alpha_x}{v}, \tag{B.4}$$

$$\varrho_y = \frac{\sin\alpha_y}{v}, \tag{B.5}$$

need to be extracted from the traveltimes $t(x, y)$. This is accomplished by taking the partial derivatives in x- and y-direction of the rearranged traveltimes:

$$\varrho_x = \frac{\partial t}{\partial x}, \tag{B.6}$$

$$\varrho_y = \frac{\partial t}{\partial y}. \tag{B.7}$$

These ray parameters describe a ray connection a certain position at the datum with a certain position at the acquisition surface and can, therefore, be utilized for the selection of source/receiver pairs at the surface belonging to the possible reflection points.

C

Estimation of the eigenvalues for the Hessian matrix of the corrected traveltime function

The aim of this appendix is to explain why both eigenvalues of the Hessian matrix of the half-corrected traveltime function Γ are said to be positive. This is derived here for the situation of a flat target reflector, assuming that this is also representative for target reflectors that are not strongly curved.
In Chapter 3 the number n of positive eigenvalues of the Hessian matrix of the half-corrected traveltimes:

$$A_{jk} = \left[\frac{\partial^2 \Gamma(\hat{\mathbf{x}}_r)}{\partial x_{r_j} \partial x_{r_k}} \right], \tag{C.1}$$

with

$$\Gamma(\mathbf{x}_s, \mathbf{x}_r) = -t_t(\mathbf{x}_s, \mathbf{x}_r) + \tau_r(\mathbf{x}_r), \tag{C.2}$$

is required for the derivation of the integral expression describing the DMR method. For a flat target reflector at depth z_r and the new datum at depth z_d the required

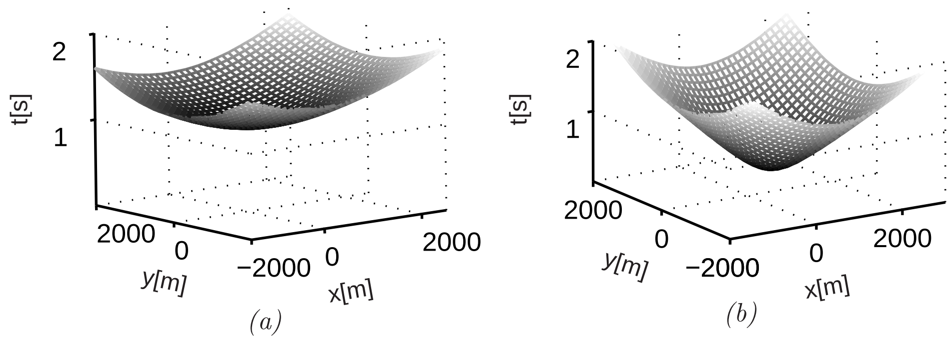

Figure C.1: *Comparison of the traveltime curves of (a) the reflection event and (b) the time correction for* $\mathbf{x}_s = (0\,m, 0\,m)$, $\hat{\mathbf{x}}_r = (500\,m, 0\,m)$, $v_1 = 1500\,{}^m/_s$, $v_{RMS} = 2000\,{}^m/_s$, $z_r = 1000\,m$ *and* $z_d = 500\,m$.

traveltimes t_t and time shifts τ_r can be expressed as:

$$t_t = \frac{2}{v_{RMS}}\sqrt{(\frac{x_r - x_s}{2})^2 + (\frac{y_r - y_s}{2})^2 + z_r^2}, \tag{C.3}$$

$$\tau_r = \frac{1}{v_1}\sqrt{(x_r - \tilde{x}_r)^2 + (y_r - \tilde{y}_r)^2 + z_d^2}. \tag{C.4}$$

Here, v_{RMS} denotes the RMS-velocity along a ray traveling from the considered source $\mathbf{x}_s = (x_s, y_s)$ via the target reflector to the receiver $\mathbf{x}_r = (x_r, y_r)$ at the surface. v_1 describes the velocity of the datum layer, and $\tilde{\mathbf{x}}_r = (\tilde{x}_r, \tilde{y}_r)$ describes the receiver position at the new datum. Figure C.1 provides a comparison of these traveltime curves for certain values of $\mathbf{x}_s$ and $\tilde{\mathbf{x}}_r$ clearly showing that the curvature of τ_r is considerably larger than the curvature of t_t.
Because of this, it can be assumed that the half-corrected traveltime Γ has a positive curvature in the vicinity of the stationary phase point $\hat{\mathbf{x}}_r$. Hence, it can be approximated by an hyperboloid t_h of the form:

$$t_h = \sqrt{1 + \frac{(x_r - \hat{x}_r)^2}{a_h^2} + \frac{(y_r - \hat{y}_r)^2}{a_h^2}} - b_h, \tag{C.5}$$

with a_h and b_h being two parameters defining the curvature and the shift in vertical direction, respectively. In Figure C.2 Γ is compared to such an hyperboloid.
The approximation made here is also valid for a dipping target reflector, because the reflector dip mainly causes the apex position of the traveltime curve to shift while its shape is approximately retained. The hyperboloid can then be described as:

$$t_h = \sqrt{1 + \frac{(x_r - \hat{x}_r)^2}{a_h^2} + \frac{(y_r - \hat{y}_r)^2}{c_h^2}} - b_h, \tag{C.6}$$

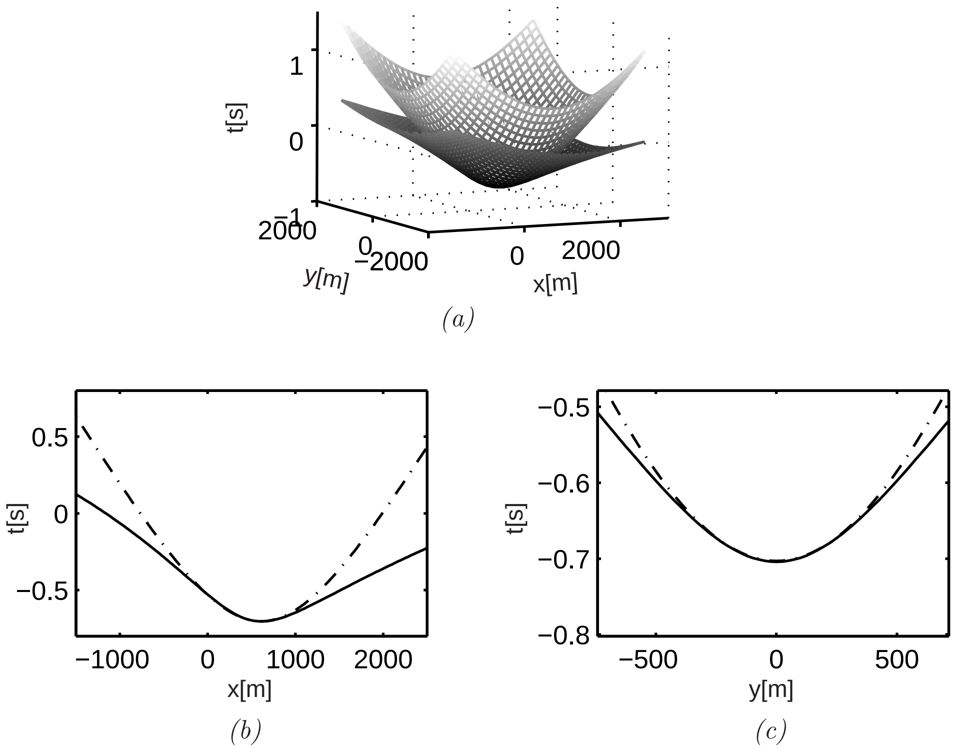

Figure C.2: *Comparison of the half-corrected traveltime curve Γ (solid line) and the hyperboloid t_h (dashed-dotted line) in (a) 3D, (b) along $y_r = \hat{y}_r$ and (c) along $x_r = \hat{x}_r$.*

with different curvatures in x- and y-direction.
The eigenvalues belonging to the Hessian matrix of Γ can be approximated by the eigenvalues of the Hessian matrix A_h belonging to a hyperboloid as described in Equation C.5:

$$A_h = \begin{bmatrix} \frac{\partial t_h^2}{\partial x_r^2} & \frac{\partial t_h^2}{\partial x_r \partial y_r} \\ \frac{\partial t_h^2}{\partial y_r \partial x_r} & \frac{\partial t_h^2}{\partial y_r^2} \end{bmatrix}. \tag{C.7}$$

According to Bartsch [1994], the eigenvalues $\zeta_{1,2}$ of any given 2×2-matrix D can be calculated using the following expression:

$$\zeta_{1,2} = \frac{1}{2} \left[(d_{11} + d_{22}) \pm \sqrt{4 d_{12} d_{21} + (d_{11} - d_{22})^2} \right]. \tag{C.8}$$

For the given problem the eigenvalues have to be derived for A_h, hence:

$$d_{11} = \frac{\partial t_h^2}{\partial x_r^2} = \frac{1}{a_h^2} \frac{[1 + \frac{(y_r - \hat{y}_r)^2}{c_h^2}]}{\left[\sqrt{1 + \frac{(x_r - \hat{x}_r)^2}{a_h^2} + \frac{(y_r - \hat{y}_r)^2}{c_h^2}}\right]^3}, \tag{C.9}$$

$$d_{12} = d_{21} = \frac{\partial t_h^2}{\partial x_r \partial y_r} = \frac{-1}{a_h c_h} \frac{(x_r - \hat{x}_r)(y_r - \hat{y}_r)}{\left[\sqrt{1 + \frac{(x_r - \hat{x}_r)^2}{a_h^2} + \frac{(y_r - \hat{y}_r)^2}{c_h^2}}\right]^3}, \tag{C.10}$$

$$d_{22} = \frac{\partial t_h^2}{\partial y_r^2} = \frac{1}{c_h^2} \frac{[1 + \frac{(x_r - \hat{x}_r)^2}{a_h^2}]}{\left[\sqrt{1 + \frac{(x_r - \hat{x}_r)^2}{a_h^2} + \frac{(y_r - \hat{y}_r)^2}{c_h^2}}\right]^3}. \tag{C.11}$$

Here, it can clearly be seen that d_{11} and d_{22} will both have positive, real values, and, furthermore, that the multiplication of d_{12} and d_{21} will have a positive, real result. It can thus be concluded that the radicand of Equation C.8 will be real and positive, too; i.e. the first eigenvalue ζ_1 has to be positive.
In order to prove that ζ_2 is positive, it has to be shown that:

$$d_{11} + d_{22} - \sqrt{4 d_{12} d_{21} + (d_{11} - d_{22})^2} > 0, \tag{C.12}$$

or, after reformulating this expression, that:

$$d_{11} d_{22} > d_{12} d_{21}. \tag{C.13}$$

Substituting Equations C.9-C.11 yields:

$$\frac{1}{a_h^2 c_h^2} \frac{[1 + \frac{(x_r - \hat{x}_r)^2}{a_h^2}][1 + \frac{(y_r - \hat{y}_r)^2}{c_h^2}]}{\left[\sqrt{1 + \frac{(x_r - \hat{x}_r)^2}{a_h^2} + \frac{(y_r - \hat{y}_r)^2}{c_h^2}}\right]^6} > \frac{1}{a_h^4 c_h^4} \frac{(x_r - \hat{x}_r)^2 (y_r - \hat{y}_r)^2}{\left[\sqrt{1 + \frac{(x_r - \hat{x}_r)^2}{a_h^2} + \frac{(y_r - \hat{y}_r)^2}{c_h^2}}\right]^6}, \tag{C.14}$$

and after further simplification:

$$1 + \frac{(x_r - \hat{x}_r)^2}{a_h^2} + \frac{(y_r - \hat{y}_r)^2}{c_h^2} > 0. \tag{C.15}$$

This statement is certainly true and, therefore, the second eigenvalue ζ_2 is positive as well.

D

The construction of a contour of source/receiver pairs with rays reaching a certain reflection point under identical angle of incidence

The aim of this appendix is to explain how a contour at a new, flat datum level, as it is assumed throughout this thesis, can be constructed, which indicates the positions of all source/receiver pairs $\tilde{\mathbf{x}}^{'}_{s,r}$ at this datum belonging to rays that reach a certain reflection point under an identical angle of incidence.
The contour at the new datum indicates the intersection of the datum plane and a cone, which has its apex at the possible reflection point belonging to the time sample that needs to be reconstructed. Consequently, the contour at the new datum is determined by the characteristics of the cone: its apex position $\mathbf{x}_{iso}$, its opening angle φ, which is twice the angle of incidence α, and its axis of rotation $\tilde{\mathbf{x}}_{c,0}$ (see Figure D.1). Besides the apex position $\mathbf{x}_{iso}$, two points on the contour – the source position $\tilde{\mathbf{x}}_s$ at the new datum and the receiver position $\tilde{\mathbf{x}}_r$ at the new datum – are known. These three points define the vectors (see also Figure D.2):

$$\tilde{\mathbf{x}}_{c,s} = \tilde{\mathbf{x}}_s - \mathbf{x}_{iso}, \;\; \tilde{\mathbf{x}}_{c,r} = \tilde{\mathbf{x}}_r - \mathbf{x}_{iso}, \tag{D.1}$$

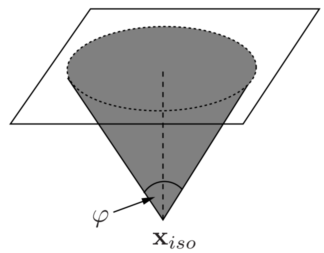

Figure D.1: *Infill cone, which indicates all rays belonging to different source/receiver pairs at the datum that reach the reflection point with an identical angle of incidence.*

which are part of the cone. They can be utilized to calculate the opening angle φ by means of their scalar product:

$$\varphi = \arccos\left(\frac{\tilde{\mathbf{x}}_{c,s}\tilde{\mathbf{x}}_{c,r}}{|\tilde{\mathbf{x}}_{c,s}||\tilde{\mathbf{x}}_{c,r}|}\right). \tag{D.2}$$

Furthermore, it is known that:

[**1**] the rotation axis intersects the datum plane at some point $\tilde{\mathbf{x}}_0$ on the straight line in the datum plane connecting $\tilde{\mathbf{x}}_s$ and $\tilde{\mathbf{x}}_r$ (see Figure D.2). This straight line can be described by its slope m_0 and its intercept b_0 with the y-axis:

$$m_0 = \frac{\tilde{y}_r - \tilde{y}_s}{\tilde{x}_r - \tilde{x}_s}, \;\; b_0 = \tilde{y}_s - \frac{\tilde{y}_r - \tilde{y}_s}{\tilde{x}_r - \tilde{x}_s}\tilde{x}_s. \tag{D.3}$$

Hence, the components of $\tilde{\mathbf{x}}_0$ have to satisfy the following equation:

$$\tilde{y}_0 = m_0\tilde{x}_0 + b_0. \tag{D.4}$$

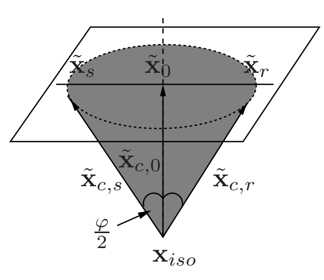

Figure D.2: *Definition of the rotation axis of the infill cone.*

[2] the rotation axis, whose direction is given by the following vector:

$$\tilde{\mathbf{x}}_{c,0} = \tilde{\mathbf{x}}_0 - \mathbf{x}_{iso}, \tag{D.5}$$

and $\tilde{\mathbf{x}}_{c,s}$ intersect each other with half the opening angle. Hence, the components of $\tilde{\mathbf{x}}_0$ have to satisfy the following equation:

$$\frac{\tilde{\mathbf{x}}_{c,s}\tilde{\mathbf{x}}_{c,0}}{|\tilde{\mathbf{x}}_{c,s}||\tilde{\mathbf{x}}_{c,0}|} = \cos\frac{\varphi}{2}. \tag{D.6}$$

Thus, $\tilde{\mathbf{x}}_0$ can be found by combining Equations D.4 and D.6.
Once the direction of the rotation axis and its intersection with the datum have been defined, the contour at the datum can be determined in a similar way. All points $\tilde{\mathbf{x}}^{'}_{s,r}$ on this contour have to be positioned somewhere along straight lines in the datum plane, which can be described as the straight line connecting $\tilde{\mathbf{x}}_s$ and $\tilde{\mathbf{x}}_r$ rotated around $\tilde{\mathbf{x}}_0$ by $\vartheta \in [0, 2\pi)$. This is illustrated in Figure D.3. In other words, the contour points have to satisfy the following equation:

$$\tilde{y}^{'}_{s,r} = \tan\left(\arctan\left(m_0\right) + \vartheta\right)\tilde{x}^{'}_{s,r} + \left(\tilde{y}_0 - \tan\left(\arctan\left(m_0\right) + \vartheta\right)\tilde{x}_0\right). \tag{D.7}$$

And, since the contour points lie on the cone, the vectors $\tilde{\mathbf{x}}^{'}_{c,s}$ and $\tilde{\mathbf{x}}^{'}_{c,r}$:

$$\tilde{\mathbf{x}}^{'}_{c,s} = \tilde{\mathbf{x}}^{'}_s - \mathbf{x}_{iso}, \;\; \tilde{\mathbf{x}}^{'}_{c,r} = \tilde{\mathbf{x}}^{'}_r - \mathbf{x}_{iso}, \tag{D.8}$$

both have to intersect the rotation axis $\tilde{\mathbf{x}}_{c,0}$ with half the opening angle. That is, the contour points have to satisfy the following equations:

$$\frac{\tilde{\mathbf{x}}^{'}_{c,s}\tilde{\mathbf{x}}_{c,0}}{|\tilde{\mathbf{x}}^{'}_{c,s}||\tilde{\mathbf{x}}_{c,0}|} = \cos\frac{\varphi}{2}, \tag{D.9}$$

$$\frac{\tilde{\mathbf{x}}^{'}_{c,r}\tilde{\mathbf{x}}_{c,0}}{|\tilde{\mathbf{x}}^{'}_{c,r}||\tilde{\mathbf{x}}_{c,0}|} = \cos\frac{\varphi}{2}. \tag{D.10}$$

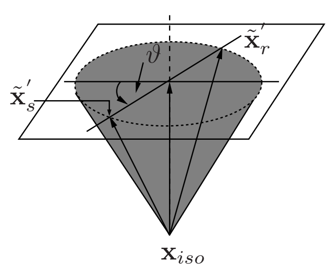

Figure D.3: *The contour, which indicates all source/receiver pairs at the datum belonging to rays which reach the same reflection point with an identical angle of incidence, is constructed by rotation around* $\tilde{\mathbf{x}}_{c,0}$.

Now, all contour points $\tilde{\mathbf{x}}'_{s,r}$ can be found by combining Equations D.7, D.9 and D.10.

Note, again, that these derivations are only valid for a locally flat datum layer between the redatumed source and the redatumed receiver. If it is intended to extend the approach to arbitrary datum layers, the construction of the contour needed for the infill of missing data has to be modified accordingly.

E

Notation, Symbols and Abbreviations

E.1 Notation

For the notation in this thesis the following conventions have been adopted:

- Scalars are given by lower-case normal font, e.g. x.
- Vectors are given by lower-case bold font, e.g. $\mathbf{x}$. The elements of vectors indicating positions in a Cartesian coordinate system are given by lower case normal font subscripted by the name of the vector, e.g. $(x_{iso}, y_{iso}, z_{iso})$ belonging to $\mathbf{x}_{iso}$.
- Matrices are given by upper-case normal font, e.g. A. One element of a matrix is denoted by an upper-case normal font with a double subscript, e.g. $A_{i,j}$ means element (i, j) of matrix A.
- The determinant of a matrix is given by an upper-case calligraphic font, e.g. $\mathcal{A}$.
- Parameters related to sources are denoted by the subscript s in normal font, parameters related to receivers are denoted by the subscript r in normal font, e.g $\mathbf{x}_r$.

- Positions at the acquisition surface are denoted by a vector $\mathbf{x}$.
- Positions at the new datum level are denoted by a vector $\tilde{\mathbf{x}}$.
- Stationary phase points are denoted by a vector $\hat{\mathbf{x}}$.
- Source/receiver positions, which can be used to infill missing traces are denoted by $\mathbf{x}^{'}$ at the acquisition surface and by $\tilde{\mathbf{x}}^{'}$ at the datum level.

E.2 Symbols

In the following symbols that occur frequently are briefly explained. Symbols that occur infrequently are not listed. Their meaning will be clear from the text.

Scalars

symbol	description
p	seismic wavefield in the space-time domain
P	seismic wavefield in the space-frequency domain
t	time
ω	angular frequency
k	wavenumber
t_{red}	time sample to be redatumed
t_L	possibly contributing time sample on locus L
$\tau_{s,r}$	one-way traveltime between sources at the acquisition surface and the new datum, and receivers at the acquisition surface and the new datum, respectively. This equals the time shift applied during redatuming
t_t	two-way traveltime of a reflection event at the true reflector recorded at the acquisition surface
$t_{t,KSR}$	traveltime of a reflection event in a half-redatumed data set
t_e	traveltime of the missing time sample
Δt_{DTR}	difference in traveltime between the missing time sample and the time sample used for reconstruction
Γ	half-corrected traveltime of a reflection event for the DMR method ($\Gamma = -t_t + \tau_r$)

Γ_{DMR}	fully corrected traveltime of a reflection event for the DMR method ($\Gamma_{DMR} = -t_t + \tau_r + \tau_s$)
Γ_{KSR}	fully corrected traveltime of a reflection event for the KSR method ($\Gamma_{KSR} = -t_{t,KSR} + \tau_s$)
$\mathcal{A}$	determinant of A (related to Γ)
$\mathcal{A}_{DMR}$	determinant of A_{DMR} (related to Γ_{DMR})
$\mathcal{A}_{KSR}$	determinant of A_{KSR} (related to Γ_{KSR})
a	amplitude
a_{sr}	amplitude of a missing time sample
$a_{s'r'}$	amplitude of a time sample used for reconstruction
a_{DTR}	amplitude correction applied for the infill
r	distance between two points
$r_{s,r}$	distance between a source at the acquisition surface and the new datum and a receiver at the acquisition surface and the new datum, respectively
α	emergence angle at a certain point between the local raypath and the inward pointing normal vector
$\alpha_{s,r}$	emergence angle at $\mathbf{x}_{s,r}$ between the local raypath and the inward pointing normal vector of the acquisition surface
v	velocity
v_{RMS}	RMS velocity
v_1	velocity of the datum layer
v_{NMO}	redatumed stacking velocity
v_2	redatumed stacking velocity chosen to describe the medium below the datum for a certain redatumed time sample
a_{ell}	long axis of the ellipsoid describing the isochrone of possible reflection points
b_{ell}	short axis of the ellipsoid describing the isochrone of possible reflection points
$\delta_{x,y}$	local dip of the ellipsoid in x, y-direction
θ	azimuth of a certain point $\mathbf{x}_{iso}$ on the isochrone
ϕ	polar angle of a certain point $\mathbf{x}_{iso}$ on the isochrone
ε	relative error
ε_O	relative error of focal point position
ε_ϱ	relative error of ray parameter

ε_S	relative error in the position of a source/receiver pair

- **Vectors**

symbol	description
$\mathbf{x}_{s,r}$	source/receiver position at the acquisition surface
$\tilde{\mathbf{x}}_{s,r}$	source/receiver position at the new datum
$\mathbf{x}_{iso}$	point on the isochrone of possible reflection points
$\hat{\mathbf{x}}_{s,r}$	stationary source/receiver at the acquisition surface
$\mathbf{x}'_{s,r}$	source/receiver position of a trace used for the infill of missing data
$\tilde{\mathbf{x}}'_{s,r}$	source/receiver positions on the infill contour at the new datum level
$\boldsymbol{\varrho}$	ray parameter consisting of the components (ϱ_x, ϱ_y)
$\boldsymbol{\varrho}_{s,r}$	ray parameter belonging to the ray between the considered reflection point and a source/receiver at the new datum
$\mathbf{n}$	normal vector

- **Matrices**

symbol	description
A	Hessian matrix of Γ
A_{DMR}	Hessian matrix of Γ_{DMR}
A_{KSR}	Hessian matrix of Γ_{KSR}

E.3 Abbreviations

abbreviation	meaning
1D	one dimensional
2D	two dimensional
3D	three dimensional
KDM	Kirchhoff data mapping
NMO	normal move-out
DMO	dip move-out
AMO	azimuthal move-out

DMR	data mapping approach to redatuming
KSR	Kirchhoff summation approach to redatuming
CFP	Common Focus Point
RMS	root mean square
TDO	topographic datuming operator
DTR	DELPHI trace replacement
OMO	offset move-out
SCO	shot continuation operator
EFI	Experimental Facility for Imaging
ZMAART	Ziggy Model Acquisition and the ART of physical modeling

Bibliography

Aki, K., and Richards, P. G., 2002, Quantitative Seismology: University Science Press, 2nd edition.

Al-Ali, M., and Blacquiere, G., 2005, Velocity-independent determination of 3D focusing operators using cross-spreads: 75th Ann. Internat. Mtg., Soc. of Expl. Geophys., 1830–1833.

Alkhalifah, T., and Bagaini, C., 2004, Cost-effective datuming in presence of rough topography and complex near-surface: 74th Ann. Internat. Mtg., Soc. of Expl. Geophys., 2024–2027.

Alkhalifah, T., and Bagaini, C., 2006, Straight-rays redatuming: A fast and robust alternative to wave-equation-based datuming: Geophysics, **71**, no. 3, U37–U46.

Aminzadeh, F., Burkhard, N., Nicoletis, L., Rocca, F., and Wyatt, K., 1994, SEG/EAEG 3-D modeling project: 2nd update: The Leading Edge, **13**, no. 9, 949–952.

Aminzadeh, F., Burkhard, N., Long, J., Kunz, T., and Duclos, P., 1996, Three dimensional SEG/EAEG models — an update: The Leading Edge, **15**, no. 2, 131–134.

Bagaini, C., and Alkhalifah, T., 2003, One Step Better than Static Corrections The Topographic Datuming Operator: 65th Meeting, Eur. Assn. Geosci. Eng., C07.

Bagaini, C., and Spagnolini, U., 1996, 2-D continuation operators and their applications: Geophysics, **61**, no. 6, 1846–1858.

Bartsch, H. J., 1994, Taschenbuch mathematischer Formeln: Fachbuchverlag Leipzig – Köln.

Berkhout, A. J., 1997a, Pushing the limits of seismic imaging, part I: prestack migration in terms of double dynamic focusing: Geophysics, **62**, no. 3, 937 – 953.

——— 1997b, Pushing the limits of seismic imaging, part II: integration of prestack migration, velocity estimation and AVO analysis: Geophysics, **62**, no. 3, 954 – 969.

Berryhill, J. R., and Kim, Y. C., 1986, Deep-water peglegs and multiples - Emulation and suppression: Geophysics, **51**, no. 12, 2177–2184.

Berryhill, J. R., 1979, Wave-equation datuming: Geophysics, **44**, no. 8, 1329 – 1344.

Berryhill, J. R., 1984, Short note: Wave-equation datuming before stack: Geophysics, **49**, no. 11, 2064 – 2066.

Berryhill, J. R., 1986, Submarine canyons: Velocity replacement by wave-equation datuming before stack: Geophysics, **51**, no. 8, 1572 – 1579.

Bevc, D., 1995, Imaging under rugged topography and complex velocity structure: Ph.D. thesis, Stanford University.

Bevc, D., 1997, Flooding the topography: Wave-equation datuming of land data with rugged acquisition topography: Geophysics, **62**, no. 5, 1558 – 1569.

Biondi, B., Fomel, S., and Chemingui, N., 1998, Azimuth moveout for 3-D prestack imaging: Geophysics, **63**, no. 2, 574–588.

Biondi, B., 2001, Kirchhoff imaging beyond aliasing: Geophysics, **66**, no. 2, 654–666.

Biondi, B., 2006, 3-D Seismic Imaging:, Investigations in Geophysics Soc. of Expl. Geophys., in press.

Blacquiere, G., and Koek, A. E., 1997, 3-D seismic experiments with the Delft modeling facility: 67th Ann. Internat. Mtg., Soc. of Expl. Geophys., 16–19.

Blacquiere, G., Debeye, H. W. J., Wapenaar, C. P. A., and Berkhout, A. J., 1989, 3D table-driven migration: Geophysical Prospecting, **37**, no. 8, 925–958.

Bleistein, N., and Jaramillo, H., 2000, A platform for Kirchhoff data mapping in scalar models of data acquisition: Geophysical Prospecting, **48**, no. 1, 135–161.

Bleistein, N., 1984, Mathematical methods for wave phenomena: Academic Press, Inc.

Cerveny, V., 2001, Seismic ray theory: Cambridge University Press.

Chang, W. F., and McMechan, G. A., 1989, 3D acoustic reverse-time migration: Geophysical Prospecting, **37**, no. 3, 243–256.

Chang, W. F., and McMechan, G. A., 1990, 3D acoustic prestack reverse-time migration: Geophysical Prospecting, **38**, no. 7, 737–756.

Claerbout, J. F., and Doherty, S., 1972, Downward continuation of seismograms: Geophysics, **37**, no. 5, 741 – 768.

Claerbout, J. F., 1985, Imaging the Earth's Interior: Blackwell Sciences Publications.

Crawley, S., Clapp, R., and Claerbout, J., 1999, Interpolation with smoothly nonstationary prediction-error filters: 69th Ann. Internat. Mtg., Soc. of Expl. Geophys., 1154–1157.

Deregowski, S., 1986, What is DMO: First break, **4**, no. 7, 7 – 24.

Dix, C. H., 1955, Seismic velocities from surface measurements: Geophysics, **20**, no. 1, 68–86.

Duijndam, A. J. W., Schonewille, M. A., and Hindriks, C. O. H., 1999, Reconstruction of band-limited signals, irregularly sampled along one spatial direction: Geophysics, **64**, no. 2, 524–538.

Energy Information Administration, 2005, International Energy Outlook: Office of Integrated Analysis and Forecasting, U.S. Department of Energy.

Farmer, P., Jones, I., Zhou, H., Bloor, R., and Goodwin, M., 2006, Application of reverse time migration to complex imaging problems: First Break, **24**, no. 9, 65–74.

Gazdag, J., and Sguazzero, P., 1984, Migration of seismic data by phase-shift plus interpolation: Geophysics, **49**, no. 2, 124 – 131.

Gazdag, J., 1978, Wave equation migration with the phase-shift method: Geophysics, **43**, no. 7, 1342 – 1351.

Gisolf, A., 2002, Infilling of sparse 3D seismic data for 3D focusing operator estimation: 72nd Ann. Internat. Mtg., Soc. Expl. Geophys., 1272 – 1275.

Hale, D., 1991, Dip Moveout Processing: Soc. of Expl. Geophys.

Hill, N. R., 1990, Gaussian beam migration: Geophysics, **55**, no. 11, 1416–1428.

Hill, N. R., 2001, Prestack Gaussian-beam depth migration: Geophysics, **66**, no. 4, 1240–1250.

Hindriks, C., and Verschuur, D. J., 2001, CFP approach to the complex near surface: 71st Ann. Internat. Mtg., Soc. Expl. Geophys., 1863 – 1866.

Hindriks, K. O. H., Duijndam, A. J. W., and Schonewille, M. A., 1997, Reconstruction of two-dimensional irregularly sampled wavefields: 67th Ann. Internat. Mtg., Soc. of Expl. Geophys., 1163–1166.

Holberg, O., 1988, Towards optimum one-way wave propagation: Geophysical Prospecting, **36**, no. 2, 99–114.

Hubral, P., 1983, Computing true amplitude reflections in a laterally inhomogeneous earth: Geophysics, **48**, no. 8, 1051 – 1062.

Kabir, M. M. N., and Verschuur, D. J., 1995, Restoration of missing offsets by parabolic Radon transform: Geophysical Prospecting, **43**, no. 3, 347–368.

Kelamis, P. G., Verschuur, D. J., Berkhout, A. J., and Erickson, K. E., 1999, Velocity-independent datuming of seismic data: 69th Ann. Internat. Mtg., Soc. Expl. Geophys., 441–444.

Kelamis, P. G., Erickson, K. E., Verschuur, D. J., and Berkhout, A. J., 2002, Velocity-independent redatuming of seismic data: A new approach to the near-surface problem in land seismic data processing: The Leading Edge, **21**, no. 8, 730 – 735.

Larkin, S. P., and Levander, A., 1996, Wave-equation datuming for improving deep crustal seismic images: Tectonophysics, **264**, 371 – 379.

Marsden, D., 1993, Static corrections – a review, Part I: The Leading Edge, **12**, no. 1, 43 – 49.

Martini, F., and Bean, C., 2002a, Application of pre-stack wave equation datuming to remove interface scattering in sub-basalt imaging: First Break, **20**, no. 6, 395 – 403.

——— 2002b, Interface scattering versus body scattering in subbasalt imaging and application of pre-stack wave equation datuming: Geophysics, **67**, no. 5, 1593 – 1601.

McMechan, G. A., 1982, Determination of source parameters by wavefield extrapolation: Geophysical Journal of the Royal Astronomical Society, **71**, 613–628.

McMechan, G. A., 1983, Migration by extrapolation of time-dependent boundary values: Geophysical Prospecting, **31**, no. 3, 413–420.

Merriam Webster. Online Dictionary, `http://www.m-w.com`.

Oxford Dictionary of English. 1989, Oxford University Press, 2nd edition.

Pica, A., Poulain, G., David, B., Magesan, M., Baldock, S., Weisser, T., Hugonnet, P., and Herrmann, P., 2005, 3D surface-related multiple modeling: The Leading Edge, **24**, no. 3, 292–296.

Schalkwijk, K. M., Wapenaar, C. P. A., and Verschuur, D. J., 2003, Adaptive decomposition of multicomponent ocean-bottom seismic data into downgoing and upgoing P- and S-waves: Geophysics, **68**, no. 3, 1091–1102.

Sheriff, R. E., 2002, Encyclopedic Dictionary of Applied Geophysics: Soc. of Expl. Geophys., 4th edition.

Shtivelman, V., and Canning, A., 1988, Datum correction by wave-equation extrapolation: Geophysics, **53**, no. 10, 1311 – 1322.

Spagnolini, U., and Opreni, S., 1996, 3-D shot continuation operator: 66th Ann. Internat. Mtg., Soc. of Expl. Geophys., 439–442.

Spitz, S., 1991, Seismic trace interpolation in the F-X domain: Geophysics, **56**, no. 6, 785–794.

Staude, O., 1882, Ueber die Fadenconstructionen des Ellipsoides: Mathematische Annalen, **20**, 147 – 184.

Stoffa, P., Fokkema, J., de Luna Freire, R., and Kessinger, W., 1990, Split-step Fourier migration: Geophysics, **55**, no. 4, 410 – 421.

Tegtmeier, S., Gisolf, A., and Verschuur, D. J., 2004, 3D sparse-data Kirchhoff redatuming: Geophysical Prospecting, **52**, no. 6, 509 – 521.

Telford, W. M., Geldart, L. P., and Sheriff, R. E., 1990, Applied Geophysics: Cambridge University Press.

Thorbecke, J. W., and Berkhout, A. J., 1994, 3-D recursive extrapolation operators: An overview: 64th Ann. Internat. Mtg., Soc. of Expl. Geophys., 1262–1265.

Thorson, J. R., and Claerbout, J. F., 1985, Velocity-stack and slant-stack stochastic inversion: Geophysics, **50**, no. 12, 2727–2741.

van de Rijzen, M. J., Verschuur, D. J., and Gisolf, A., 2003, Data-driven meets model-driven – 3D-CFP operator updating: EAGE/SEG Summer Research Workshop, Eur. Assn. Geosci. Eng., T08.

van de Rijzen, M., Gisolf, A., and Verschuur, D. J., 2004, Infilling of sparse 3D data for 3D focusing operator estimation: Geophysical Prospecting, **52**, no. 6, 489 – 507.

van Veldhuizen, E. J., and Blacquiere, G., 2005, Integrated approach to acquisition geometry analysis: 75th Ann. Internat. Mtg., Soc. of Expl. Geophys., 1–4.

Verschuur, D., and Marhfoul, B. E., 2005, Estimation of Complex Near Surface Focusing Operators by Global Optimization: 67th Meeting, Eur. Assn. Geosci. Eng., A035.

Vidale, J. E., 1988, Finite-difference calculation of traveltimes: Bulletin of the Seismological Society of America, **78**, no. 6, 2062–2076.

Vidale, J. E., 1990, Finite-difference calculation of traveltimes in three dimensions: Geophysics, **55**, no. 5, 521–526.

Wapenaar, C. P. A., Peels, G. L., Budejichy, V., and Berkhout, A. J., 1989, Inverse extrapolation of primary seismic waves: Geophysics, **54**, no. 7, 853 – 863.

Wapenaar, C. P. A., 1993, Kirchhoff-Helmholtz downward extrapolation in a layered medium with curved interfaces: Geophysical Journal International, **115**, 445 – 455.

Wiggins, J. W., 1984, Kirchhoff integral extrapolation and migration of nonplanar data: Geophysics, **49**, no. 8, 1239 – 1248.

Wiggins, J. W., 1988, Attenuation of complex water-bottom multiples by wave equation-based prediction and subtraction: Geophysics, **53**, no. 12, 1527–1539.

Zwartjes, P., 2005, Fourier reconstruction with sparse inversion: Ph.D. thesis, Delft University of Technology.

Summary

Redatuming of Sparse 3D Seismic Data

The purpose of a seismic survey is to produce an image of the subsurface providing an overview of the earth's discontinuities. The obtained image can be interpreted by geologists, geophysicists or reservoir engineers. The aim of seismic processing - including procedures like temporal and spatial filtering, traveltime corrections and, finally, the migration of the reflection energy - is to recreate this image. The seismic method is especially well suited for the exploration and the monitoring of hydrocarbon reservoirs.

A majority of the algorithms, which are applied for seismic processing, are optimized for regularly sampled data referenced to a flat surface and for a simple velocity distribution in the subsurface. In reality, data are collected at irregularly sampled, rugged surfaces and/or with complex structures in the subsurface. As a pre-processing step, the seismic data can be *redatumed* to a new reference surface prior to further processing, which satisfies the requirements mentioned above. Redatuming virtually places sources and receivers at another level without moving them.

The methodology most commonly used for redatuming is the so-called Kirchhoff summation redatuming (KSR). It has been applied successfully to 2D data sets.

The redatuming of pre-stack data by means of the KSR approach is applied in two separate steps, one to redatum the receivers and one to redatum the sources. Each step requires the computation of the Rayleigh II integral over the coordinates of the considered sources and receivers, respectively. This integral can be derived from

the acoustic wave equation. It allows the calculation of the seismic wavefield at any point below the acquisition surface by means of a weighted sum of the wavefield measurements at the surface; i.e. for the redatuming of 2D pre-stack data by means of the KSR approach a 2D integral has to be computed, for the redatuming of 3D pre-stack data a 4D integral has to be computed. The KSR method requires the input data set to be densely sampled in both source and receiver coordinates at the acquisition surface to avoid aliasing artifacts.

The weighting functions account for the propagation effects between the surface points and the target point at the new datum, in terms of traveltimes and amplitudes. In practice, they are unknown and need to be estimated from the seismic data (data-driven approach) or from a given velocity model of the datum layer (model-driven approach).

Nowadays, the amount of 3D data increases, which makes it more and more important to develop a feasible method for the redatuming of 3D pre-stack data. However, all commonly used 3D acquisition geometries deliver data sets that are sparse in at least one of the coordinates, meaning that the KSR approach is not directly applicable. Hence, a new redatuming methodology had to be developed, which is applicable to sparsely sampled 3D data.

In this thesis, data mapping redatuming (DMR) is presented. The choice has been made to formulate the redatuming process in terms of a data mapping problem, similar to well-known techniques as, for example, dip move-out (DMO) correction and azimuthal move-out (AMO) correction. For the DMR approach, firstly, all time samples of the input data set are identified which are possibly contributing to the output sample considered. To achieve this, certain assumptions about the velocity model below the new datum level are made. It is assumed that the medium below the new datum level can be described by the redatumed stacking velocities, which can be extracted from the input data by conventional velocity analysis. Furthermore, the potential reflectors below the datum are assumed not to be strongly curved. Then, a weighted stack is applied to the possibly contributing time samples, which yields the sought-after time sample of the considered redatumed trace. This is different from the conventional methods. However, in this new DMR approach, the number of traces involved in the calculation of one output sample is reduced considerably as well as the dimensionality of the integral expression describing the process. Only a 2D integral needs to be calculated to compute one output sample compared to a 4D integral for the conventional KSR approach.

The DMR approach is in general applicable to all sorts of input data sets, but, as already mentioned, the primary interest of this work was to develop an approach applicable to data sets that do not have a dense areal coverage of sources and receivers at the acquisition surface. For the DMR approach it can still happen that the required traces have not been acquired, even if it uses considerably less traces per output sample. In case this happens, the DMR approach needs to be combined with a data infill procedure.

The information about the possible reflection points belonging to the time sample considered, which can be obtained from the assumptions of the medium below the new datum level made for the DMR approach, can be used to apply the Delphi trace replacement (DTR) method to infill missing data. The DTR method can be categorized as a simplified data mapping technique, which employs the redundancy of seismic data. The general assumption underlying this approach is that the reflectivity of a certain reflection point at a target reflector is independent of the azimuth. This suggests that traces recorded at two different source/receiver pairs contain identical information regarding the target reflector if the rays belonging to the considered reflection event reach the same reflection point with an identical angle of incidence. As a consequence, the missing time sample, which belongs to a certain reflection event, can be replaced by a time sample on an acquired trace, which belongs to a reflection at the same reflection point with the same angle of incidence with respect to this point. Certainly, the acquired time sample has to be corrected first for differences in the wave propagation, which cannot be considered azimuthal independent. By combining the DMR approach with the proposed infill method the new approach to redatuming becomes applicable to 3D data sets from conventional acquisition geometries.

The newly developed approach for redatuming has been evaluated on several data examples. The applicability of the proposed DMR methodology has been tested with positive outcome on fully sampled synthetic 2D and 3D data sets and on a 2D field data set. It has been shown, that the DMR methodology produces results that are kinematically and dynamically almost identical to the results of the conventional KSR approach, as it was intended to. It has, furthermore, been shown that the DMR method is, indeed, relatively insensitive with respect to the background medium chosen to describe the subsurface below the new datum level. The use of redatumed stacking velocities was already sufficient to achieve correct results. Even the use of grossly incorrect velocities for the medium below the new datum yielded results with only minor errors in the timing and the amplitudes of the redatumed events.

Furthermore, the applicability of the DMR method combined with the proposed DTR approach to infill missing data has been examined. It has been applied to sparsely sampled synthetic and realistic 3D data sets. The results of these tests were satisfactory as well. The results of the DMR approach combined with the infill and applied to sparsely sampled input data were kinematically and dynamically almost identical to the results of the DMR approach applied to fully sampled 3D input data, as was aimed for. It can thus be stated that all research objectives have been achieved.

Additionally, further applications of the DMR approach have been examined. The methodology has been modified such that it can be applied for the redatuming of PS-data, and a new concept for the prediction of datum layer-related multiples by means of the DMR methodology has been developed. The applicability of the modified redatuming approach and the new concept for multiple prediction, both, have been evaluated on numerical 2D data sets with a positive outcome.

Sandra Tegtmeier-Last

Samenvatting

Redatuming van schaarse 3D seismische data

Het doel van een seismisch onderzoek is een beeld van de ondergrond te verkrijgen die een overzicht van de discontinuïteiten van de aarde levert. Het verkregen beeld kan door geologen, geophysici of reservoir-ingenieurs worden geïnterpreteerd. Het doel van seismische data verwerking - d.m.v. van procedures zoals het tijdelijke en ruimtelijke filteren, looptijd correcties en, tenslotte, de migratie van de gereflecteerde energie - is dit beeld te creëren. De seismische methode is vooral geschikt voor de exploratie en de controle van koolwaterstof reservoirs.
Een meerderheid van de algoritmen, die in de seismische data verwerking worden toegepast, is geoptimaliseerd voor regelmatig bemonsterde data gemeten op een vlakke oppervlakte en voor een eenvoudige snelheidsdistributie in de ondergrond. In werkelijkheid zijn de seismische data onregelmatig bemonsterd en ze worden gemeten op een ruwe oppervlakte en/of met complexe structuren in de ondergrond. In dit geval kunnen de seismische data worden *geredatumed* naar een nieuwe referentie oppervlakte (*datum*) die aan de hierboven vermelde eisen voldoet, voorafgaand aan verdere stappen. Redatuming plaatst echter bronnen en ontvangers op een ander niveau zonder hen daadwerkelijk te bewegen.
De methodologie die het meest voor redatuming wordt gebruikt is het zogenaamde Kirchhoff sommatie redatuming (KSR). Het is al met succes toegepast op 2D data. Het redatuming van pre-stack data door middel van de KSR methode wordt uitgevoerd in twee afzonderlijke stappen, het redatuming van de ontvangers en het

redatuming van de bronnen. Elke stap vereist de berekening van het Rayleigh II integraal over de coördinaten van de bronnen en de ontvangers. Dit integraal kan uit de akoestische golf-vergelijking worden afgeleid. Het staat de berekening van een seismische golfveld op iedere punt onder de acquisitie oppervlakte toe door middel van een gewogen sommatie van de metingen aan deze oppervlakte; d.w.z. voor het redatuming van seismische 2D pre-stack data door middel van KSR moet een 2D integraal worden berekend, voor het redatuming van 3D pre-stack data moet een 4D integraal worden berekend. De KSR methode vereist dicht bemonsterde data in zowel bron- als ontvangers-coördinaten aan de acquisitie oppervlakte om aliasing artefacten te voorkomen.
De wegingsfuncties beschrijven de een-weg propagatie tussen de oppervlakte-punten en het doelpunt op het nieuwe datum, in termen van looptijden en amplitudes. In de praktijk zijn zij onbekend en moeten worden geschat uit de gemeten seismische data (data-gedreven benadering) of van een snelheidsmodel van de datum laag (model-gedreven benadering).
Tegenwoordig neemt de hoeveelheid van gemeten 3D data toe, wat betekent dat het ontwikkelen van een toepasbare methode voor het redatumen van 3D pre-stack data steeds belangrijker wordt. Alle gebruikelijke 3D acquisitie-geometrieën leveren data sets op die in minstens één van de coördinaten schaars zijn. Dat betekend dat de KSR methode niet rechtstreeks toepasbaar is. Daarom moest een nieuwe redatuming methodologie worden ontwikkeld, die wel van toepassing is voor schaarse 3D data.
In dit proefschrift wordt het zogenaamde data mapping redatuming, de DMR methode geïntroduceerd. Hier is de keuze gemaakt om het redatuming proces in termen van een data mapping probleem te formuleren, vergelijkbaar met bekende technieken zoals, bijvoorbeeld, de dip move-out (DMO) correctie en de azimuthal move-out (AMO) correctie. Voor de DMR methode worden, ten eerste, alle tijdsamples van de input data geïdentificeerd die misschien tot het beschouwde output sample bijdragen. Om dit te kunnen bereiken worden enkele veronderstellingen over het snelheidsmodel onder het nieuwe datum gemaakt. Men veronderstelt dat het medium onder het nieuwe datum kan worden beschreven door stack snelheden gerelateerd aan het nieuwe datum. Deze snelheden kunnen uit de input data worden gehaald door conventionele snelheidsanalyse. Verder wordt verondersteld dat de potentiële reflectoren onder het datum niet sterk gekromd zijn. Er wordt een gewogen sommatie toegepast op de mogelijk bijdragende tijdsamples met als resultaat het gezochte tijdsample van het geredatumde signaal. Dit is verschillend van de conventionele methodes. In de DMR methode wordt het aantal signalen dat is betrokken bij de berekening van één output-sample aanzienlijk verminderd, net als de dimensionaliteit van het integraal die het proces beschrijft. Er moet slechts een 2D integraal worden berekend om één output-sample te verkrijgen terwijl er een 4D integraal voor de conventionele KSR methode nodig is.
De DMR methode is in het algemeen van toepassing op alle soorten input data, maar het primaire doel van dit werk was het ontwikkelen van een redatuming methode die wel toepasbaar is op data die er geen dichte bedekking van bronnen en ontvangers aan het acquisitie oppervlak hebben. Zelfs voor de DMR methode kan het gebeuren

dat de vereiste signalen niet zijn gemeten, ook al heeft deze methode aanzienlijk minder signalen per output-sample nodig. Voor het geval dat dit gebeurt moet de DMR methode met een infill procedure worden gecombineerd.

De informatie over de mogelijke reflectie punten die tot de beoogde tijdsample behoren, die uit de veronderstellingen over het medium onder het nieuwe datum kan worden verkregen die voor de DMR methode worden gemaakt, kan worden gebruikt om de DELPHI *trace replacement* (DTR) methode voor de infill van ontbrekende data toe te passen. De DTR methode kan als een vereenvoudigde data mapping techniek worden gecategoriseerd, die gebruik maakt van de redundantie van seismische data. De algemene veronderstelling, waar deze methode op gebaseerd is, is dat de reflectiviteit van een bepaald reflectie punt onafhankelijk is van de azimut. Dit stelt voor dat de signalen die bij twee verschillende bron/ontvanger-paren worden geregistreerd identieke informatie betreffende een reflectie punt bevatten als de stralen, die tot de beschouwde reflectie behoren, hetzelfde reflectie punt onder een identieke invalshoek bereiken. In dit geval kan het ontbrekende tijdsample, dat tot een bepaalde reflectie behoort, worden vervangen door een tijdsample op een spoor die wel gemeten is en tot een reflectie behoort aan het zelfde reflectie punt met dezelfde invalshoek. Alleen moet het zo gekozen tijdsample eerst voor de verschillen in de golf propagatie worden gecorrigeerd, die niet als azimutaal onafhankelijk kan worden beschouwd. Door de DMR methode met de voorgestelde infill methode te combineren wordt de nieuwe methode voor het redatuming wel toepasbaar op 3D data van conventionele acquisitie-geometrieen.

De ontwikkelde DMR methode voor redatuming is geëvalueerd op verschillende voorbeelden. De toepasbaarheid van de voorgestelde methodologie is getest op volledig bemonsterde synthetische 2D en 3D data en op een echte 2D data set. De uitkomsten van deze tests waren positief. De DMR resultaten en de resultaten van de conventionele KSR methode zijn kinematisch en dynamisch bijna identiek. Verder kan men zien dat de DMR methode inderdaad vrij ongevoelig is voor de keuze die is gemaakt om het medium onder het nieuwe datum te beschrijven. Het is al voldoende stack snelheden te gebruiken die gerelateerd zijn aan het nieuwe datum. Zelfs als onjuiste snelheden voor het medium onder de nieuwe datum worden gebruikt zijn er slechts kleine fouten in de timing en de amplitude van het geredatumde resultaat te zien.

De toepasbaarheid van de DMR methode gecombineerd met de voorgestelde DTR methode voor de infill van ontbrekende data is ook onderzocht. Het was toegepast op schaarse synthetische en realistische 3D data. De resultaten van deze tests waren eveneens bevredigend. De resultaten van de DMR methode met infill toegepast op schaarse data zijn kinematisch en dynamisch bijna identiek aan de resultaten van de DMR methode toegepast op volledige 3D input data. Men kan dus concluderen dat alle doelstellingen van dit onderzoek zijn bereikt.

Verder zijn een tweetal andere toepassingen van de DMR methode onderzocht. De methodologie is dusdanig gewijzigd dat het voor het redatuming van PS-data kan worden gebruikt. Bovendien is een nieuw concept ontwikkeld voor de voorspelling van meervoudige reflecties gerelateerd aan die datumlaag door middel van de DMR methodologie. De toepasbaarheid van de gewijzigde redatuming methode voor PS-data en van het nieuwe concept voor de voorspelling van meervoudige reflecties zijn allebei geëvalueerd op numerieke 2D data met een positief resultaat.

Sandra Tegtmeier-Last

Curriculum vitae

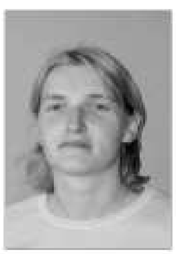

Sandra Tegtmeier-Last was born in Hameln, Germany on July 19, 1976. She attended secondary school at the Viktoria-Luise-Gymnasium in Hameln, where she received her 'Abitur' in June 1996. In September of the same year she started the study of geophysics at the Ruhr-Universität in Bochum and received the 'Diplom', which is equivalent to a MSc., in October 2001 (graded 'with distinction'). Her thesis was awarded with the 'Preis an Studierende 2001'. During her studies she spent two months with Schlumberger Geco-Prakla (now WesternGeco) in Gatwick, UK for an internship.

From December 2001 to September 2006 she was part of the Delphi research consortium at the Faculty of Applied Sciences at the Delft University of Technology. There, she conducted the PhD research, which led to this thesis.

In November 2006 she joined the Chevron Coorporation in San Ramon, US.

Acknowledgements

At this point, as I literally reached the last page of my thesis, it is time to thank all people who contributed in any way to the results presented on the previous pages.
There are several things one needs to have to actually perform the research, produce results and write the thesis: a project, professional, financial and mental support.
Ik wil daarom mijn dankwoord beginnen met mijn promotoren professor Gisolf en Eric Verschuur. Hun professionele ondersteuning hebben deze proefschrift mogelijk gemaakt. Ik dank professor Gisolf en voor het letten op de theoretische details van dit onderzoek en voor het nauwkeurige lezen en corrigeren van mijn proefschrift. Ook al was dit proces van het ontwikkelen van die details af en toe pijnlijk, het was wel leerzaam en absoluut de moeite waard.
Een grote dank ook aan Eric, voor de taalloze discussies, vele ideeën, theoretische en praktische hulp en het "net een stukje verder pushen" dan ik zelfs soms wilde. Ook dat was de moeite waard.
Ik wil ook graag professor Berkhout bedanken voor de mogelijkheid om deze onderzoek te verrichten in de Delphi omgeving.
Another thing needed at some point is data. I got the opportunity to test my 2D algorithm on a data set provided by Saudi Aramco and I would like to thank Saudi Aramco for this. Furthermore, I would like to thank Mustafa Al'Ali for providing the operators for the data set. En dank aan Bouchaib, Eric en Jan voor de operatoren voor die waterbak data.
A vital component of this research project is, of course, the financial and professional support of sponsors of the Delphi consortium. The experience of the sponsors leading to critical remarks and fruitful discussions during the meetings certainly helped

a lot in this project.
Ich möchte mich außerdem gerne bei Jörg Schleicher bedanken, dessen Tipps und Hinweise in der Anfangsphase die Arbeit in die richtige Richtung gelenkt haben.
Voor de ontwikkeling van de DTR methode waren ook de discussies met Gijs Vermeer heel erg belangrijk. Bedankt daarvoor.
Ook de technische (en morele) ondersteuning was heel erg belangrijk voor dit onderzoek. Ik ben veel dank verschuldigd aan Edo, Henry, Paul en Margaret. Ook wil ik graag Geerit van Dijk en Erwin Broer bedanken voor hun steun met die waterbak data.
En dan, "mental/moral" (en professionele) support: Dank aan mijn oude/recente collegas Kees, Paul, Mohammed, Mustafa, Ayon, Justyna, Dana, Lars, Pascal, Hans, Niels voor vele gezellige uren aan de TU, lunches en gezellige trips naar diverse meetings. Bijzondere dank aan mijn kamergenoot Maurice. Er zijn zeker niet veel mensen die in staat zijn om de altijd "optimistische" Sandra te tolereren. De tijd samen op een kamer heb ik in ieder geval genoten en zal ik zeker nooit vergeten. Ook dank aan Barbara en Geert-Jan, die niet alleen door actieve/passieve sportieve activiteiten voor de nodige afleiding van de wetenschap hebben gezorgd.
Dank ook aan mijn oude een nieuwe collega Edith voor gezellige koffiepauzes, jetlag-zwem-sessies, tips wat betreft promotieregelement en verhuizing, IKEA trips, Thanksgiving-Dinner- pogingen en het delen van de ene of andere dessert.
Außerdem sind da noch eine ganze Menge Menschen in Delft denen ich das Überleben zu verdanken habe. Birte und Wim, Lena, Nikolai, Julia, Alex Danke dafür, daß Delft schön war. Danke für entspannte Abende und Wochenenden.
Wichtig auf dem Weg zur und während der Doktorarbeit ist aber vor allem die Familie. Meine Eltern haben mit Ihrer Erziehung den Grundstein gelegt. Meine Mutter hat dadurch, daß sie war, wie sie war, viel zu dem beigetragen, was ich heute bin. Und meinem Vater möchte ich dafür danken, daß er mich und insbesondere alle meine Auswanderungsentscheidungen immer unterstützt hat.
Vielen Dank auch an meine Schwester. Es hat zwar einige Zeit gedauert, bis wir uns zusammengerauft hatten, aber die Zeit in Delft war toll.
Und dann, die letzten Worte und den größten Dank an Thorsten, dessen Anteil an dieser Arbeit und an meinem Leben nicht in Worte zu fassen ist. Ich hoffe, daß in nicht allzu ferner Zukunft auch die physische Distanz, die uns trennt, nicht mehr in umgekehrtem Verhältnis zur gefühlten Nähe sein wird.